

Design of Innovative Access Protocols for Cell-less Architectures

Tareq Al-shami

PhD

University of York

Electronic Engineering

June 2020

Abstract

Traditionally, wireless architectures have relied on cells where a user is served only by one base station. This conventional approach suffers from severe inter-cell interference particularly at the cell-edge. Thus, it is essential to rethink the design of the wireless architecture and shift from a cell-centric design to a cell-less architecture. Cell-less architectures where cell boundaries are eliminated and a user can be jointly served by multiple base stations have the potential to tackle inter-cell interference and provide satisfactory services to all users. The aim of this thesis is to investigate the performance of cell-less architectures in heterogeneous networks.

The first part of this thesis focuses on user-centric JT-CoMP as it is one of the main elements that form cell-less architectures. A novel user-centric approach that can effectively identify CoMP users that can obtain signal-to-interference-plus-noise-ratio (SINR) gain without wasting bandwidth is proposed. Results have shown that the proposed approach is more effective in balancing SINR gain and loss of bandwidth compared with the traditional approaches.

In the second part of this thesis, joint user-centric JT-CoMP clustering and multi-cell resource allocation is studied. A resource matching approach is proposed to support multi-cell resource allocation. In addition, a hybrid approach where users at the edge can be jointly served by CoMP and no CoMP is proposed to efficiently utilise the bandwidth. According to the results, the hybrid approach achieves better user throughput and bottom 5% throughput compared with the traditional JT-CoMP scheme.

Finally, the performance of a cell-less architecture that utilises JT-CoMP or zero forcing (ZF) as interference mitigation techniques is investigated. To address inter-cluster interference in cell-less architectures, macro base stations are connected to multiple central processing units (CPUs). Results have demonstrated the strength of cell-less architectures in improving SINR levels and throughput compared with cell-centric approaches.

Contents

Abstract

List of Figures

List of Tables

Acknowledgements

Declaration

1 Introduction.....	14
1.1 Motivation.....	14
1.2 Hypothesis.....	15
1.3 Objectives.....	16
1.4 Thesis Outline	16
2 Literature Review	18
2.1 Introduction.....	18
2.2 5G Heterogeneous Networks	19
2.3 Interference Management in 5G Heterogeneous Networks.....	20
2.3.1 Inter-cell Interference Coordination	21
2.3.2 Coordinated Multipoint Transmission.....	21
2.4 Radio Propagation and Channel Modelling.....	28
2.5 Shannon's Channel Capacity Theorem	30
2.6 Radio Access Network Architectures	30
2.6.1 Cell-centric Architecture.....	30
2.6.2 C-RAN Architecture	31
2.6.3 Cell-free Architecture	32

2.6.4	Cell-less Architecture	34
2.7	Spatial Modelling of Base Stations	35
2.7.1	Grid Models	35
2.7.2	Stochastic Models	36
2.8	Conclusion	41
3	User-centric JT-CoMP Clustering	43
3.1	Introduction	43
3.2	System Model	45
3.2.1	System Layout	45
3.2.2	Outage Probability Metric	47
3.3	User-centric Clustering Approaches	47
3.3.1	Power Level Difference	48
3.3.2	RSS Threshold	49
3.3.3	SINR Threshold	50
3.3.4	Proposed User-centric Algorithm	51
3.4	Definition of Regions and Cooperation Set	54
3.5	Performance Evaluation	56
3.5.1	Impact of Limiting the Maximum UC Cluster Size	66
3.5.2	Impact of BS Densification.....	70
3.5.3	Impact of Spatial Modelling of SC BSs	73
3.6	Conclusion	74
4	Joint Multi-Cell Resource Allocation and User-centric Clustering in JT-CoMP.....	77
4.1	Introduction	77
4.2	System Model	79
4.3	Set Definitions of CoMP and non-CoMP Users Per Base Station.....	79
4.4	Multi-cell Radio Resource Management	81

4.4.1	Challenges of Resource Allocation in User-Centric JT-CoMP	83
4.4.2	Resource Matching Approach	84
4.4.3	Bandwidth Allocation	86
4.4.4	Bandwidth Underutilisation Problem	87
4.4.5	Impact of JT-CoMP on Base Station Loading	91
4.5	Performance Comparison	93
4.6	Conclusion	104
5	5G Cell-less Architecture	107
5.1	Introduction	107
5.2	System Model	108
5.2.1	Performance Metrics	111
5.3	Performance Evaluation	111
5.3.1	Impact of CPU Densification	116
5.3.2	Impact of Different Cluster-edge Distances	119
5.3.3	Complexity of Zero Forcing	123
5.4	Conclusion	125
6	Conclusions and Future Work.....	127
6.1	Conclusions	127
6.2	Novel Contributions	131
6.2.1	User-centric JT-CoMP Clustering Approach	131
6.2.2	Resource Matching Approach	131
6.2.3	Multi-cell Radio Resource Management	132
6.2.4	JT-CoMP-No CoMP Hybrid Approach	133
6.2.5	Development of a Novel Cell-less Architecture	133
6.3	Future Work	134
6.3.1	Load Balancing in Cell-less Architectures	134
6.3.2	Energy Efficient Cell-less Architectures	134

6.3.3	Cell-less Millimetre Wave Systems.....	134
6.3.4	Multi-objective Cell-less Architecture.....	135
6.3.5	Cell-less Architecture: a Stochastic Geometry Approach	135

Glossary

References

List of Figures

Figure 2.1: JT-CoMP where a user can be served by multiple base stations jointly [19].	23
Figure 2.2: Coordinated beamforming in CoMP.	24
Figure 2.3: The traditional cell-centric architecture.....	31
Figure 2.4: C-RAN architecture [75].	32
Figure 2.5: Cell-free architecture.	33
Figure 2.6: Cell-less architecture.	35
Figure 2.7: A realisation of a hexagonal model with $v = 5$	36
Figure 2.8: A realisation of PPP with $\lambda_p = 0.01$	38
Figure 2.9: A realisation of type 2 MHPP with $\lambda_p = 0.01$ and $\delta = 5$	40
Figure 2.10: A realisation of type 2 MHPP with $\lambda_p = 0.006$ and $\delta = 7$	40
Figure 3.1: System model	46
Figure 3.2: Minimum SINR with CoMP to achieve rate gains ranging from 2 to 8.	53
Figure 3.3: An example of non-CoMP and CoMP regions. A1 denotes non-CoMP regions while A2 and A3 denote CoMP regions with cluster sizes of 2 and 3, respectively.	54
Figure 3.4: Percentage of non-CoMP and CoMP UEs for the PLD, RSS and SINR approaches when $c_{max}=8$	59
Figure 3.5: Percentage of UEs with cluster sizes of 1, 2, 4, 6, and 8 for the PLD approach.....	60
Figure 3.6: Percentage of UEs with cluster sizes of 1, 2, 4, 6, and 8 for the RSS approach.....	60
Figure 3.7: Percentage of UEs with cluster sizes of 1, 2, 4, 6, and 8 for the SINR approach.....	61
Figure 3.8: Percentage of UEs with cluster sizes of 1, 2, 4, 6, and 8 for the proposed approach.....	62
Figure 3.9: Percentage of winners and losers for the PLD, RSS and SINR approaches when $c_{max}=8$	64
Figure 3.10: Outage probability with no CoMP and with the PLD (6 dB), RSS (-57 dBm), SINR (3 dB), and the proposed UC JT-CoMP approaches.....	66

Figure 3.11: Number of winners and losers in the PLD approach when the maximum cluster size is limited to 2, 4, 6, and 8.	68
Figure 3.12: Number of winners and losers in the RSS approach when the maximum cluster size is limited to 2, 4, 6, and 8.	69
Figure 3.13: Number of winners and losers in the SINR approach when the maximum cluster size is limited to 2, 4, 6, and 8.	69
Figure 3.14: Percentage of winners in the proposed approach when the maximum cluster size c_{max} is limited to 2, 4, 6, and 8.	70
Figure 3.15: Percentage of winners and losers in the PLD approach for sparse (56 BSs/km ²), medium (80 BSs/km ²), and dense (104 BSs/km ²) deployment.	71
Figure 3.16: Percentage of winners and losers in the RSS approach for sparse (56 BSs/km ²), medium (80 BSs/km ²), and dense (104 BSs/km ²) deployment.	72
Figure 3.17: Percentage of winners and losers in the SINR approach for sparse (56 BSs/km ²), medium (80 BSs/km ²), and dense (104 BSs/km ²) deployment.	72
Figure 3.18: Percentage of winners in the proposed approach for sparse (56 BSs/km ²), medium (80 BSs/km ²), and dense (104 BSs/km ²) deployment.	73
Figure 3.19: The performance of JT-CoMP in pure PPP networks compared repulsive PPP networks with when the PLD approach is implemented.	74
Figure 4.1: An example illustrating the set of CoMP and non-CoMP UEs of a base station.	81
Figure 4.2: An example of half bandwidth assignment.	83
Figure 4.3: An example of resource mismatching for CoMP regions.	85
Figure 4.4: An example solved by the proposed resource matching approach.	86
Figure 4.5: The bandwidth underutilisation problem. An overlapping region with a heavily loaded macro base station and a small cell base station is shown in (a) while (b) shows an overlapping region with two small cell base stations where the bandwidth underutilisation problem is less severe.	89
Figure 4.6: The proposed hybrid approach where a hybrid user (UE 1) can be served by no CoMP and JT-CoMP simultaneously.	90
Figure 4.7: Some potential load distributions in JT-CoMP.	92
Figure 4.8: Outage probability with no CoMP and with the PLD (6 dB), RSS (-57 dBm), SINR (3 dB), and the proposed UCCA approaches when $c_{max} = 2$	95
Figure 4.9: User throughput with and without JT-CoMP. In JT-CoMP, full bandwidth assignment is considered.	96

Figure 4.10: Cell-edge throughput with and without JT-CoMP. In JT-CoMP, full bandwidth assignment is considered.....	98
Figure 4.11: A comparison between no CoMP, the traditional JT-CoMP and the hybrid approach in terms of overall user throughput. In the traditional JT-CoMP and the hybrid approach, full bandwidth assignment is considered.....	99
Figure 4.12: A comparison between no CoMP, the traditional JT-CoMP and the hybrid approach in terms of cell-edge throughput. In the traditional JT-CoMP and the hybrid approach, full bandwidth assignment is considered.....	100
Figure 4.13: A comparison of assigning half bandwidth, full bandwidth, and double bandwidth for CoMP users in terms of user throughput when the hybrid approach is implemented.....	101
Figure 4.14: A comparison of assigning half bandwidth, full bandwidth, and double bandwidth for CoMP users in terms of cell-edge throughput when the hybrid approach is implemented.	102
Figure 4.15: Macro-cell-edge throughput with and without CoMP. Full bandwidth assignment is considered when the JT-CoMP and the hybrid approach are implemented.	104
Figure 5.1: System model	109
Figure 5.2: Outage probability with the cell-centric approach, the hybrid cell-less scheme (CLH1 and CLH2), and the cell-less zero forcing scheme (CLZF1 and CLZF2).	114
Figure 5.3: User throughput with the cell-centric approach, the hybrid cell-less scheme (CLH1 and CLH2), and the cell-less zero forcing scheme (CLZF1 and CLZF2).	115
Figure 5.4: Bottom 5% throughput with the cell-centric approach, the hybrid cell-less scheme (CLH1 and CLH2), and the cell-less zero forcing scheme (CLZF1 and CLZF2).	116
Figure 5.5: An example of CPU densification in cell-less architectures.	118
Figure 5.6: The impact of CPU densification on the outage probability performance.	119
Figure 5.7: The impact of different cluster-edge distances on the performance of the outage probability.....	120
Figure 5.8: Two different cases of double CPU association.....	122
Figure 5.9: The impact of allowing small cell base stations to connect to two CPUs..	123
Figure 5.10: Complexity of the zero forcing scheme when different number of users and different number of base stations are considered.....	124

List of Tables

Table 2.1: Specifications of different node types in heterogeneous networks20

Acknowledgements

First and foremost, all praises are due to Allah, the Almighty, the greatest of all, and the Most Merciful, on whom we rely for guidance and sustenance.

I would like to express my deepest gratitude to my first supervisor Prof. David Grace for his excellent and continuous support, valuable suggestions, and constructive comments. I appreciate all of his contributions of time, support and ideas. I would also like to express my gratitude to my second supervisor Prof. Alister Burr and my thesis advisor Dr. Paul Mitchell for their valuable guidance and suggestions.

Thanks go to all my friends at the communication technologies research group for their help and support since the first day I started my PhD study.

Sincere thanks go to my family who always encourages and supports me during every stage of my personal and academic life

Finally, I would like to thank the European Commission for financially aiding this research through the H2020-ITN-5Gaura project.

Declaration

This work has not previously been presented for an award at this, or any other, University. To the best knowledge of the author, all the work presented in this thesis is original. All sources are acknowledged as references.

Some of the work in this thesis has been published, submitted, or is planned for submission to conferences, journals, and project deliverables. A list is provided below.

Journal Papers

1. T. M. Shami, D. Grace, A. Burr, and J. S. Vardakas, "Load balancing and control with interference mitigation in 5G heterogeneous networks," *EURASIP Journal on Wireless Communications and Networking*, vol. 2019, no. 1, p. 177, 2019.
2. T. M. Shami, D. Grace, and A. Burr, "Joint User-centric Clustering and Multi-cell Radio Resource Management in Coordinated Multipoint Joint Transmission," *Wireless Personal Communications*, [Under review]
3. T. M. Shami, D. Grace, and A. Burr, "User-centric Clustering in Coordinated Multipoint Joint Transmission Heterogeneous Networks," to be submitted to *Transactions on Emerging Telecommunications Technologies*
4. T. M. Shami, D. Grace, and A. Burr, "Inter-cluster Mitigation in cell-less Networks," to be submitted to *IEEE Transactions on Mobile Computing*
5. M. D. Zakaria, D. Grace, P. D. Mitchell, T. M. Shami, and N. Morozs, "Exploiting User-Centric Joint Transmission–Coordinated Multipoint With a High Altitude Platform System Architecture," *IEEE Access*, vol. 7, pp. 38957-38972, 2019.

Conference Papers

1. T. M. Shami, D. Grace, A. Burr, and M. D. Zakaria, "User-centric JT-CoMP clustering in a 5G cell-less architecture," in 2018 IEEE 29th Annual International Symposium on Personal, Indoor and Mobile Radio Communications (PIMRC), 2018, pp. 177-181: IEEE.

2. T. M. Shami, D. Grace, A. Burr, and M. D. Zakaria, "Radio resource management for user-centric JT-CoMP," in *2018 15th International Symposium on Wireless Communication Systems (ISWCS)*, 2018, pp. 1-5: IEEE.
3. M. D. Zakaria, D. Grace, P. D. Mitchell, and T. M. Shami, "User-centric JT-CoMP for high altitude platforms," in *2018 26th International Conference on Software, Telecommunications and Computer Networks (SoftCOM)*, 2018, pp. 1-6: IEEE.

Project Deliverables

1. T. M. Shami, D. Grace, and A. Burr, 5GAura D1: Medium Access Control Protocols for Cell-less 5G Architectures, 2017
2. T. M. Shami, D. Grace, and A. Burr, 5GAura D2: User-centric Algorithms in 5G Cell-less Architectures, 2017
3. T. M. Shami, D. Grace, and A. Burr, 5GAura D3: Multi-cell Radio Resource Management in Coordinated Multipoint Joint Transmission, 2019

CHAPTER 1

Introduction

Contents

1.1 Motivation.....	14
1.2 Hypothesis.....	15
1.3 Objectives.....	16
1.4 Thesis Outline	16

1.1 Motivation

The rapid growth in the number of wireless devices and the emerging new applications are forcing a rethink in the design and architecture of cellular wireless networks. Future wireless networks are expected to require the design of novel architectures that are capable of meeting high-end requirements such as the high demand for mobile data. The massive mobile data demand creates a substantial burden on the capacity of current wireless networks that mainly rely on the conventional cellular base stations. Therefore, it is crucial to enhance the capacity by providing more radio resources per unit area. This capacity enhancement is a key element to the success of the enhanced mobile broadband 5th generation (5G) use case where 5G users can communicate in crowded places such as festivals, sports events, and airports. Enhanced mobile broadband in 5G promises to provide 1000x of capacity and throughput improvement over the 4th generation (4G) network [1].

One of the main simplest and most effective approaches towards the success of 5G is the deployment of heterogeneous networks (HetNets) that consist of high transmission power base stations such as macro base stations and low transmission power base stations (pico and femto base stations). The main advantages of HetNet deployments are that they can increase the capacity of the network and provide users with a better link quality since users are closer to base stations. Several techniques such

as coordinated multipoint joint transmission (JT-CoMP), enhanced inter-cell interference coordination (eICIC), and zero forcing (ZF) have been proposed to aid the deployment of HetNets in order to enhance the spectrum efficiency and provide high capacity [2]. These technologies introduce new numerous challenges as their successful implementation relies on a high degree of cooperation and more information exchange. Thus, it is crucial to develop innovative mechanisms that address such challenges in order to support the deployment of effective HetNets.

Historically, wireless system architectures have relied on cells where a UE that is located within a cell boundary is served by one base station only. This cell-centric design has always suffered from inter-cell interference that has been a major concern in the wireless field. Due to recent trends in wireless communication over the past few years such as massive densification of HetNets and the JT-CoMP technique, the architecture of wireless systems is moving from a cell-centric to a cell-less design. A cell-less architecture can be defined as “elimination of cell boundaries and freedom for users to associate with multiple base stations simultaneously”. The first step of designing a cell-less architecture is to develop innovative solutions that can address the challenges in HetNets and JT-CoMP as they are two main elements of a cell-less architecture. Additional innovative strategies are needed to completely design a cell-less architecture that can reduce the cooperation complexity that exists in cell-centric architectures.

1.2 Hypothesis

The research presented in this thesis is guided by the following hypothesis.

Exploiting a cell-less architecture that utilises promising technologies such as joint transmission coordinated multipoint and zero forcing can play an essential role towards meeting the 5G requirements in terms of improving the system capacity.

Future wireless architectures are expected to be cell-less and the exploitation of an innovative cell-less architecture will have a significant impact on the overall system performance. The performance effectiveness of the cell-less architecture is evaluated based on improvements to outage probability and capacity achieved by the cell-less architecture. Another important assessment of the cell-less architecture is evaluating the

throughput performance of users with poor link quality when operating in a cell-centric architecture. This assessment is essential to prove that a cell-less architecture provides good services to all users. Simulation experiments and a comprehensive performance evaluation have been performed to prove the hypothesis.

1.3 Objectives

According to the hypothesis, the objectives of the thesis is listed as follows.

- Development of a novel user-centric JT-CoMP clustering approach that can balance signal-to-interference-noise-ratio (SINR) gain and loss of bandwidth.
- Development of efficient multi-cell radio resource allocation that can support 5G cell-less architectures.
- Designing a 5G cell-less architecture that can exploit JT-CoMP and zero forcing techniques in order to improve the outage probability and the system capacity.

1.4 Thesis Outline

The organisation of the rest of thesis is as follows.

A literature review that presents the related work to this thesis is provided in Chapter 2. The chapter starts by introducing HetNets as a key enabler towards the success of 5G. It discusses its promises as well as challenges. It then focuses on interference mitigation techniques that promise to tackle inter-cell interference in HetNets. More specifically, it provides a comprehensive review on user-centric JT-CoMP clustering which is a main element of realising a cell-less architecture. It also reviews the research work that has been carried out on zero forcing in HetNets. Finally, the chapter provides a review on different spatial modelling strategies for small cell base stations.

Chapter 3 presents in detail the most common and recent user-centric JT-CoMP clustering algorithms. It also develops a new user-centric algorithm that attempts to balance between SINR gain and loss of bandwidth that might occur as a result of restricting all cooperating base stations from reusing radio resources allocated to their

CoMP users. Considering the existing and the developed user-centric clustering approaches, set theory is used to provide mathematical definitions of CoMP and non-CoMP areas as well as to define the cooperative set of base stations that can serve a certain user. The effectiveness of the proposed user-centric clustering algorithm is evaluated and compared with the existing user-centric clustering approaches. The chapter also describes simulation experiments to find effective thresholds for the existing user-centric JT-CoMP clustering approaches. Finally, it investigates the impact of limiting the maximum user-centric cluster size, base station densification, and spatial modelling of small cell base stations.

Chapter 4 develops multi-cell radio resource allocation in 5G JT-CoMP HetNets. The challenges in allocating resources from multiple base stations are presented. A novel resource matching approach is proposed to resolve the problem of resource mismatching in the number of radio resources provided by any two cooperating base stations. Moreover, a hybrid approach that allows a user to operate in both CoMP and no CoMP modes simultaneously is proposed. The proposed hybrid approach is compared with the traditional JT-CoMP scheme in order to evaluate its effectiveness.

Chapter 5 develops a 5G cell-less architecture that exploits the proposed user-centric clustering approach and the proposed hybrid approach. Chapter 5 also proposes to allow macro, pico, or femto base stations located at the edge of central processing units (CPUs) to be connected to multiple CPUs in order to reduce inter-cluster interference. The performance of zero forcing and the hybrid approach is compared when a cell-less architecture is considered. Also, Chapter 5 compares the performance of a cell-less design where each base station is connected to only one CPU with another case where cell-edge base stations are connected to multiple CPUs. Finally, the chapter investigates the impact of CPU densification on the system performance.

Chapter 6 concludes this thesis. It also provides the novel contributions of the research. Finally, it provides a list of potential future research directions.

CHAPTER 2

Literature Review

Contents

2.1	Introduction	18
2.2	5G Heterogeneous Networks	19
2.3	Interference Management in 5G Heterogeneous Networks	20
2.3.1	Inter-cell Interference Coordination	21
2.3.2	Coordinated Multipoint Transmission	21
2.4	Radio Access Network Architectures	30
2.4.1	Cell-centric Architecture.....	30
2.4.2	C-RAN Architecture	31
2.4.3	Cell-free Architecture	32
2.4.4	Cell-less Architecture	34
2.5	Spatial Modelling of Base Stations	35
2.5.1	Grid Models	35
2.5.2	Stochastic Models	36
2.6	Conclusion	41

2.1 Introduction

Designing a cell-less architecture requires deployment of heterogeneous networks to deliver more radio resource per unit area. In addition, a cell-less network implements CoMP as an interference mitigation technique where users are served by their x strongest base stations. The focus of this chapter is to present related background knowledge and to provide a review of established studies related to the scope of this thesis.

The organisation of this chapter is as follows. Section 2.2 presents 5G heterogeneous networks. Interference mitigation techniques in heterogeneous networks are discussed in Section 2.3. Section 2.4 and Section 2.5 provide an overview of radio propagation and Shannon's channel capacity theorem, respectively. Section 2.6 describes the traditional and recent promising radio access network architectures. Next, spatial modelling of macro and small cell base stations is discussed in Section 2.7. Finally, Section 2.8 concludes this chapter.

2.2 5G Heterogeneous Networks

Heterogeneous networks often consist of macro base stations and small cell base stations that have different transmission power, sizes, and coverage areas. A macro base station transmits with high power ranging from 5 W to 40 W [3] and it can provide coverage to a large area reaching up to 30 kilometres or more. Due to the high transmission power, air conditioners are typically needed to maintain suitable temperatures in the surrounding environments of macro base stations. The large size, high cost, and high power consumption of macro base stations restrict them from being densely deployed and benefitting from frequency reuse. Nevertheless, the existence of macro base stations in future wireless networks is still essential. Unlike small cell base stations, macro base stations, due to their large cells, do not cause high handover frequency which is crucial to support users with high mobility. In addition, they can be deployed in rural regions as they can cover large areas. Small cell base stations such as pico and femto base stations have lower transmission power, smaller size, and provide coverage to smaller areas compared with macro base stations. The transmission power of pico base stations varies from 250 mW to 2 W in outdoor environments and 100 mW or less in indoor deployments [3]. Pico base stations can provide coverage to small areas having a radius of 200 metres or less. Another small cell base station type is femto where its serving area ranges from 10 to 50 metres and its transmission power is 100 mW or less [3]. Based on their access mode, femto base stations can be categorised into three classes: open access, closed access, or hybrid. Open access gives permission to any user to be served by a femto base station whereas closed access prevents any user with no subscription from granting access. In hybrid access, all users are allowed to access femto base stations with a higher priority given to subscribers. The design and functionality of femto base stations is built in this way in order to reduce costs and

ensure privacy and security [4]. Table 2.1 compares the transmission power, coverage range, backhaul connections, and cost of macro, pico and femto base stations. The deployment of heterogeneous networks promises to significantly improve the capacity and coverage of future wireless networks particularly in high traffic demand areas such as airports, sport events, and city centres [5] [6]. The capacity is improved by densifying the number of base stations per unit area and reusing the spectrum while placing small cell base stations at dead zones can significantly provide better coverage. Although using heterogeneous networks is a straightforward and an effective approach to enhance the capacity and coverage of the network, its deployment creates many challenges that need to be addressed.

Table 2.1: Specifications of different node types in heterogeneous networks

Node Type	Transmission power	Coverage range	Cost	Backhaul
Macro	5 W-40 W	30 kilometres or more	High	S1 interface
Pico	250 mW- 2 W (outdoor) ≤100 mW (indoor)	≤200 metres	Low	X2 interface
Femto	≤100 mW	≤ 50 metres	Low	Internet IP

2.3 Interference Management in 5G Heterogeneous Networks

The deployment of heterogeneous networks in 5G has the potential to introduce severe inter-cell interference [7]. According to [8], four main reasons have a direct influence in increasing the level of interference. Firstly, the dense deployments of base stations in a small geographical area. Secondly, the access restriction modes in heterogeneous networks that can be public or private. Thirdly, base stations in each tier have different transmission powers which leads to different coverage areas. Finally, inappropriate resource allocation techniques. Several techniques such as ICIC and CoMP transmission have been proposed by 3GPP to address the foregoing four factors.

2.3.1 Inter-cell Interference Coordination

3GPP introduced ICIC in Release 8 in order to mitigate inter-cell interference at the cell-edge area. In ICIC, base stations communicate via an x2 interface and exchange messages that help to optimise scheduling radio resources for cell-edge users. ICIC in Release 8 is not specifically designed to support heterogeneous networks; thus, eICIC is introduced in Release 10 to better aid the deployment of heterogeneous networks [9]. The major enhancement is time domain ICIC represented by almost blank sub-frames (ABSs). ABSs do not include user data; however, it contains reference signals as well as control channels sent with reduced power. In eICIC, macro base stations transmit ABS that follows a specific pattern. Macro base stations communicate with small cells via an x2 interface informing them about the ABS pattern. During ABS periods, small cell base stations can transmit data to their users who can achieve better SINR and throughput since interference from muted macro base stations is reduced.

eICIC has been extensively implemented in heterogeneous networks due to its effectiveness in reducing inter-cell interference [10-13]. It also has shown significant enhancement in terms of improving the SINR levels of cell-edge users in heterogeneous networks that apply the cell range expansion (CRE) technique [14-18] as it can help to reduce the interference caused by macro base stations at the CRE region.

2.3.2 Coordinated Multipoint Transmission

The concept of CoMP has been introduced by 3GPP in Release 11 in order to mitigate inter-cell interference. In the same release, a study on the physical layer aspects of CoMP has been conducted for LTE networks. The benefits of CoMP have been evaluated in homogeneous macro networks and heterogeneous networks. In both networks, static clustering has been implemented. The simulation results have shown that CoMP can provide significant enhancement in terms of spectral efficiency particularly for cell-edge users [19]. CoMP has been further enhanced (feCoMP) by 3GPP in Release 15 where specification support for non-coherent JT-CoMP has been provided [20] [21]. As described in Release 16, CoMP can be utilised to enhance ultra-reliable, low-latency communication as it can provide redundant links with spatial diversity.

CoMP has the potential to reduce inter-cell interference, increase system throughput, and improve performance of cell edge users [22, 23]. The fundamental concept of CoMP is to convert the downlink interference signal into a useful signal through a joint transmission approach or to avoid inter-cell interference by coordinated beamforming. Based on the availability of user data among cooperating base stations and scheduling complexity, CoMP has been classified by 3GPP into the two following main categories [24].

1) Joint Transmission

In JT-CoMP, multiple base stations cooperate and transmit the same data to a user simultaneously. To perform this, user data must be available at all cooperating base stations. According to 3GPP, a user can be served by a number of a cooperating base stations non-coherently or coherently [19]. In non-coherent transmission, cooperating base stations jointly send the same data to a particular user without ensuring coherent combination at the user [25]. At the user side, the non-coherent signals are added resulting in received power gain. Coherent transmission is the case when the cooperating set of base stations of a user have detailed knowledge of channel state information (CSI) of the links between them and their served user [26]. Due to the knowledge of CSI, coherent combination at the user side can be achieved by precoding data that is transmitted simultaneously from a set of cooperating base stations to an intended user with prior phase alignment as well as tight synchronisation [27]. Figure 2.1 shows an example of JT-CoMP.

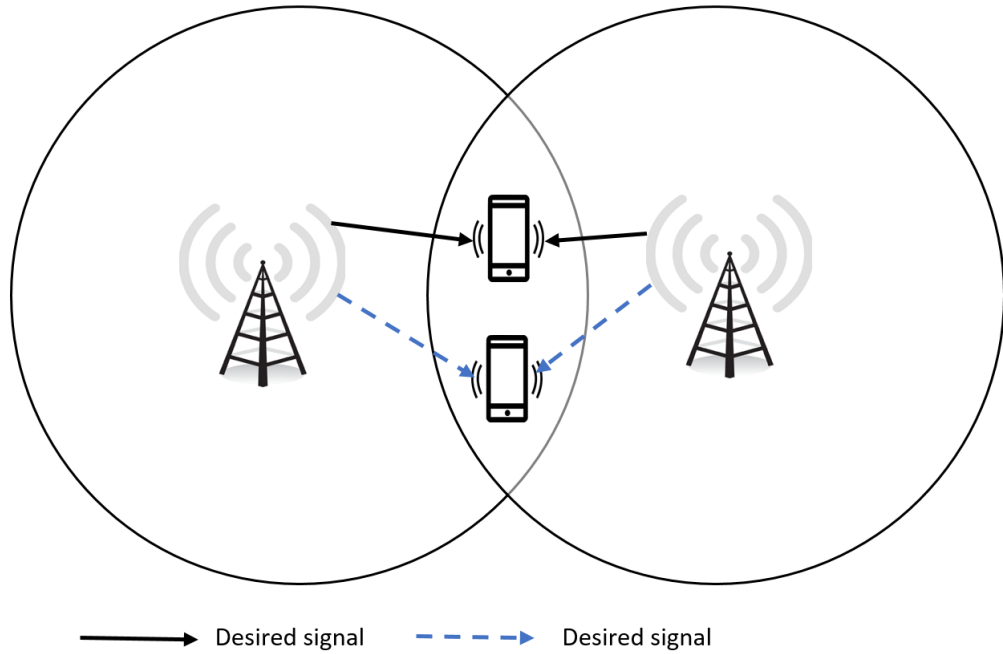


Figure 2.1: JT-CoMP where a user can be served by multiple base stations jointly [19].

2) Coordinated Scheduling/Beamforming (CS/CB)

In CS/CB, only the serving base station has the user data while CSI is shared among cooperating base stations. In other words, multiple base stations cooperate and share scheduling/beamforming information. In the case of CS, cooperating base stations attempt to minimise interference by carefully scheduling radio resources for users. The idea of CS is similar to eICIC; however, they are different in terms of the sharing period [28] and the amount of shared user data [29]. Sharing periods in CS and eICIC are approximately a millisecond and a hundred millisecond [28], respectively. Due to the short sharing period of CS, better resource scheduling can be achieved even in the case when the channel condition of a user changes rapidly [30]. CB reduces interference by selecting beamforming weights that steer the signals of interfering base stations towards the null space of an intended user.

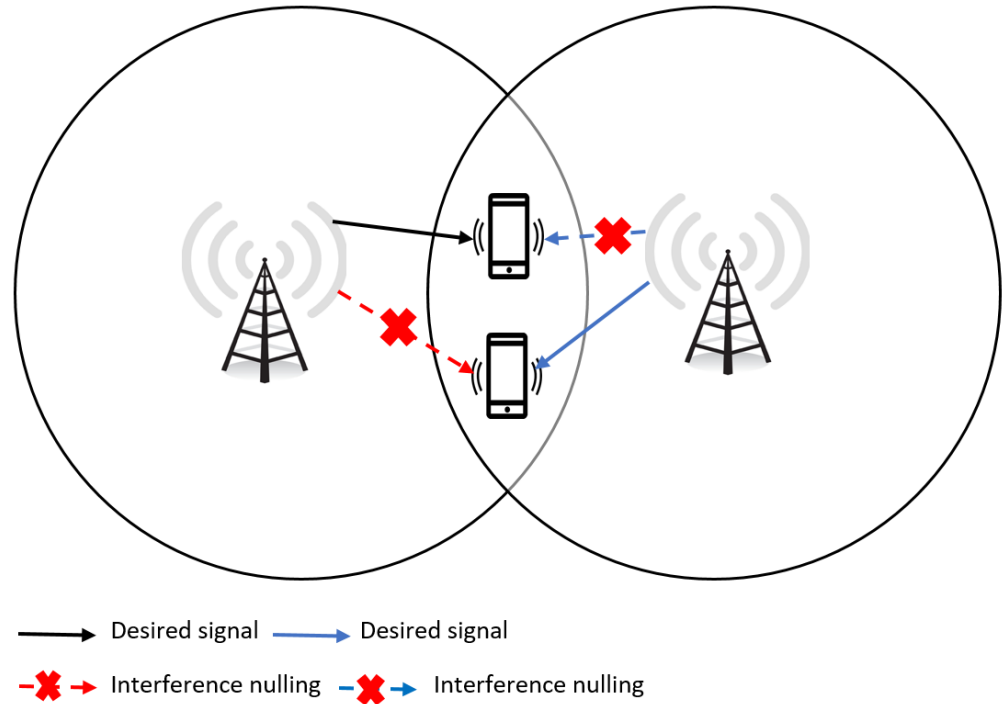


Figure 2.2: Coordinated beamforming in CoMP.

Clustering in CoMP

In a wireless CoMP network, it is impractical to let all base stations cooperate because that would lead to prohibitive complexity and overheads. In addition, according to [31], a CoMP network with many cooperating base stations has a negligible performance improvement compared to one that consists of just a few. To address the aforementioned problem, base stations are clustered and cooperation is performed within a cluster. A too small cluster size may not provide the expected CoMP improvements. On the contrary, increasing the cluster size improves CoMP gains but at the expense of excessive overhead and backhaul capacity requirements [31]. In addition, a big cluster size might be inefficient in terms of energy consumption [32]. Therefore, finding an effective cluster size is required in order to maximise the benefits of CoMP. Generally, clustering in CoMP can be grouped into static and user-centric clustering.

1) Static Clustering

Static clustering is a simple form of clustering where a number of neighbouring base stations form a fixed cluster that does not change over time. Several research works [31, 33-39] have implemented static clustering in order to increase the SINR levels

particularly at the cell edge. Static clustering, which is based on fixed topologies, can be used when the network topology does not change. This static approach is less complex and it can be a suitable candidate for LTE-A networks [23]. One of the basic and practical options of implementing static clustering is to allow cooperation only within cells in a co-located site which eliminates the need for data exchanges between sites [23]. Unfortunately, static clustering will not be able to provide expected gains for 5G networks because of the dynamic network topology, i.e., small cells will not be active all the time and users will randomly deploy small cells at unknown locations [23, 40]. As a result, dynamic user-centric clustering is required as it can adapt to changes in the network [23].

2) User-centric Clustering

In user-centric clustering, each user has his own set of cooperating base stations that cooperate to serve him. This approach divides users into two types: non-CoMP users and CoMP users. Non-CoMP users are served by one base station only while CoMP users can be served by two base stations or more. This division is essential since allowing all users to operate in CoMP can severely reduce the availability of radio resources. A major challenge in user-centric clustering is finding an effective user-centric cluster size that can balance between the SINR enhancement and the wastage of radio resources.

The work in [41] [42] has shown that the user-centric clustering approach outperforms static clustering in terms of average as well as cell-edge throughput. Significant research on user-centric JT-CoMP has been carried out focusing on finding an effective user-centric cluster size and allocating resources efficiently in CoMP networks. However, the majority of the research work has addressed these two issues separately [41-44].

In [41], a user-centric clustering algorithm is developed to enhance the throughput of cell-edge users. Optimal and low complex suboptimal algorithms are proposed and their average and cell-edge throughput performance is compared against the static clustering approach. The results showed that the proposed user-centric JT-CoMP clustering algorithms are more efficient than static clustering in terms of average and cell-edge throughput. The authors in [42] proposed a user-centric clustering approach in a single-tier network in order to tackle inter-cell interference. The idea of the proposed clustering

scheme is to let each user measure the average path loss and decide its potential serving base stations. After this measurement, a user forms its own cluster according to a given objective function that maximises the normalised goodput. Results showed that the proposed user-centric approach performs better than the static clustering approach. In [43], the authors proposed a user-centric JT-CoMP clustering approach where a user operates in the CoMP mode only if its second strongest received power is comparable with the power it receives from the strongest base station. The work in [44] proposed a user-centric clustering approach with the objective of maximising energy efficiency in heterogeneous networks. In [45], JT-CoMP has been applied to improve the energy efficiency and overall throughput. A user forms its own CoMP cluster by selecting the two base stations that provide the maximum SINR. Results have demonstrated that cooperation can achieve up to 26% energy savings.

The work in [46] applied non-coherent JT-CoMP to reduce inter-cell interference in ultra-dense heterogeneous networks where macro base stations are distributed hexagonally and small cell base stations are distributed based on a Poisson point process (PPP). The authors analysed the coverage performance in the hexagonal-PPP network and it was shown that the JT-CoMP coverage probability decreases exponentially as the density of small cell base stations increases. Considering non-coherent transmission in PPP networks, the authors in [47] proposed a location-dependent cooperation approach where users located at the cell centre area, cell edge area, and cell corner area are served by the strongest one, two, and three base stations, respectively. The sizes of the three areas are controlled by a cooperation level parameter n in the range of $[0,1]$ where a value of 1 indicates full cooperation and a value of 0 indicates no cooperation. The results have shown that a moderate n value can enhance the signal-to-interference ratio (SIR) performance.

The state-of-the-art research on JT-CoMP has shown the ability of JT-CoMP to improve the coverage area significantly [48-51]; nevertheless, JT-CoMP reduces the availability of physical resource blocks (PRBs) since a CoMP user must be assigned identical PRB(s) from all of its cooperating base stations to transmit the same data, meaning that these PRB(s) cannot be reused by any of the cooperating base stations. Thus, it is essential to consider resource allocation when investigating the performance of JT-CoMP.

Though most of the research in the state-of-the-art has tackled user-centric clustering and radio resource allocation separately, some research has attempted to jointly address this clustering and resource allocation problem [40, 52-55] using the PLD approach. The authors in [52] proposed a two-step joint clustering/scheduling algorithm with the aim of balancing the load in heterogeneous networks. The first step of the proposed algorithm utilises game theory to design a load-aware clustering approach. According to the clustering results obtained from the first step, the second step implements graph colouring to optimise utilisation of radio resources.

Recently, the authors in [55] addressed joint user-centric clustering and resource assignment using graph colouring with the aim of maximising spectral efficiency. With the help of graph colouring, the user-centric clustering and resource allocation are solved independently. First, a user-centric clustering is constructed in three stages: anchoring, exploration, and confirmation. After the construction of the user-centric clusters, a two-stage graph-based resource assignment approach is developed. The work in [50] utilised JT-CoMP user-centric clustering to address inter-cell interference in a high altitude platform (HAP) system. A novel user-centric clustering algorithm is developed where a user forms its own cooperating base stations based on the SINR levels. The performance of JT-CoMP in HAP systems is compared against the traditional no CoMP approach and ICIC scheme. According to the obtained results, JT-CoMP outperforms a no CoMP system and ICIC in terms of coverage probability as well as per user throughput with the highest gain achieved by cell-edge users. The reason that JT-CoMP performs better than ICIC is because ICIC only eliminates the most dominant interfering signal whereas JT-CoMP removes and converts it into a useful signal as well, resulting in higher SINR levels and throughput gain.

Decoupling the control plane from the data plane is an emerging wireless architecture that has been proposed to satisfy the 5G requirements. In this architecture, macro base stations are responsible for providing coverage and support control signalling, whereas small cell base stations that are located within the coverage area of macro base stations handle data traffic. Recently, the authors in [40] applied JT-CoMP in a decoupled control/data architecture with the objective of balancing the load and maximising the spectral efficiency. In the proposed approach, a user will form its own cluster of x base stations that provide the best received power as long as that x does not

go beyond a maximum cluster size. The results showed that the proposed algorithm is effective in balancing the load especially in dense environments. However, the authors did not investigate the impact of choosing power level difference (PLD) values on the performance of CoMP and non-CoMP users. Also, it focuses only on user-centric clustering without focusing on radio resource management. Following the work in [40], [56] developed a load balancing algorithm with the aim of reducing the number of users that obtain less than a certain data rate threshold.

The following summarises the recent advances in JT-CoMP:

- 1) The work in [41-44] investigated the performance of user-centric JT-CoMP clustering without taking radio resource management into account.
- 2) The majority of the research on JT-CoMP identifies CoMP users based on PLD [40, 41, 43, 51, 54, 57, 58].
- 3) Recent research [40, 51, 54, 57, 58] has addressed joint user-centric clustering and resource allocation where identifying CoMP users is still based on PLD.

2.4 Radio Propagation and Channel Modelling

The propagation of wireless signals is influenced by the surrounding environments where traveling signals can experience reflection, diffraction and scattering by buildings, walls, trees, and a variety of objects. As a result, a wireless device may receive a signal that is formed constructively or destructively by a number of signals coming from different paths with different phases and time delays. This phenomenon is known as multipath fading. Generally, fading can be categorised into large-scale fading or small-scale fading [59]. Large-scale fading can be presented by pathloss and shadowing whereas small-scale fading is characterised by multipath [60]. In this thesis, large-scale fading is only considered because clustering decisions are based on long term received power levels.

The following presents large-scale fading which consists of pathloss and shadow fading.

Path loss

Path loss is the reduction of a signal's power as it travels through the environment [60]. Path loss in dB can be mathematically written as follows:

$$PL = 10 \log_{10} \left(\frac{P_T}{P_R} \right) \quad (2.1)$$

where P_T is the transmitted power and P_R is the received power.

A signal can propagate in free space where it does not experience attenuation or reflections. In this case, free-space path loss model can be used. Nevertheless, most of the wireless devices communicate in complex environments where the free-space path loss model becomes inaccurate [60]. Thus, extensive efforts, mainly based on measurement results, have been made to develop models that can provide accurate predication of path loss in such environments. 3GPP have developed a number of path loss models for heterogeneous networks that operate in frequencies ranging from 2 to 6 GHz while considering different scenarios such as hotspot, indoor, urban micro, and urban macro environments [61].

Shadow Fading

A traveling signal over a long distance is usually blocked by a number of objects which causes random variations of the original signal when received at a certain distance. Therefore, a model that can represent these random variations is needed. The most well-known shadow fading model is the log-normal shadowing. This model has been validated in indoor and outdoor environments and it has proved its effectiveness in providing accurate modelling of the attenuation in the received power [62, 63]. The log-normal shadowing assumes random ratio between the transmit and received power $\vartheta = \frac{P_T}{P_R}$ with a log-normal distribution that can be mathematically written as [60]:

$$p(\vartheta) = \frac{\eta}{\sqrt{2\pi} \sigma_{\vartheta_{dB}} \vartheta} \exp \left[-\frac{(10 \log_{10} \vartheta - \mu_{\vartheta_{dB}})^2}{2\sigma_{\vartheta_{dB}}^2} \right], \vartheta > 0 \quad (2.2)$$

where $\eta = 10/\ln 10$, $\vartheta_{dB} = 10 \log_{10}(\vartheta)$, $\sigma_{\vartheta_{dB}}$ and $\mu_{\vartheta_{dB}}$ are the standard deviation and mean of ϑ_{dB} in dB, respectively.

2.5 Shannon's Channel Capacity Theorem

Shannon's capacity theorem provides the capacity limits of wireless channels. In order to successfully receive bits with a probability of error $\rightarrow 0$, Shannon has proved that the maximum transmission rate is given as follows:

$$R = B \log_2(1 + SNR) \quad (2.3)$$

where SNR is the signal to noise ratio. This theorem provides the theoretical limits that is difficult to reach in practise. Due to a number of factors such as channel attenuation, there exists a large gap between the real performance and this limit [64].

2.6 Radio Access Network Architectures

2.6.1 Cell-centric Architecture

Traditionally, the wireless architecture has been based on cell-centric design where a number of cells exist and a user connects only to one of them. In addition, both baseband processing and radio functions are performed in each base station. One of the major limitations of the conventional cellular architecture is its poor performance in tackling inter-cell interference [65]. Another drawback of the traditional cell-centric networks is radio resource underutilisation. Figure 2.3 provides an example of the traditional cell-centric architecture. To overcome the drawbacks of the conventional wireless architecture, several architectures such as cloud radio access network (C-RAN), cell-free, and cell-less have been recently proposed.

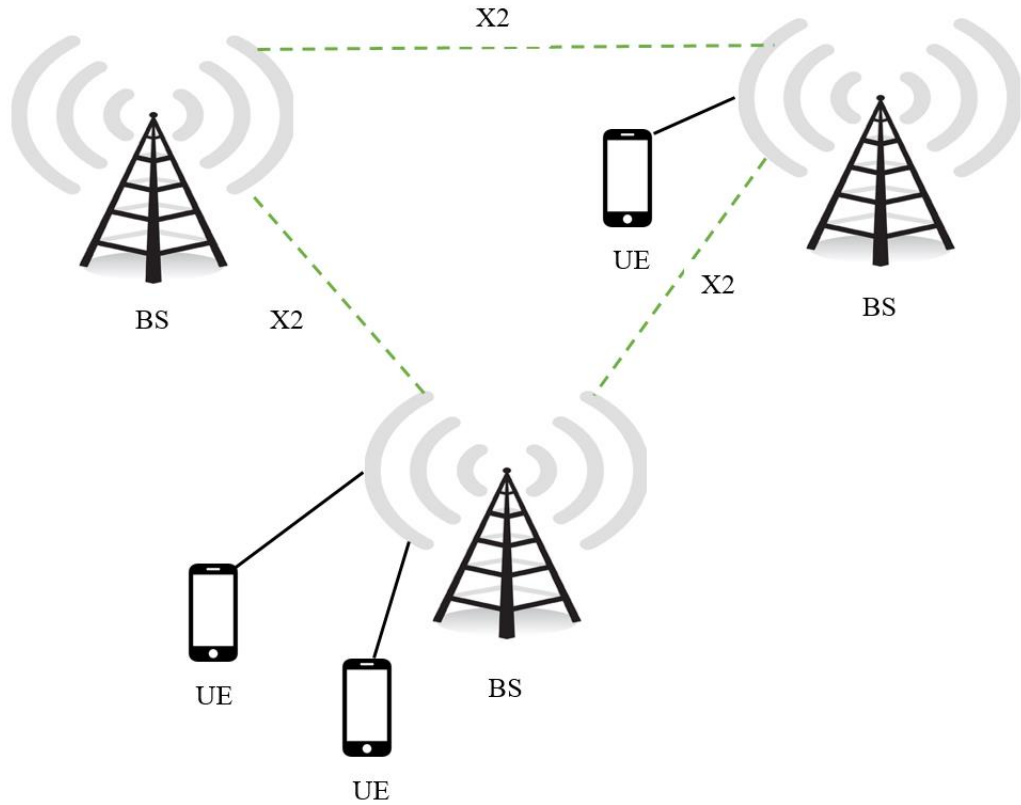


Figure 2.3: The traditional cell-centric architecture.

2.6.2 C-RAN Architecture

C-RAN is a centralised wireless architecture that attempts to reduce the burden on base stations by moving the baseband units (BBUs) located at a number of base stations into a centralised BBU pool. C-RAN was initially introduced in [66] while the work in [67] explained the architecture in detail. The main elements of this architecture are: remote radio heads (RRHs), BBU pool, and front-haul that connects RRHs to their associated BBU. Besides performing radio functionalities, RRHs are responsible to deliver signal coverage for users. A BBU pool consists of a number of BBUs that act as virtual base stations which facilitate the implementation of eICIC and CoMP resulting in increased spectral efficiency and throughput [7]. Figure 2.4 depicts the architecture of C-RAN.

C-RAN has attracted the attention of the wireless industry such as Huawei, ZTE, and Orange [7] and academia [68-71] due to the advantages it can provide over the traditional cell-centric architecture. Besides cost and energy savings and increased throughput, C-RAN can efficiently support the implementation of CoMP which is

crucial particularly for heterogeneous networks [7, 72, 73]. Nevertheless, C-RAN can suffer from significant delay particularly when providing local services since processing is performed at remote locations [74].

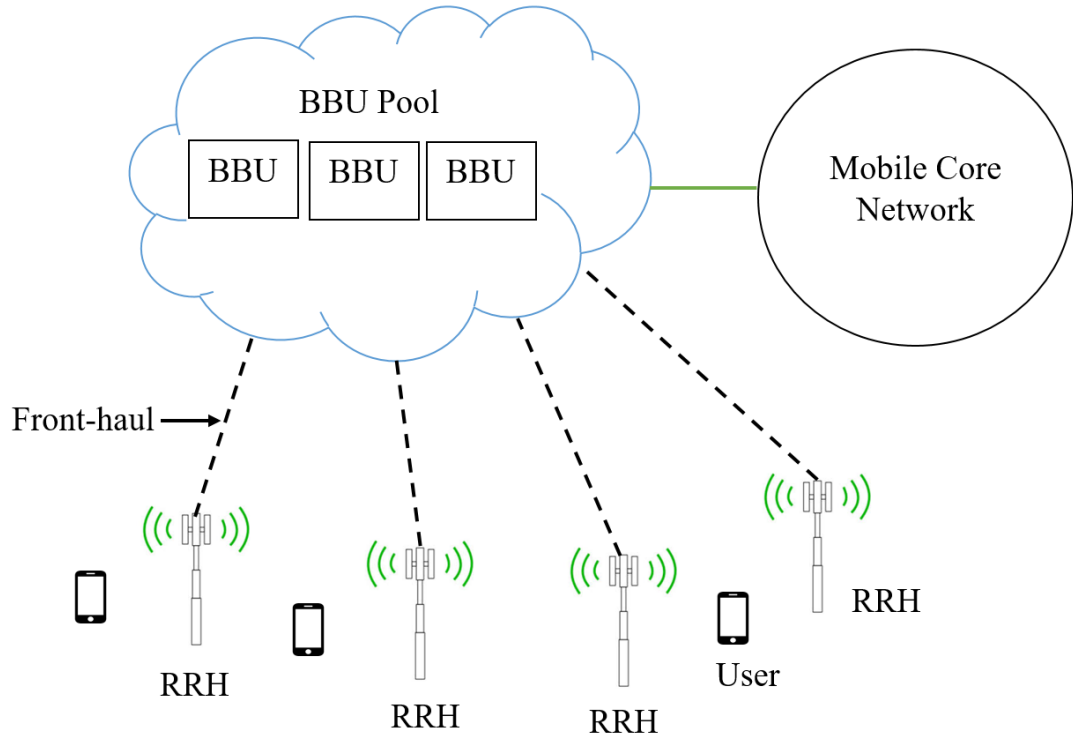


Figure 2.4: C-RAN architecture [75].

2.6.3 Cell-free Architecture

A cell-free architecture, widely known as cell-free massive MIMO, is a recent wireless technology that was initially proposed in [76]. The term cell-free indicates that cell boundaries are removed and a user can be jointly served by all access points in the network [77]. A cell-less network is another architecture that eliminates cell boundaries; however, a user in this wireless architecture is served only by a subset of base stations selected in a user-centric manner. As shown in Figure 2.5, a cell-free network consists of a number of access points connected by front haul connections to CPUs. The initial procedure for a UE to access a cell-free network might follow the same steps as in long-term evolution (LTE) [26] or 5G new radio (5G-NR) [78] which are purely cellular. During the inactive mode, a UE performs cell search in order to find the best cell to be attached to. At this stage, the cell-free architecture follows the same steps of a cellular network. The network becomes completely cell-free during the data transmission phase, i.e., active mode.

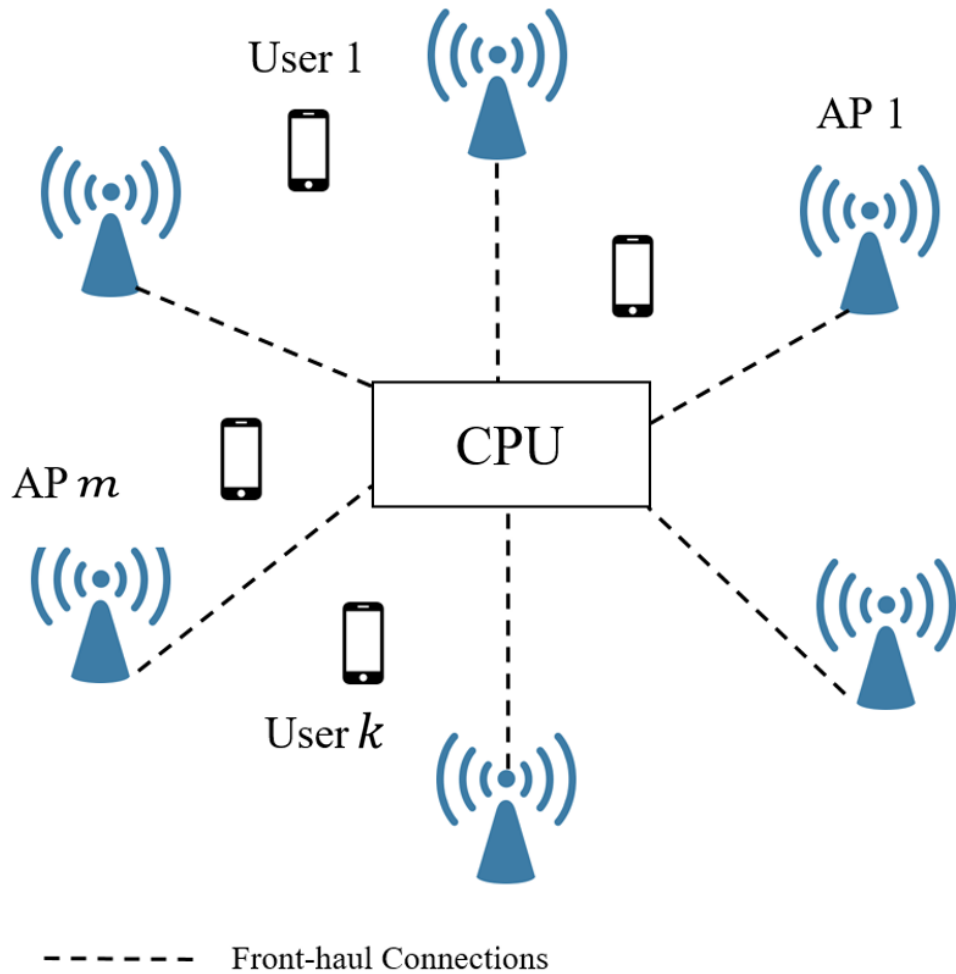


Figure 2.5: Cell-free architecture.

In a cell-free architecture, L access points jointly cooperate to serve a smaller number of users K where $L \gg K$. The work in [76] compared the performance of a cell-free architecture with a small-cell cellular network. According to the obtained results, a cell-free network can achieve ten-fold enhancement in terms of per-user downlink throughput. This significant throughput improvement is due to the macro-diversity and the favourable propagation. Despite the ten-fold improvement, the authors did not consider inter-cluster interference which is a major concern in cell-free networks. Taking inter-cluster interference into account would limit the performance of cell-free architectures since users at a cluster edge would receive severe interference from base stations located in neighbouring clusters. As described in [79], the authors in [76] assumed a COST-Hata propagation model [80] that is suitable for macro cell

environment where base stations are placed more than 30 m above the ground and users are at least 1 km away from base stations. In [80], the developers of this propagation model stated that this model must not be used for small cells. In addition, no shadowing is assumed when a user is at distance less than 50 m from a base station. For the aforementioned reasons, the propagation model used in [76] is inaccurate in cell-free and small cell environments where base stations can be located less than 30 m above ground and users could experience shadowing if they were closer than 50 m from a base station. Some other work on cell-free design [81-84] has also followed the same propagation model presented in [76]. The work in [79] evaluated the performance of a cell-free architecture using a better propagation model that matches the 3GPP model [61] for urban environments. The results in [79] showed that cell-free architecture can still achieve significant spectral efficiency over the cellular scheme provided that a fully centralised network is implemented. Although a cell-free architecture has shown its superiority over the conventional cellular systems, it is impractical since it assumes that all base stations communicate and transmit data to all users. In practice, a user receives strong signal only from a sub-set of base stations in the network while the strength of the received signals from the rest of base stations is poor. This motivates to design an architecture where only a carefully selected number of base stations that promise to provide significant benefits to a user should be involved to serve this user.

2.6.4 Cell-less Architecture

A cell-less architecture follows the same design as a cell-free network except that a user is served only by a sub-set of base stations in the network. The selection of base stations that serve a certain user is based on user-centric approach where each user has an individual set of cooperating base stations. Figure 2.6 provides an example of a cell-less architecture.

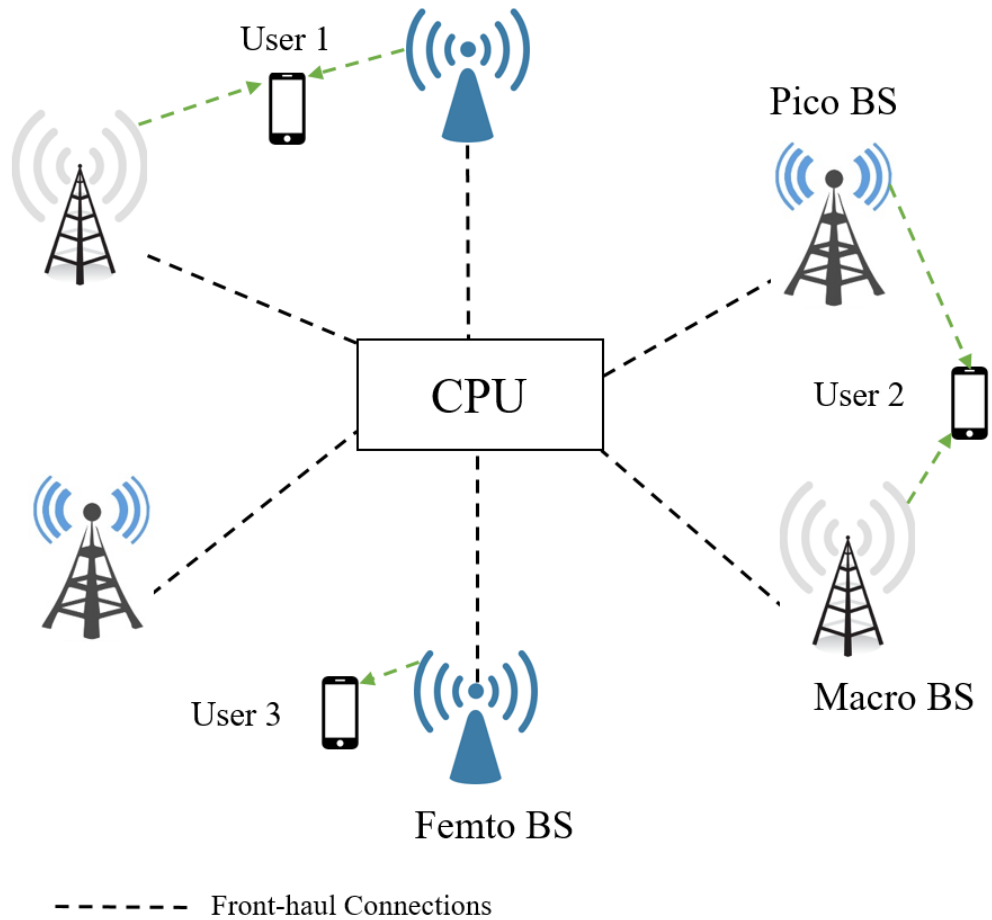


Figure 2.6: Cell-less architecture.

2.7 Spatial Modelling of Base Stations

The spatial distribution of base stations has a direct influence on the system performance of wireless networks since radio power is distance dependent. In other words, the accuracy of results is highly dependent on the spatial models. The topology of 5G networks is expected to be sophisticated due to the dense deployments of small cells. Thus, it is essential to consider more realistic spatial models that can represent the actual deployments of base stations. The most two common spatial models for wireless networks are presented in the following.

2.7.1 Grid Models

Base stations in grid spatial models are located in a 2D space. Homogenous networks have been modelled based on the grid model because cell planning is

performed in order to find optimal locations of macro base stations. The wireless research community in both academia and industry have been using grid models to distribute macro base stations when evaluating the performance of wireless systems [85]. The most common grid model that has been used in the wireless community to model macro base stations is the hexagonal lattice.

Considering a 2D space, the hexagonal lattice $E \subset \mathbb{R}^2$ can be mathematically described as follows:

$$E = \left\{ v \left(\frac{1}{2}s + o, \frac{\sqrt{3}}{2}s + \sqrt{3}t \right) : s, o, t \in \mathbb{Z} \right\} \quad (2.4)$$

where v is the inter-site distance that determines the density of base stations. Figure 2.7 shows an example of a hexagonal lattice where base stations are hexagonally distributed in the area with an inter-site distance of 500 m. This inter-site distance results in a base station density of $10/\text{km}^2$.

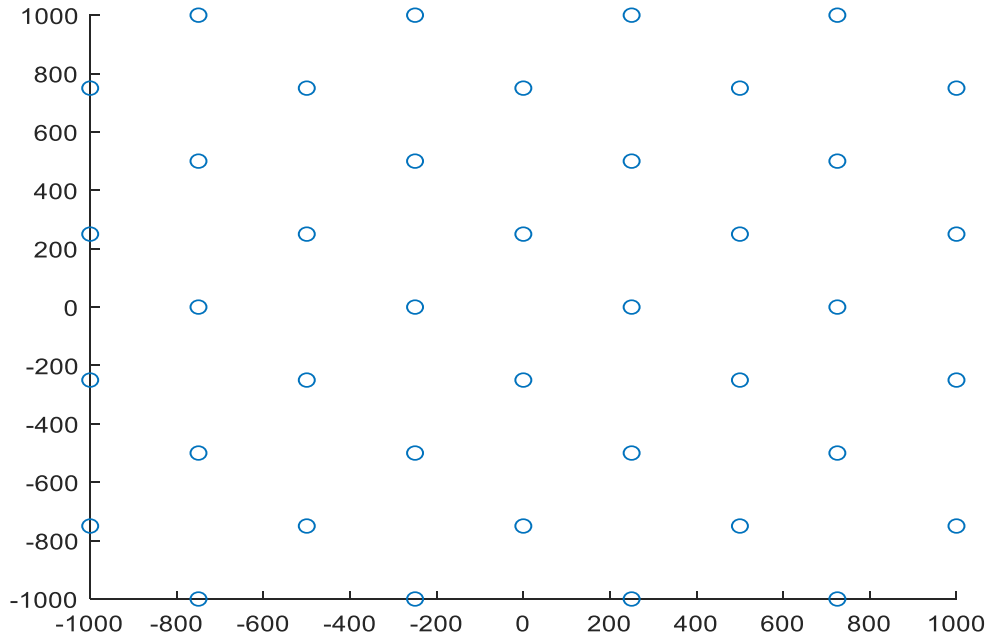


Figure 2.7: A realisation of a hexagonal model with $v = 5$.

2.7.2 Stochastic Models

Cell planning to deploy small cell base stations is less likely to be performed due to the dense number of small cells and the permission to allow users to deploy some small

cells [86]. Thus, random deployment of small cell base stations causes spatial modelling of wireless networks to be more complicated and it restricts the usage of grid model. As grid models are not suitable to model random networks, a stochastic model is needed in order to better capture the randomness of small cell networks.

Stochastic geometry, a new spatial modelling method, has been recently used to model the randomness of small cell networks. Stochastic geometry is a mathematical tool that does not only capture the randomness of small cell locations but it can also provide tractable and precise performance bounds [87-89]. In stochastic geometry theoretical analysis, performance metrics are derived based on expectations of numerous realisations [88]. In simulation-based environments, stochastic spatial models can better represent the deployment of small cell base stations compared with grid models as they can capture the randomness.

The geographical distribution of small cell base stations is generally represented by point processes. In wireless networks, a point process $\Phi = \{x_i, i \in \mathbb{N}\}$ can be defined as a random collection of base stations that reside in the Euclidean space \mathbb{R}^2 [90]. A point process Φ is usually interpreted in terms of a random counting measure that counts the number of points that falls in any set $B \subset \mathbb{R}^2$. It is defined mathematically as follows [90]:

$$\psi(B) = \sum_{x_i \in \Phi} \mathbb{1}(x_i \in B) \quad (2.5)$$

Several kinds of point processes can be formed by applying clustering, thinning, and superposition to the fundamental point process. This chapter presents only two of the most common point processes, i.e., PPP and Hard core PPP, which have been extensively used in the area of wireless communications as well as in this thesis for modelling the locations of base stations.

Poisson Point Process

A point process Φ is classified a Poisson point process Φ_p if and only if:

- 1) The number of points $\psi(B)$ that reside in any bounded set B is a Poisson random variable.

- 2) The number of points $\psi(B_1), \psi(B_2), \dots, \psi(B_z)$, are independent for any z disjoint sets B_1, B_2, \dots, B_z [91].

Considering a PPP in an Euclidean space \mathbb{R}^2 with an intensity of λ_p whose unit is points/area, the probability that there are k points that falls in set B is written as [90]:

$$\mathbf{P}(\psi(B) = k) = \exp(-\lambda\pi r^2) \frac{(\lambda\pi r^2)^k}{k!} \quad (2.6)$$

PPP has been extensively utilised in the wireless field due to its tractability which helps to better understand the system performance; however, its weakness is that there is a probability that two points can be located close to each other or one on the top of the other which is unrealistic in modelling the locations of base stations. Figure 2.8 provides an example of a PPP with an intensity $\lambda_p = 0.01$. As can be seen from Figure 2.8, there are some points that are extremely close to each other.

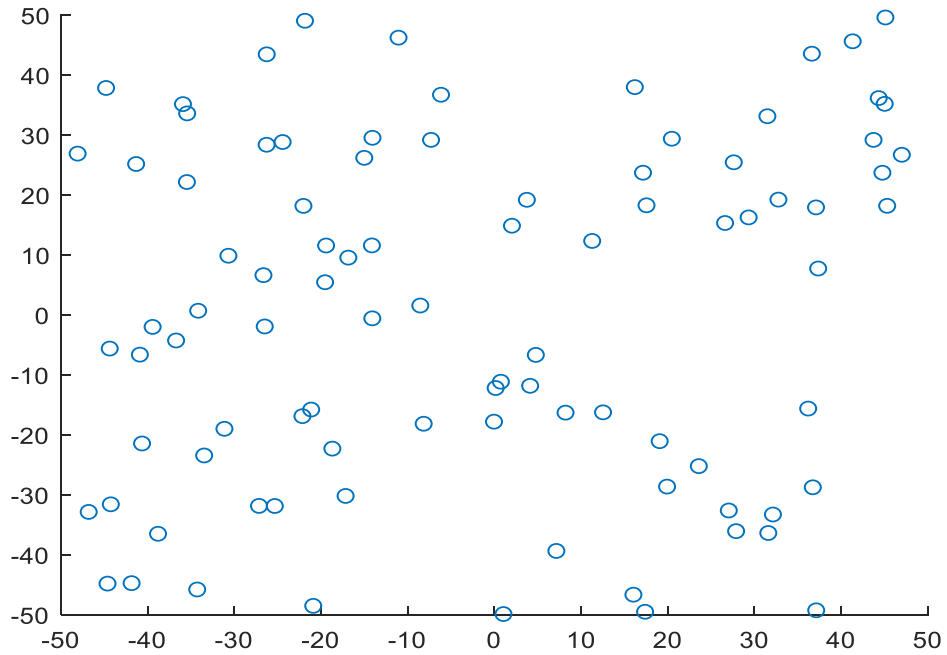


Figure 2.8: A realisation of PPP with $\lambda_p = 0.01$.

Hard Core Poisson Point Process

A Hard-core Poisson point process is a repulsive point process where the distance between any point and its closest point must be larger than a predefined distance known as a hard-core distance δ . This type of point process is usually initiated by a parent PPP then a thinning process is applied where unqualified points that violate the hard-core requirement are deleted [91]. One of the most popular hard-core point processes in the wireless community is the Matern Hard-core Point Process (MHPP) which is used in this thesis.

MHPP has two main different types: type 1 and type 2. In both types, a dependent thinning process is applied after forming a parent PPP that has an intensity of λ_p . The thinning process of type 1 MHPP removes any pair of points if the distance between them is smaller than a hard-core distance δ . During the type 2 MHPP thinning process, each primary point is assigned an independent random mark that has a uniform distribution in the range (0,1). Considering a repulsion distance of δ , a primary point is removed if there exist another primary point that has a smaller mark.

The retaining probability of a primary point is defined as follows [91, 92]:

$$\mathbf{P}(x_i \in \Phi_m \text{ } x x x_i \in \Phi_p) = \frac{1 - \exp(-\lambda_p \pi \delta^2)}{\lambda_p \pi \delta^2} \quad (2.7)$$

The final result presented by equation (2.7) are shown in [91, 92] while the work in [86] provides the derivation in detail.

In this thesis, a type 2 MHPP is used to model the locations of small cell base stations due to its capability of capturing randomness, popularity, and it is repulsion feature that can better represent realistic deployment of small cell base stations. Figure 2.9 shows a realisation of type 2 MHPP with an intensity of $\lambda_m = 0.01$ and a repulsion distance $\delta = 5$. As Figure 2.9 shows, no two points coexist with a distance less than 5 m. Figure 2.10 shows another type 2 MHPP realisation with an intensity of $\lambda_m = 0.006$ and a repulsion distance $\delta = 7$.

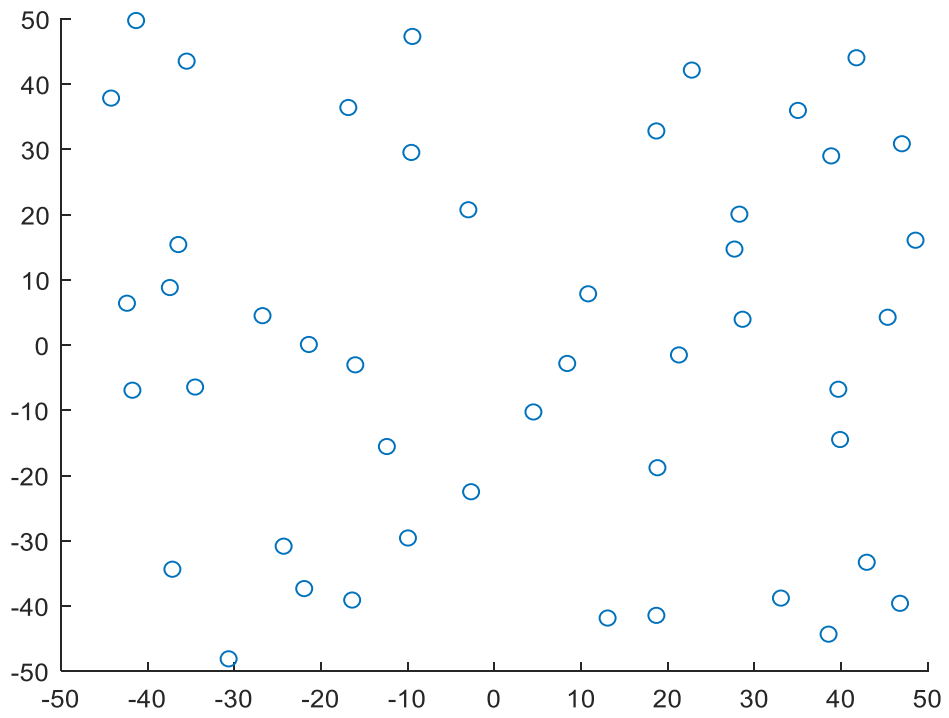


Figure 2.9: A realisation of type 2 MHPP with $\lambda_p = 0.01$ and $\delta = 5$.

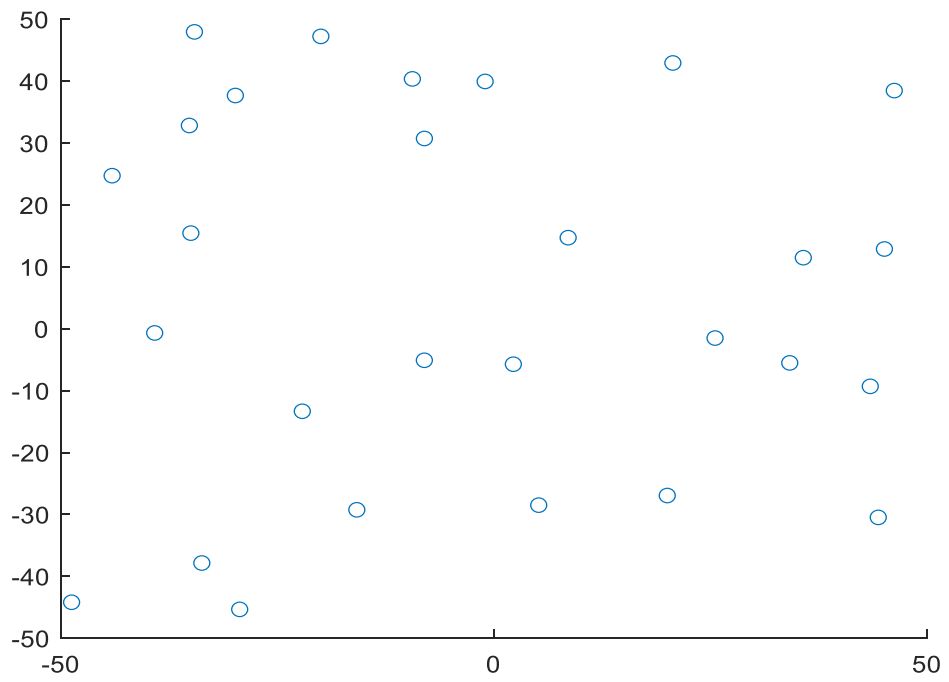


Figure 2.10: A realisation of type 2 MHPP with $\lambda_p = 0.006$ and $\delta = 7$.

2.8 Conclusion

A review on background information and established research work related to this thesis has been presented in this chapter. The state-of-the-art has focused on heterogeneous networks as it is a straightforward and an effective approach to improve coverage and capacity of future wireless networks. The coverage can be enhanced by placing small cell base stations at dead zones while the capacity is improved by densifying small cell base stations that reuse the spectrum. The existence of macro cells particularly in rural areas is still crucial in the next generations of wireless networks as they can cover large areas. Moreover, macro cells do not suffer from high handover frequency enabling them to support high mobility users. Although the deployment of heterogeneous networks is a promising approach towards the success of future wireless systems, its major drawback is inter-cell interference that needs to be tackled.

Inter-cell interference mitigation techniques such as JT-CoMP, eICIC and have been investigated. The main focus has been on the user-centric JT-CoMP approach due to its superiority over static JT-CoMP clustering and eICIC. JT-CoMP faces two main constraints to maximising system capacity, which are operating with an effective user-centric clustering algorithm that can balance between SINR gain and the wastage of radio resources and the lack of an efficient multi-cell resource allocation scheme. Therefore, it is essential to develop an efficient algorithm that can identify which UEs will benefit from operating in a JT-CoMP mode and how to efficiently allocate radio resources from multiple base stations. User-centric clustering is a main element of cell-less architectures and it will be used in later work.

Recent and popular radio access network architectures have been presented. The traditional cell-centric architecture relies on cells and each user is served by only one base station. The main limitation of this architecture is its poor performance in reducing inter-cell interference. C-RAN that consists of RRHs connected to a pool of BBUs has been proposed to improve spectral efficiency, throughput and resource utilisation. However, due to remote processing, significant delay can occur which is undesirable particularly when providing local services. Recently, the cell-free architecture has been introduced and it has shown great performance in terms of improving per user throughput. Nevertheless, it is based on the assumption that a UE is served by all access points in the network which is not practical and unnecessary. Cell-less design where a

user is served only by base stations that can provide sufficient power is not well studied yet.

Spatial modelling of macro and small cell base stations have been presented. The hexagonal model as the most famous grid model has been introduced as it can arguably better represent the deployment of macro base stations. However, it is not suitable for small cell base stations since it cannot capture their randomness. The randomness in the deployment of small cell base stations has increased the need for stochastic models. HPPP has been extensively used due to its tractability; however, it is unrealistic in wireless systems as two points can be located extremely close to each other. By applying thinning, the fundamental PPP can be changed into another PPP form named MHPP which has a repulsion feature that separates any two points by a minimum distance. Stochastic geometry is utilised in later chapters to model the locations of small cell base stations.

CHAPTER 3

User-centric JT-CoMP Clustering

Contents

3.1	Introduction	43
3.2	System Model	45
3.2.1	System Layout	45
3.2.2	Outage Probability Metric	47
3.3	User-centric Clustering Approaches	47
3.3.1	Power Level Difference	48
3.3.2	RSS Threshold	49
3.3.3	SINR Threshold	50
3.3.4	Proposed User-centric Algorithm	51
3.4	Definition of Regions and Cooperation Set	54
3.5	Performance Evaluation	56
3.5.1	Impact of Limiting the Maximum UC Cluster Size	66
3.5.2	Impact of BS Densification.....	70
3.5.3	Impact of Spatial Modelling of SC BSs	73
3.6	Conclusion	74

3.1 Introduction

User-centric JT-CoMP clustering is one of the main elements that drives the current wireless cell-centric architecture to move into a cell-less architecture. In user-centric JT-CoMP clustering, BSs are allowed to serve users even if these users are located out of their cell coverage. Allowing all UEs to operate using the JT-CoMP mode can significantly improve the SINR levels. However, this approach reduces the availability of radio resources as all cooperating BSs must reserve identical PRBs for the user they

serve and they cannot reuse them. User-centric clustering is a promising approach that can address this problem where each UE selects its own set of cooperative BSs that promise to provide significant SINR gain. In this chapter, a cluster is defined as the set of cooperative BSs that jointly transmit the same data to an intended user. A cluster size of one indicates no cooperation (non-CoMP mode) where the user is served by the strongest BS. A cluster size of c , where c is greater than one, indicates that there are c BSs that cooperate to serve a cell-edge user (JT-CoMP mode). The most common user-centric clustering approach that has been used in the literature is the PLD approach where a BS is allowed to cooperate only if its average received power is comparable with the strongest received power. Another user-centric clustering approach is the RSS approach where a UE can add a BS to its cooperative set if the average power received from this BS is stronger than a certain threshold. SINR clustering is a recent user-centric clustering approach where a BS can join the cooperation set if the SINR of a UE is below a specific threshold. Since these three approaches are heuristic, it is important to find effective thresholds that can achieve the best performance. Although the existing UC approaches attempt to restrict any UE with marginal SINR gain to operate in CoMP mode, there is no proof that these approaches can provide an effective balance between the SINR gain and the loss of bandwidth. To provide this balance, a new UC clustering approach is proposed. In the proposed UC clustering approach, a UE is allowed to operate in the CoMP mode only if its rate with CoMP is higher than c times its rate without CoMP, where c is its cluster size.

The organisation of this chapter is as follows. The system model is described in Section 3.2. Section 3.3 presents the algorithms of the existing UC clustering approaches and the proposed approach. In Section 3.4, set theory is utilised to provide mathematical definitions of the CoMP and non-CoMP regions for all UC clustering approaches. Section 3.5 compares the effectiveness of the proposed algorithm against the existing UC clustering approaches in terms of outage probability and the balance between the SINR gain and the loss of bandwidth. The impact of limiting the maximum cluster size and BS densification on the performance of JT-CoMP is investigated. In addition, Section 3.5 compares the performance of JT-CoMP when SC BSs are spatially distributed according to the pure PPP and repulsive PPP models. In pure PPP, the number of points that lie in any bounded set $\mathcal{B} \subset \mathbb{R}^2$ is a Poisson random variable and the number of points residing in any other disjoint set is independent. In addition, pure

PPP does not restrict any two points that belong to the same set from being close to each other. A repulsive PPP is a hard core point process where any two points are separated by a minimum repulsion distance δ . Finally, Section 3.6 concludes this chapter.

3.2 System Model

A three-tier downlink cellular network that consists of M macro BSs, P pico BSs, F femto BSs, and K users is considered. Each BS and each user are considered to be equipped with a single antenna. Two different cases are studied: non-CoMP and JT-CoMP. In the non-CoMP case, all users are served by one BS only. In the JT-CoMP case, user-centric clustering is employed where each UE decides whether it should operate in non-CoMP or CoMP mode. In the non-CoMP mode, a UE is served by the BS that provides the strongest received power. If a UE decides to operate in the CoMP mode, then it is served by the c_{max} strongest BSs where c_{max} is the maximum UC cluster size. A UE can be served by BSs that belong to different tiers. OFDMA as a multi access radio technology is considered. It is assumed that macro and SC BSs reuse the same radio resources, i.e., a reuse factor of one. Non-coherent joint transmission is considered in this chapter: cooperating BSs jointly send the same data to a particular user without ensuring coherent combination at the user [25]. At the user side, the non-coherent signals are added resulting in received power gain. Non-coherent JT-CoMP is used because it eliminates the process of CSI exchange and its associated overheads. Implementing JT-CoMP without knowledge of CSI restricts multi-user MIMO communications as well as distributed precoding; however, JT-CoMP can benefit from diversity gain [65, 93, 94]. The system model is shown in Figure 3.1.

3.2.1 System Layout

The locations of macro BSs in some studies [95, 96] have been modelled as a PPP network; however, in practice, operators deploy macro BSs after careful planning [97, 98] with some restrictions due to geographical limitations [99]. In [97-99], it is argued that it is more practical to assume hexagonal deployment of macro BSs. This argument is also consistent with what 3GPP recommends [61]. Thus, macro BSs are spatially distributed based on a hexagonal deployment.

To better represent the randomness that exists in the actual deployment of SC BSs in real networks, pico and femto BSs are distributed according to a PPP. Two spatial PPP models are studied: pure PPP and repulsive PPP. Pure PPP is the case where BSs might be located close to each other or even one on the top of the other. In repulsive PPP, any two BSs are separated by a minimum separation distance δ . In pure PPP, pico and femto BSs are distributed according to two independent pure PPPs Φ_p and Φ_f with densities of λ_p and λ_f , respectively. In the case of the repulsive PPP, the parent PPPs Φ_p and Φ_f are modified by implementing the repulsive dependent thinning which results in type II MHPP Φ_{pm} and Φ_{fm} with a repulsion distance δ_p and δ_f , respectively [87]. Users are also spatially distributed according to another PPP Φ_k with a density of λ_k .

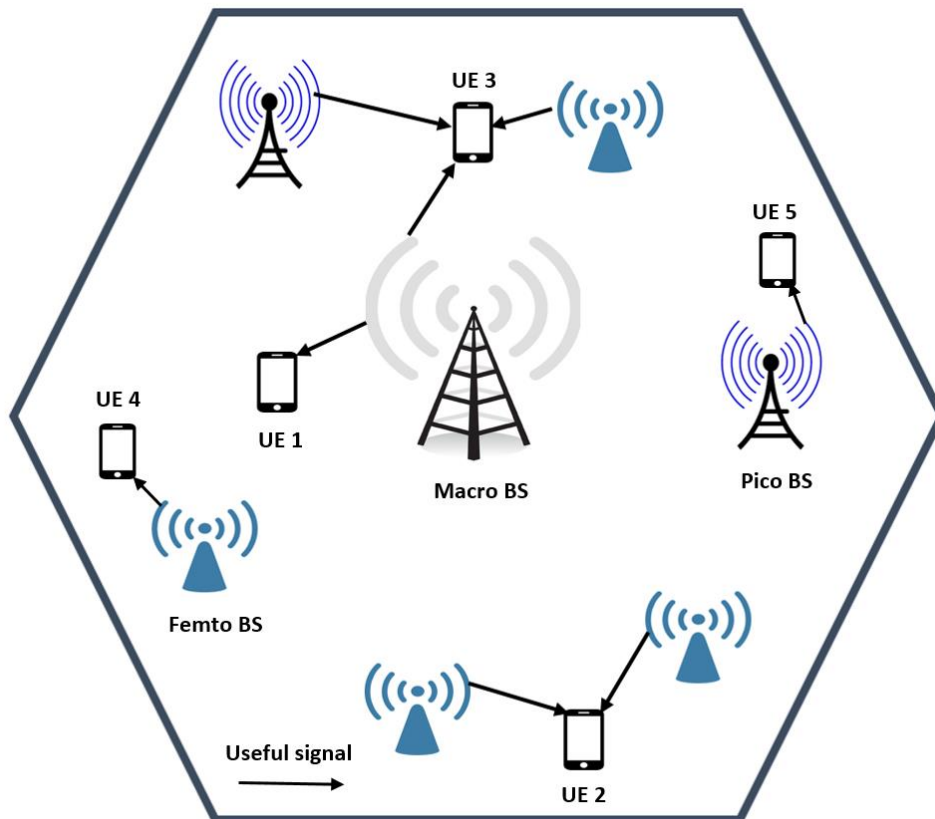


Figure 3.1: System model

3.2.2 Outage Probability Metric

This chapter focuses on analysing the outage probability. The outage probability is defined as the probability that the SINR of a UE is below a specific threshold θ . The SINR that is received by UE_k is calculated as follows [40]:

$$SINR_k = \frac{P_{Tx} \sum_{j \in C_k} |g_{kj}|^2}{P_{Tx} \sum_{i \in \mathcal{J}/C_k} |g_{ki}|^2 + \sigma^2} \quad (3.1)$$

where P_{Tx} is the transmit power of a BS, C_k is the set of cooperative BSs of UE k , g_{ki} is the channel gain between BS i and user k which consists of path loss and shadowing and σ^2 is the noise power. Since clustering decisions are based on long term received power levels, fast fading averages out [40].

The SINR of a UE in (3.1) clearly depends on its cluster size. If a UE decides to operate as a CoMP UE with a cluster size larger than 1, then the dominant interference signal(s) will be eliminated and converted into useful signal(s) resulting in a significant SINR gain. The outage probability can be mathematically expressed as follows:

$$P(SINR < \theta) \quad (3.2)$$

3.3 User-centric Clustering Approaches

In user-centric clustering, each user forms its own set of cooperative BSs independently based on a certain rule in order to eliminate the most harmful interfering signals and convert them into useful signals. Users in user-centric clustering can operate in a non-CoMP or a CoMP mode. In a non-CoMP mode, a user is associated with the strongest BS only, i.e., a cluster size of one. Generally, users closest to a base station operate in a non-CoMP mode due to the high power they receive from their strongest BS. A user is associated with multiple BSs in the case where it chooses to operate in JT-CoMP mode. Users at the cell-edge would operate in JT-CoMP mode in order to reduce the high interference that comes from their neighbouring BSs. In the literature, several user-centric approaches have been used to identify the set of BSs that can cooperate to serve a typical user. For any user-centric clustering approach, each UE measures the average power it receives from neighbouring BSs as follows:

$$P_{ki}^{rx} = P_{ki}^{tx} |g_{ki}|^2, i \in \mathcal{J} \quad (3.3)$$

where P_{ki}^{rx} is the average power that is received by UE_k from $BS i$, P_{ki}^{tx} is the power transmitted by $BS i$ to UE_k , g_{ki} is the channel gain between UE_k and $BS i$ which consists of path loss and shadowing.

After the measurement of the average received power, the set of average received powers of a UE are sorted in a descending order as follows:

$$P_{k1}^{rx} > P_{k2}^{rx} > \dots P_{kl}^{rx} \quad (3.4)$$

where P_{k1}^{rx} is the strongest power received by UE_k , P_{k2}^{rx} is the second strongest power received by UE_k and so on.

The calculations of (3.3) and (3.4) are the first two steps to identify the set of cooperative BSs of a UE. The following presents common and recent existing user-centric clustering approaches in details. In addition, it proposes a new user-centric clustering algorithm.

3.3.1 Power Level Difference

PLD measures the strength of the average received power by a user k from the strongest BS compared to the average received power by the same user from the i^{th} BS. For example, a PLD value of 10 dB between the strongest BS and the second strongest BS indicates that the average received power from the strongest BS is 10 times stronger than the average received power from the second strongest BS. The benefit of this measurement is that it can determine the BSs giving rise to the strongest interfering signals and convert them into useful signals. In the PLD user-centric clustering scheme, a UE forms its own cluster of BSs based on the comparison of the average powers it receives from neighbouring BSs. If the received power from the second strongest, third strongest, ..., i^{th} strongest BSs are comparable with the strongest BS, then the user selects the i strongest BSs as its own cluster. This comparison is referred as the PLD and it is mathematically written as follows:

$$\frac{P_{k1}^{rx}}{P_{ki}^{rx}} < \beta, i \in \mathcal{J} \quad (3.5)$$

where β is the power level difference threshold that identifies whether a UE should operate in CoMP or non-CoMP mode. The power level β is a threshold choice between

CoMP and non-CoMP mode because it can determine the relative strength between the strongest and second strongest received power. Algorithm 3.1 shows the steps that each UE in the PLD approach needs to perform in order to find its cluster size. An effective β prevents users with marginal SINR gain from operating in CoMP mode which saves the available bandwidth from being wasted. This restriction enables efficient use of the bandwidth and as a result improves the capacity of the system. It is clear that a large PLD value attracts more UEs to operate in CoMP mode and vice versa. The selection of an effective PLD value is extremely important since a small PLD value restricts some cell-edge users to be served only by the strongest BS although they still receive high interference from the second strongest BS. On the contrary, a large PLD value admits UEs that may not significantly improve their SINR if they operated in CoMP mode since the power they receive from the second strongest BS is negligible compared with the strongest BS. Moreover, allowing users with marginal SINR improvement to operate in CoMP mode would waste the available resources and as a consequence non-CoMP users would be left with fewer radio resources. This illustrates that it is crucial to choose an effective PLD value that can balance between SINR gain and loss of radio resources.

Algorithm 3.1 PLD algorithm

```

1: for all  $k \in \mathcal{K}$  do
2: Measure the average received powers from neighbouring BSs based on (3.3)
3: Sort the average received powers based on (3.4)
4: for  $S = 1$  to  $C_{max}$ 
5:   if  $\frac{P_{k1}^{rx}}{P_{k(S+1)}^{rx}} < \beta$  is true then
6:      $|C_k| = S + 1$ 
7:   else
8:     if  $S = 1$  then
9:        $|C_k| = 1$ 
10:      Break
11:     else
12:        $|C_k| = S$ 
13:     end if
14:   end if
15: end for
16:end for

```

3.3.2 RSS Threshold

A user-centric JT-CoMP clustering approach that allows a number of BSs to jointly send multiple copies of the same data to a user is proposed in [100]. In the proposed approach, each user forms its own cooperative cluster based on long-term measurements

of RSS. The x BSs other than the strongest BS that provide sufficiently strong RSS are involved to cooperate. In other words, BS i (with the exception of the strongest BS) is admitted to cooperate only if it provides an average RSS above a certain threshold α . This requirement can be mathematically written as follows:

$$P_{ki/i=1}^{rx} > \alpha \quad (3.6)$$

Algorithm 3.2 provides the steps that show how a UE determines its cluster size when the maximum cluster size is c_{max} .

Algorithm 3.2 RSS algorithm

```

1: for all  $k \in \mathcal{K}$  do
2: Measure the average received powers from neighbouring BSs based on (3.3)
3: Sort the average received powers based on (3.4)
4: for  $S = 1$  to  $C_{max}$ 
5:   if  $P_{k(S+1)}^{rx} > \alpha$  is true then
6:      $|C_k| = S + 1$ 
7:   else
8:     if  $S = 1$  then
9:        $|C_k| = 1$ 
10:    Break
11:   else
12:      $|C_k| = S$ 
13:   end if
14: end if
15: end for
16: end for

```

3.3.3 SINR Threshold

Recently, a new user-centric clustering approach that is based on SINR threshold is proposed [50]. In this scheme, the SINR of a UE without CoMP is calculated first. If the resultant SINR is below a specific threshold, the second strongest BS is added to the UE's cluster to cooperate, otherwise, it is served by the strongest BS only. If a UE decides to operate with CoMP, the SINR with a cluster size of 2 ($SINR^2$) is then checked if it is also below the same threshold. If it is still below the threshold, the third strongest BS is added to the UE's cooperative cluster. The work in [50] limited the maximum cluster size to 3. To include a cluster size more than 3, the same procedure is followed. Mathematically, UE k keeps increasing its cluster size until the following is met:

$$SINR_k > \gamma \quad (3.7)$$

Based on the SINR threshold approach, the steps in Algorithm 3.3 show how a UE can decide the number of BSs that need to cooperate to achieve an SINR higher than γ provided that the number of cooperative BSs does not exceed the maximum cluster size C_{max} .

Algorithm 3.3 SINR algorithm

```

1: for all  $k \in \mathcal{K}$  do
2: Measure the average received powers from neighbouring BSs based on (3.3)
3: Sort the average received powers based on (3.4)
4: Calculate  $SINR_k^1$  based on (3.1)
5:   if  $SINR_k^1 > \gamma$  then
6:      $|C_k| = 1$ 
7:   else
8:     for  $S = 2$  to  $C_{max}$ 
9:       Calculate  $SINR_k^S$  based on (3.1)
10:      if  $SINR_k^S > \gamma$  then
11:         $|C_k| = S$ 
12:      Break
13:    end if
14:  end for
15: end if
16:end for

```

3.3.4 Proposed User-centric Algorithm

A new user-centric clustering approach for JT-CoMP is proposed with the aim of balancing between SINR gain and loss of radio resources. In the proposed user-centric algorithm, a UE forms its own cluster by comparing its SINR with and without CoMP. To guarantee an effective balance between SINR gain and loss of radio resources, the reduction in radio resources caused by implementing JT-CoMP must be compensated for by the $SINR$ gain. To provide this balance, a new user-centric clustering algorithm that allows a UE to operate in CoMP mode only if its $SINR$ with CoMP can at least compensate the loss of radio resources is proposed. To guarantee an effective balance between SINR gain and loss of radio resources, the rate that a UE achieves when it operates in CoMP mode must be at least equal to c times the rate it achieves with no CoMP. This can be mathematically written as follows:

$$\log_2(1 + SINR_k^c) \geq c \log_2(1 + SINR_k^1) \quad (3.8)$$

where c is the rate gain that can be achieved when a UE operates in the CoMP mode. c also represents the user-centric cluster size as a UE that is served by c cooperative BSs must at least achieve a rate gain of c in order to balance the SINR gain

and loss of bandwidth. The system performance will degrade if a UE is served by c BSs and the resultant rate gain is less than c . The measurement of the rate using the Shannon formula is based on the average rate.

By using (3.8), the minimum $SINR_k^c$ that can achieve c rate gain can be found as follows:

$$2^{\log_2(1+SINR_k^c)} \geq 2^{c \log_2(1+SINR_k^1)} \quad (3.9)$$

$$SINR_k^c \geq (1 + SINR_k^1)^c - 1 \quad (3.10)$$

Figure 3.2 shows the minimum SINR with CoMP values that can satisfy the requirement in (3.10) in order to achieve different rate gains ranging from 2 to 8. Allowing a UE to be served by 8 BSs as in [25, 40, 42, 52] can result in significant SINR gain; however this SINR gain may still not compensate the loss of bandwidth since 8 BSs will have to reserve identical PRB(s) to serve this particular UE. As seen from Figure 3.2, if the SINR with no CoMP of a UE is 0 dB, its SINR with CoMP must be at least 4.8 dB, 11.8 dB, 18 dB, and 24 dB in order to achieve rate gains of 2, 4, 6, and 8 respectively. It is clear that allowing more than 2 BSs to cooperate requires extreme SINR gain in order to achieve a rate gain that can compensate for the loss of the bandwidth of the cooperative BSs. It is also observed that a UE must achieve more than 25 dB when it operates in CoMP mode in order to achieve 2, 4, 6, and 8 rate gains if its SINR with no CoMP is higher than 12 dB, 6 dB, 2 dB, and 0 dB respectively.

The proposed user-centric algorithm, where each UE finds its cluster size, is presented in Algorithm 3.4. Based on the proposed user-centric clustering approach, a UE computes its SINR with and without CoMP. Then, a UE chooses to operate in CoMP mode only if its SINR with CoMP is high enough to compensate the loss of radio resources.

The traditional and the proposed algorithms are user-centric algorithms where a user forms its set of BSs. Since a UE forms its own cluster by measuring the average received power, the cluster size changes according to the measurement of the average received power.

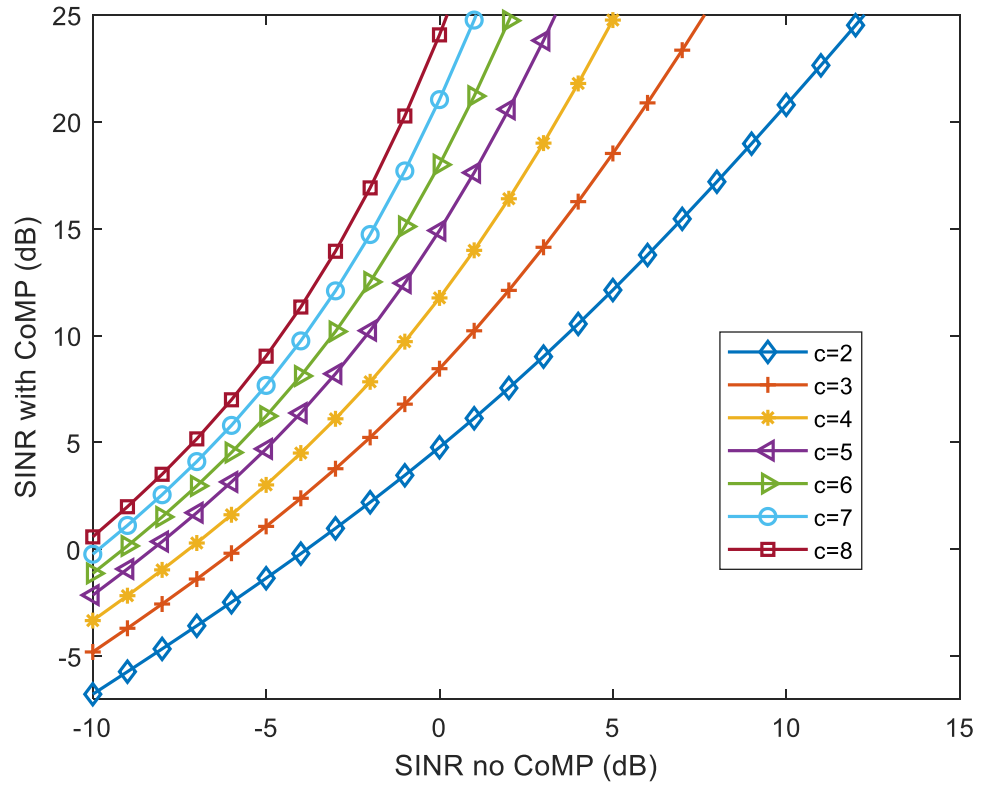


Figure 3.2: Minimum $SINR$ with CoMP to achieve rate gains ranging from 2 to 8.

Algorithm 3.4 Proposed user-centric algorithm

```

1: for all  $k \in \mathcal{K}$  do
2: Measure the average received powers from neighbouring BSs based on (3.3)
3: Sort the average received powers based on (3.4)
4: Calculate  $SINR_k^1$  based on (3.1)
5: for  $S = 1$  to  $C_{max}$ 
6: Calculate  $SINR_k^{S+1}$  based on (3.1)
7:   if (3.10) is true then
8:      $|C_k| = S + 1$ 
9:   else
10:    if  $S = 1$  then
11:       $|C_k| = 1$ 
12:      Break
13:    else
14:       $|C_k| = S$ 
15:    end if
16:  end if
17: end for
18: end for

```

3.4 Definition of Regions and Cooperation Set

In UC JT-CoMP systems, the regions that a UE can belong to can be divided into two categories: a non-CoMP region and a CoMP region. A non-CoMP region denoted as A_1 is the area where there is no cooperation and a user is served by the strongest BS only (a cluster size of one). A CoMP region can be further divided into smaller regions which are identified based on the number of serving BSs. $A_2, A_3, \dots, A_{c_{max}}$ denote two way CoMP region, three way CoMP region until c_{max} way CoMP region, respectively. Figure 3.3 shows an example illustrating non-CoMP regions (A_1), two way CoMP regions (A_2), and a three way CoMP region (A_3). It is crucial to mathematically define these regions as they represent the level of cooperation and the set of UEs located in these regions. Also, it is essential to define the set of BSs that cooperate to serve an intended user. To provide mathematical definitions of regions and the cooperation set of each user, set theory is used.

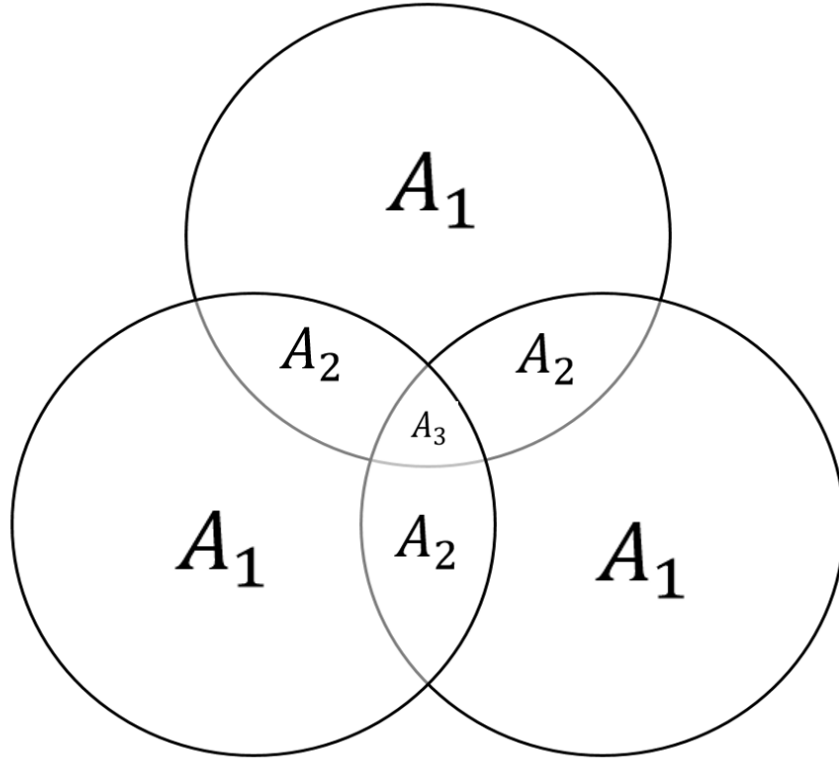


Figure 3.3: An example of non-CoMP and CoMP regions. A_1 denotes non-CoMP regions while A_2 and A_3 denote CoMP regions with cluster sizes of 2 and 3, respectively.

Since the size of each region depends on the UC clustering approach, the mathematical representations of regions for all UC clustering approaches presented in Section 3.3 are provided. PLD, RSS, SINR, and the proposed approach are numbered as approaches number 1, 2, 3, and 4, respectively. The non-CoMP region of Approach q is denoted as A_{1q} where the first subscript indicates the UC cluster size and the second subscript represents the UC clustering approach number. Similarly, CoMP regions with a UC cluster size of 2, 3, and c_{max} for Approach q are denoted as A_{2q} , A_{3q} , and $A_{c_{max}q}$, respectively.

The mathematical definitions of regions for the PLD approach can be defined as follows. First, a non-CoMP region for the PLD approach A_{11} is defined as follows:

$$A_{11} = \left\{ k \in \mathbb{R}^2 \mid \frac{P_{k2}^{rx}}{P_{k1}^{rx}} < \beta \right\} \quad (3.11)$$

CoMP regions with c cooperative BSs for the PLD approach can be written as follows:

$$A_{c1} = \left\{ k \in \mathbb{R}^2 \mid \frac{P_{k1}^{rx}}{P_{kc}^{rx}} < \beta \ \& \ \frac{P_{k1}^{rx}}{P_{k(c+1)}^{rx}} > \beta \right\} \quad (3.12)$$

Similarly, non-CoMP and CoMP regions for the RSS approach can be written as follows, respectively:

$$A_{12} = \left\{ k \in \mathbb{R}^2 \mid P_{k2}^{rx} < \alpha \right\} \quad (3.13)$$

$$A_{c2} = \left\{ k \in \mathbb{R}^2 \mid P_{kc}^{rx} > \alpha \ \& \ P_{k(c+1)}^{rx} < \alpha \right\} \quad (3.14)$$

For the SINR approach, non-CoMP and CoMP regions can be defined as follows:

$$A_{13} = \left\{ k \in \mathbb{R}^2 \mid SINR_k^1 > \gamma \right\} \quad (3.15)$$

$$A_{c3} = \left\{ k \in \mathbb{R}^2 \mid SINR_k^{c-1} < \gamma \ \& \ SINR_k^c > \gamma \right\} \quad (3.16)$$

Non-CoMP and CoMP regions for the proposed approach are defined as follows:

$$A_{14} = \left\{ k \in \mathbb{R}^2 \mid \text{SINR}_k^2 \leq (1 + \text{SINR}_k^1)^2 - 1 \right\} \quad (3.17)$$

$$A_{c4} = \left\{ k \in \mathbb{R}^2 \mid \text{SINR}_k^c > (1 + \text{SINR}_k^1)^c - 1 \ \& \ \text{SINR}_k^{c+1} \leq (1 + \text{SINR}_k^1)^{(c+1)} - 1 \right\} \quad (3.18)$$

where SINR_k^c is the SINR of user k when it operates with a cluster size of c . The cooperation set for any user in the system for UC clustering Approach q can be defined as follows:

$$C_{kq} = \begin{cases} \{x_1\}, k \in A_{1q} \\ \{x_1, x_2\}, k \in A_{2q} \\ \{x_1, x_2, \dots, x_{c_{max}q}\}, k \in A_{c_{max}q} \end{cases} \quad (3.19)$$

The cooperation set of a UE is clearly dependent on the user-centric clustering Approach.

3.5 Performance Evaluation

The performance of the PLD, RSS, SINR and the proposed user-centric JT-CoMP clustering approaches is evaluated based on snapshot simulation using MATLAB. Snapshot simulation is widely used by 3GPP [61] as well as academic researchers [101] to evaluate the performance of wireless networks.

To compare the performance of JT-CoMP against no CoMP, all UEs first operate without CoMP and then CoMP is applied for the same user set. This clearly allows the effect of the implementation of CoMP on UEs to be demonstrated. To obtain accurate statistical data, 100 snapshots are carried out.

Macro BSs are deployed hexagonally in an area 6 km x 6 km with an inter-site distance of 500 m. This inter-site distance is equivalent to a density of 8 macro BSs/km². Pico and femto BSs are randomly distributed according to repulsive PPP spatial modelling over the same area. The minimum separation distances δ_p and δ_f between any two pico BSs and any two femto BSs are set to 20 m and 10 m, respectively. The impact of different minimum separation distances δ_p and δ_f in repulsive PPP networks on the performance of JT-CoMP is studied. A comparison when the $\delta_p = 10$ m and $\delta_f = 5$ m, $\delta_p = 20$ m and $\delta_f = 10$ m, $\delta_p = 30$ m and $\delta_f =$

15 m and $\delta_p = 40$ m and $\delta_f = 20$ m is carried out. Also, the performance of UC JT-CoMP clustering in a repulsive PPP network with the four aforementioned different settings of δ_p and δ_f is compared with pure PPP. The density of pico BSs λ_{pm} and femto BSs λ_{fm} is considered to be 16 BSs/km², and 32 BSs/km², respectively. To investigate the impact of BS densification in UC JT-CoMP, sparse ($\lambda_{pm} = 16$ BSs/km² and $\lambda_{fm} = 32$ BSs/km²), medium ($\lambda_{pm} = 24$ BSs/km² and $\lambda_{fm} = 48$ BSs/km²), and dense ($\lambda_{pm} = 32$ BSs/km² and $\lambda_{fm} = 64$ BSs/km²) deployment of SCs are considered. UEs with a density of λ_k are randomly deployed according to an independent PPP over the same area. In all cases, the density of UEs λ_f is equal to 10 times the density summation of macro, pico, and femto BSs. This is set to ensure that each BS has at least one UE associated with it [102]. In the case of 8 macro BSs/km², 16 pico BSs/km² and 32 BSs/km², the density of UEs becomes 560 UE/km². UEs are equipped with a single antenna. For JT-CoMP, non-coherent joint transmission is assumed. The maximum UC cluster size is limited to 8. The impact of limiting the maximum UC cluster size is investigated where the maximum UC cluster size is limited to 2, 4, 6, and 8.

The simulation parameters are based on 3GPP recommendations to evaluate the performance of wireless networks [61]. The path loss models of the macro, pico and femto BSs are denoted by PL_m, PL_p , and PL_f are presented in (3.20), (3.21), and (3.22), respectively [61]:

$$PL_m = 128.1 + 37.6 \log_{10}(R) \quad (3.20)$$

$$PL_p = 140.7 + 36.7 \log_{10}(R) \quad (3.21)$$

$$PL_f = 127 + 30 \log_{10}(R) \quad (3.22)$$

where R is the distance in *km* between a BS and a UE. The shadowing standard deviations for the macro, pico, and femto BSs are 8 dB, 10 dB, and 10 dB, respectively. Each BS has a bandwidth of 20 MHz which consists of 100 PRBs. Assuming a noise figure of 5 dB, a 20 MHz bandwidth and a temperature of 300 K, the value of the noise floor σ^2 is -96 dBm.

To evaluate the overall performance under the worst-case interference scenario full buffer traffic is used, meaning that BSs are assumed to always have data to transmit. Since CoMP is an interference mitigation technique, it is essential to evaluate its performance under the worst-case interference scenario. Additionally, full buffer traffic is recommended by 3GPP [61] for interference analysis. Round robin, as a common resource allocation algorithm that is widely used by the wireless research community [103-105] as well as by 3GPP in its standardizations [61], is considered.

The PLD, RSS, SINR, and the proposed UC clustering approaches presented in Sections 3.3.1, 3.3.2, 3.3.3, and 3.3.4, respectively are compared in terms of outage probability and balancing the SINR gain and loss of radio resources. The PLD, RSS and SINR thresholds are varied from 1 dB to 20 dB, -50 dBm to -69 dBm, and 1 dB to 20 dB, respectively.

Figure 3.4 shows the percentage of non-CoMP and CoMP UEs for the PLD, RSS, SINR, and the proposed approaches. Since the PLD and SINR approaches are measured in dB while the RSS is in dBm, a parameter ρ ranging from 1 to 20 is used as a threshold representative for the three approaches. $\rho = 1$ represents a PLD of 1 dB, an RSS of -50 dBm, and an SINR of 1 dB whereas $\rho = 2$ represents a PLD of 2 dB, an RSS of -51 dBm, and an SINR of 2 dB, and so on. When the PLD, RSS, and SINR thresholds are 1 dB, -50 dBm, and 1 dB, the percentage of UEs that operate in CoMP mode are 9%, 22%, and 27%, respectively. Increasing the PLD value and the SINR threshold from 1 dB to 20 dB will decrease the number of non-CoMP users and the number of CoMP users will increase. For the RSS approach, the number of CoMP users increases while the number of non-CoMP users decreases when the RSS threshold decreases from -50 dBm to -69 dBm. This is because more UEs can meet the requirement in (3.5) and (3.7) if the PLD and SINR value is high, respectively. In the case of implementing the RSS approach, more UEs can meet the requirement in (3.6) if the RSS threshold is low.

Comparing the PLD, RSS, SINR and the proposed UC approaches, Figures 3.5 to 3.7 show the percentage of UEs with cluster sizes of 1, 2, 4, 6, and 8. From Figure 3.5, it can be seen that as the PLD increases from 1 dB to 7 dB, the number of UEs that operates in two ways CoMP (a cluster size of 2) increases from 8% to 24% while the number of UEs that operate with no CoMP decreases from 91% to 51%. This illustrates

that the two ways CoMP region (A_2) expands as the PLD goes from 1 dB to 7 dB while the non-CoMP region (A_1) shrinks. However, when the PLD goes above 7 dB, the two ways CoMP region starts to shrink back. This happens because UEs located at the outermost of the two ways region become three ways CoMP or c ways CoMP. In other words, three way CoMP regions and higher (A_1 to $A_{c_{max}}$) expands at the expense of the two way CoMP region as well as the non-CoMP region. Generally, every CoMP region expands at the expense of the non-CoMP region. Also, every CoMP region except the region with the highest order expands until it reaches a certain size

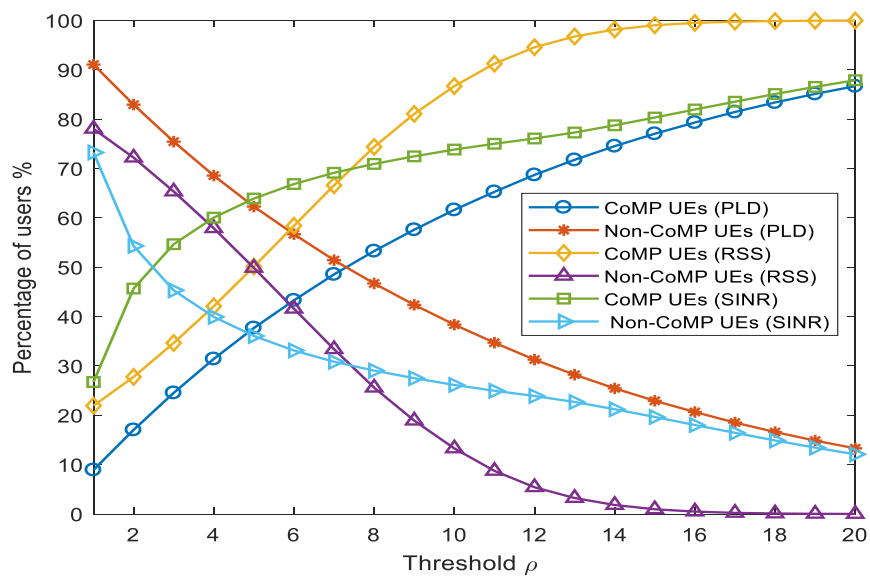


Figure 3.4: Percentage of non-CoMP and CoMP UEs for the PLD, RSS and SINR approaches when $c_{max}=8$.

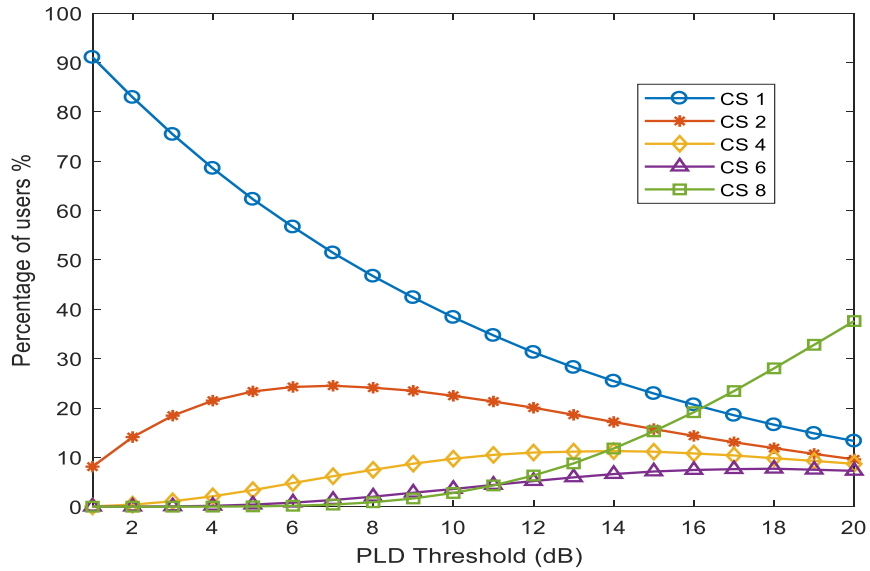


Figure 3.5: Percentage of UEs with cluster sizes of 1, 2, 4, 6, and 8 for the PLD approach

then it shrinks back. This is because a CoMP region with higher order expands at the direction of the CoMP region with lower order which forces the latter to shrink. It is also observed from Figure 3.5 that when the PLD threshold is high, such as 20 dB, the number of UEs that operate with a cluster size of 8 is 38%. This indicates that the PLD between the strongest BS and the 8th strongest BS for the remaining 62% of UEs is higher than 20 dB. In the case of a low RSS and high SINR thresholds such as -69 dBm

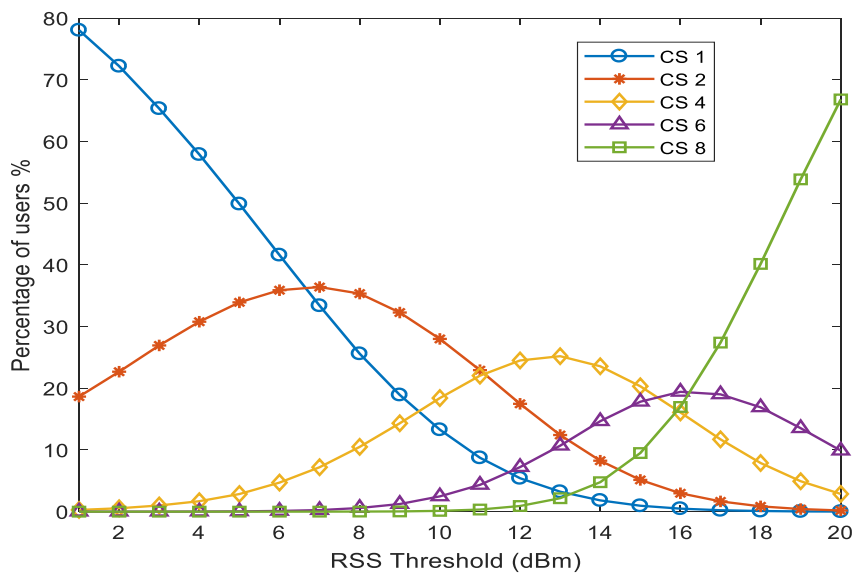


Figure 3.6: Percentage of UEs with cluster sizes of 1, 2, 4, 6, and 8 for the RSS approach

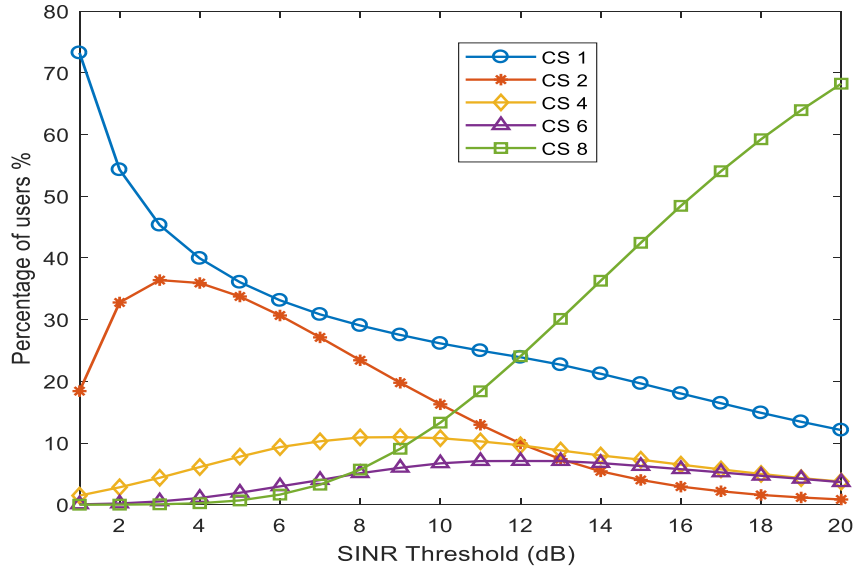


Figure 3.7: Percentage of UEs with cluster sizes of 1, 2, 4, 6, and 8 for the SINR approach

and 20 dB, the number of UEs that operate with a cluster size of 8 is 67% and 68%, respectively. It is clear that the number of UEs that operate with a cluster size of 8 in the RSS and SINR approaches are much higher compared with the PLD approach. This large number of UEs with a cluster size of 8 in the RSS approach, when the RSS threshold is -69 dBm, is because 67% of UEs can receive an average power stronger than -69 dBm from all the 8 strongest BSs. In the SINR approach when the SINR threshold is 20 dB, 68% of UEs have a cluster size of 8 because they could not achieve an SINR of 20 dB when they had a cluster size of 7. Thus, these UEs decided based on (3.7) to operate with a cluster size of 8 in order to attempt to achieve an SINR of 20 dB.

Figure 3.6 shows the percentage of UEs with cluster sizes of 1, 2, 4, 6, and 8 for the RSS approach. As seen in Figure 3.6, as the RSS decreases the number of UEs that operates in two ways CoMP increases while the number of non-CoMP UEs decreases. Similar to Figure 3.5, the two ways CoMP region expands at the expense of the no CoMP region. Also, the three ways CoMP expands at the expense of the two ways CoMP which increases the number of users with a cluster size of 3 and reduces the number of users with a cluster size of 2. In general, as the RSS threshold decreases, a region with a high order would expand forcing regions with lower order to shrink.

Figure 3.8 shows the percentage of UEs with cluster sizes of 1, 2, 4, 6, and 8 for the proposed approach. As Figure 3.8 shows, the number of non-CoMP UEs (a cluster size of 1) is 71%. This is the percentage of UEs who cannot achieve a rate gain higher than c when they operate with a cluster size of c . The total number of CoMP UEs that includes UEs with cluster sizes of 2 up to 8 is 29%. The percentage of CoMP UEs with cluster sizes of 2, 4, 6, and 8 is 7.2%, 4.3%, 2.4%, and 4.2% respectively. It is clear that the percentage of UEs with a cluster size of 2, 4, and 6 decreases as the cluster size goes from 2 to 6. This is because meeting the requirement in (3.10) becomes hard as the cluster size increases. Another reason is that a few UEs can satisfy the requirement in (3.10) when they operate with a small cluster size such as 2 and they also can satisfy the requirement when they operate with a higher cluster size such as 4. This will decrease the percentage of UEs with a cluster size of 2 and increase the percentage of UEs with a cluster size of 4. This shifting from a lower cluster size to a higher cluster size is due to the ability to satisfy the requirement in (3.10) which also explains why the percentage of UEs with a cluster size of 8 is higher than the percentage of UEs with a cluster size of 6.

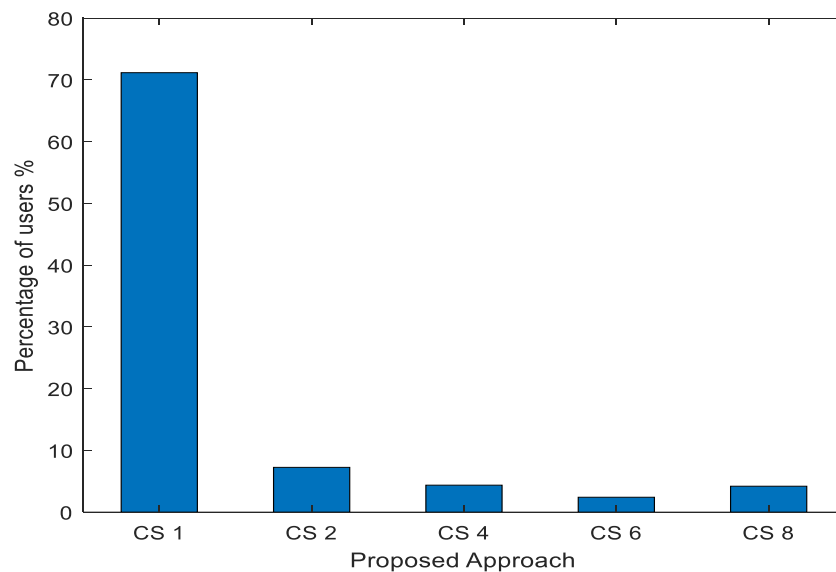


Figure 3.8: Percentage of UEs with cluster sizes of 1, 2, 4, 6, and 8 for the proposed approach

Figure 3.9 shows the percentage of users that would gain or lose throughput when the PLD, RSS, SINR, and the proposed UC JT-CoMP approaches are implemented. If a user can achieve at least c times the rate it achieves with no CoMP where c is the cluster size of this user, then this user benefits, else it loses. This is helpful to evaluate the

effectiveness of a given user-centric clustering algorithm. A good user-centric clustering algorithm should allow users to operate in CoMP mode only if a user can guarantee significant improvement in their rate, as failing to satisfy this requirement increases the number of CoMP users in the system and reduces the resource availability. The performance of the network as a whole depends on the amount of bandwidth allocated for CoMP and non-CoMP users. The definition of winners and losers in this chapter is based on the $\frac{1}{c}$ bandwidth assignment where each CoMP user is allocated $\frac{1}{c}$ of the amount of radio resources it would get when it operates in non-CoMP mode. Implementing the proposed user-centric approach and this $\frac{1}{c}$ CoMP bandwidth assignment scheme ensure that both users and the network benefit. However, it is also possible to assign CoMP users different portions of bandwidth. For instance, the full bandwidth assignment scheme allocates the same amount of bandwidth for CoMP users that they would obtain when they operate in non-CoMP mode. In full bandwidth assignment, users benefit even if they achieve less than c rate gain; however, the network loses if the user does not achieves at least c times rate. Another bandwidth allocation scheme is to assign CoMP users more than $\frac{1}{c}$ radio resources compared to what they obtain when operating in non-CoMP mode. A good example of this bandwidth allocation is a user that is served by three base stations and assigned half bandwidth. In this case, the user benefits if it achieves at least twice the rate; however, the network loses even if the user can achieve higher than twice the rate but less than c times. This bandwidth allocation for CoMP users will be explained in more detail in the next chapter. These statements about the performance of the network are true assuming perfect radio resource matching for overlapping regions and perfect load among base stations. Nonetheless, as the next chapter explains, JT-CoMP in HetNets faces a radio resource mismatching problem and load unevenness among base stations. As seen from Figure 3.9, the PLD, RSS, and SINR approaches exhibit similar behaviour where the number of winners increases until it reaches a stable point and then after a certain threshold, the number of winners starts to decrease. This is because when the PLD threshold is less than 6 dB, the cluster size of a certain CoMP user would be small (mostly 2 as seen from Figure 3.5). In addition, the average received power from each BS other than the strongest BS that belong to the user's cluster is strong due to the low value of the PLD (less than 6 dB). This helps to achieve a rate gain higher than the cluster size. However, when the PLD goes beyond 6 dB, for the same user, its cluster

size increases and the average received power of some of its cooperative BSs are weak. Due to the weakness of the average received powers from some BSs in the cooperative set and the high cluster size, it is difficult for this user to achieve a rate gain higher than its cluster size. This clearly illustrates that increasing the cluster size might degrade the system's performance. For the PLD approach, the number of winners starts to increase when the PLD increases from 1 dB until it reaches 6 dB. PLD thresholds of 5 dB to 8 dB include 25%, 25.69%, 25.62%, and 25% of winners, respectively. However, 5 dB to 8 dB PLD thresholds will also include 13%, 18%, 23%, and 29% of losers, respectively. Allowing these users to operate as CoMP users will degrade the system performance since the SINR gain of these users does not compensate the loss of resources. When the PLD and SINR thresholds go beyond 6 dB and 3 dB and the RSS threshold goes below -57 dBm, the number of winners declines and the number of losers sharply increases. For the PLD, RSS, SINR approaches, the highest number of winners is 25.69%, 23.5%, and 23.75% achieved at thresholds of 6 dB, -57 dBm, and 3 dB, respectively. Although the PLD, RSS, and SINR approaches at these thresholds attempt to include all UEs that would benefit from CoMP, they also include 18%, 50%, and 31% of losers. For the proposed approach, the number of winners and losers are 29% and 0%, respectively.

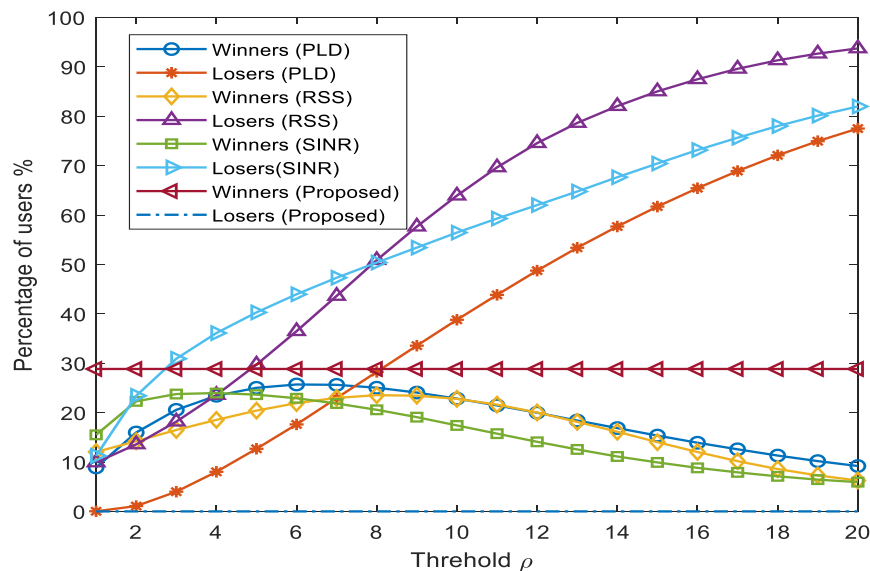


Figure 3.9: Percentage of winners and losers for the PLD, RSS and SINR approaches when $c_{max}=8$.

Figure 3.10 shows the outage probability with no CoMP and with the PLD, RSS, SINR, and the proposed user-centric JT-CoMP clustering approaches. As shown in

Figure 3.10, the highest number of winners for the PLD, RSS, and SINR is achieved when the PLD, RSS, SINR thresholds are 6 dB, -57 dBm, and 3 dB, respectively. Using other values such as a PLD threshold of 20 dB, RSS threshold of -69 dBm, and an SINR of 20 dB may result in decreasing the outage probability as many UEs would operate in CoMP mode with a high cluster size; however, such values will include many UEs that are losers as can be seen in Figure 3.9. Thus, to have a fair comparison, the PLD, RSS, and SINR thresholds that achieve the highest number of winners (a PLD of 6 dB, an RSS of -57 dBm, and an SINR of 3 dB) while the number of losers are not high are considered. Figure 3.10 shows that 73% of UEs achieve an SINR greater than 0 dB with no CoMP. By implementing JT-CoMP, a significant SINR gain is expected as JT-CoMP converts the harmful signal(s) into useful signal(s). As Figure 3.10 illustrates, 100%, 93%, 100% and 91% of users can achieve an SINR higher than 0 dB when the PLD, RSS, SINR, and the proposed approach are implemented. It is clear that implementing JT-CoMP significantly improves the SINR. Figure 3.10 shows that the RSS approach performs better than the other user-centric approaches in terms of increasing the number of UEs that achieve an SINR higher than 4.5 dB. This is because the RSS approach with a threshold of -57 dBm admits many UEs (74% of UEs as shown in Figure 3.4) to operate in CoMP even if some UEs achieve marginal SINR gain. From Figure 3.10, it is shown that the SINR approach achieves the best performance in terms of reducing the percentage of UEs that achieve less than 4.5 dB followed by the PLD, RSS, and the proposed approach. This is because the SINR approach focuses only on improving the SINR of UEs that achieve an SINR less than 3 dB. It is also shown that the performance of the RSS and the proposed approach in increasing the number of UEs that achieve an SINR higher than 4.5 dB is better than the PLD and SINR approaches. This is because the percentage of UEs that operate with cluster sizes higher than 2 in the RSS and the proposed approach is higher compared with the PLD and SINR approaches. Although the percentage of UEs that operate with cluster sizes higher than 2 in the proposed approach is not as high as in the RSS approach, the performance of the proposed approach is comparable to the RSS approach since it only allows UEs that achieve significant SINR gain to operate in CoMP mode. Generally, the SINR levels increase as the number of CoMP UEs increases. Comparing a PLD of 6 dB, RSS of -57 dBm, and an SINR of 3 dB, Figure 3.4 shows that the highest number of CoMP UEs is achieved by the RSS approach which explains the superiority of the RSS approach in terms of outage probability. The proposed approach

does not achieve the best outage probability as it only allows 29% of users to operate in JT-CoMP while the RSS allows about 68% as shown in Figures 3.8 and 3.4, respectively. This strict restriction by the proposed approach is essential in order to allow UEs with significant SINR gain only to operate in CoMP mode which in turns helps to provide an effective balance between the SINR gain and loss of radio resources. An interesting observation from Figure 3.10 is that all UEs in the SINR approach achieve SINR levels higher than 3 dB. This illustrates the strength of the SINR approach to provide a system where no UE achieves an SINR less than 3 dB. As Figure 3.10 has shown, the SINR gain clearly depends on the user-centric clustering algorithm.

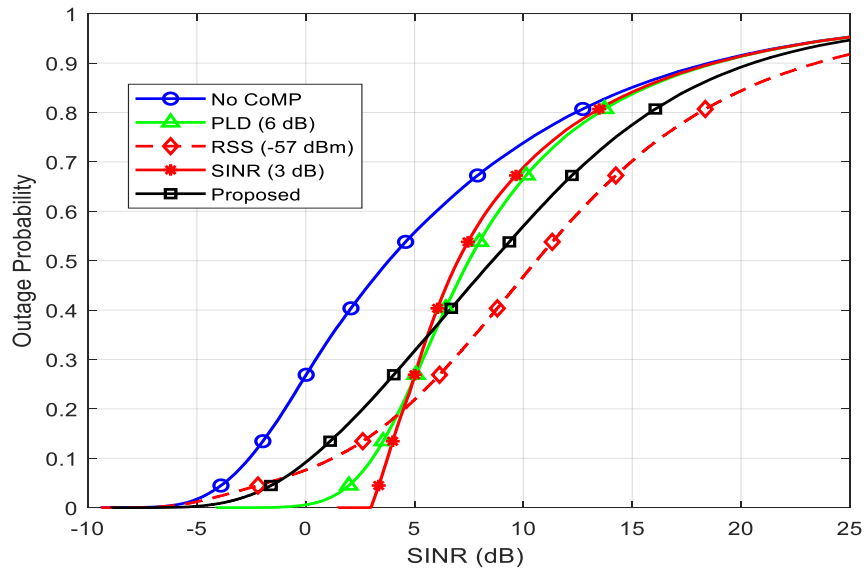


Figure 3.10: Outage probability with no CoMP and with the PLD (6 dB), RSS (-57 dBm), SINR (3 dB), and the proposed UC JT-CoMP approaches.

3.5.1 Impact of Limiting the Maximum UC Cluster Size

In JT-CoMP, limiting the maximum cluster size to c_{max} restricts a UE from being served by more than c_{max} cooperative BSs even if the requirements in (3.5), (3.6), (3.7) or 3.10 are satisfied. This limitation is necessary in order to reduce additional overhead and scheduling complexity. According to [106, 107], the complexity increases as the cluster size increases. Many research studies [108, 42, 40, 25] have limited the maximum UC cluster size to be in the range of 2 to 8.

It is important to study the impact of limiting the maximum cluster size not only on the outage probability but also on the number of winners and losers. The impact of

limiting the maximum cluster size on the outage probability has been analysed on the literature [42] where it has been shown that the outage probability decreases as the maximum cluster size increases.

The impact of limiting the maximum UC cluster size to 2, 4, 6, and 8 on the number of winners and losers for the PLD, RSS, SINR, and proposed approach is illustrated in Figures 3.11, 3.12, 3.13, and 3.14, respectively. When the maximum UC cluster size is limited to 2, increasing the PLD and SINR thresholds and decreasing the RSS threshold increases the number of winners and the number of losers as well. From Figures 3.11, 3.12, and 3.13, it is observed that the number of winners increases at a fast rate when the PLD, RSS, and SINR thresholds change from 1 dB to 6 dB, -50 dBm to -57 dBm, and 1 dB to 3 dB, respectively. However, after a certain threshold, i.e. a PLD threshold of 6 dB, an RSS threshold of -57, and a SINR threshold of 3 dB, the number of winners slightly increases while the number of losers keeps increasing at almost the same rate. Low PLD and SINR thresholds and a high RSS thresholds have a few winners because some UEs are restricted from being served by the second strongest BS even if the average received power from this BS is strong enough to help achieve a rate gain higher than 2 if it were to cooperate as the second serving BS. As the PLD and SINR increases and the RSS decreases until it reaches values of 6 dB, 3 dB, and -57 dBm, respectively, this restriction loosens and more UEs benefit since almost all second strongest BSs that can help to achieve a rate gain higher than 2 are allowed to cooperate.

As seen from Figures 3.11 to 3.13, the performance in terms of the number of winners and losers for the PLD, RSS, and SINR approaches for any threshold below 8 dB, -57 dBm, and 3 dB, respectively are identical irrespective of the maximum cluster size. This is because when the PLD and SINR thresholds are high and the RSS threshold is low, most of the users would still operate with a cluster size of 2 due to the difficulty of satisfying the requirements in (3.5), (3.6), or (3.7) even if the maximum cluster size that a UE can have is 8. When the PLD and SINR thresholds go beyond 8 dB and 3dB and the RSS threshold goes below -57 dBm, the number of winners decreases while the number of losers increases as the maximum cluster size goes from 2 to 8. When c_{max} is low, it restricts some BSs that provide insufficient average received power to cooperate even if they can satisfy the requirements in (3.5), (3.6), or (3.7). However, when c_{max} is high such as 8, these BSs would be allowed to cooperate

providing marginal SINR gain that does not help to satisfy the winner condition. For example, when $c_{max} = 2$, a CoMP UE would be served by the strongest two BSs resulting in a rate gain higher than 2. However, when $c_{max} = 8$, the same UE might be associated with the 8 strongest BSs even though some of them do not provide sufficient average received power due to the high PLD and SINR thresholds and the low RSS threshold. This can result in achieving a rate gain lower than 8.

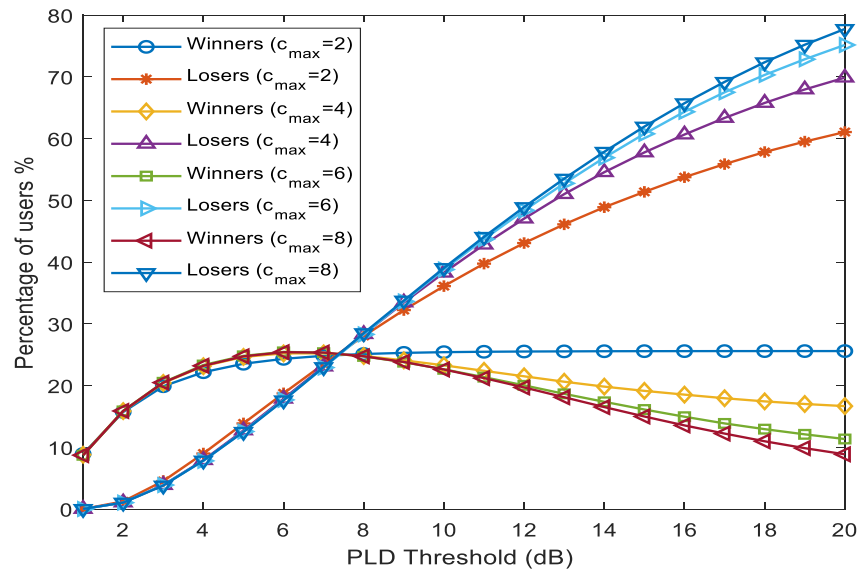


Figure 3.11: Number of winners and losers in the PLD approach when the maximum cluster size is limited to 2, 4, 6, and 8.

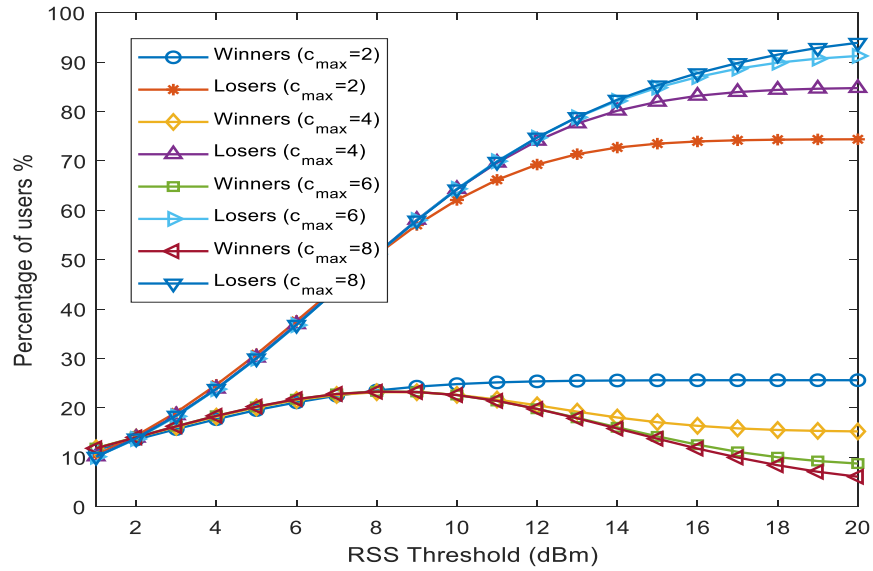


Figure 3.12: Number of winners and losers in the RSS approach when the maximum cluster size is limited to 2, 4, 6, and 8.

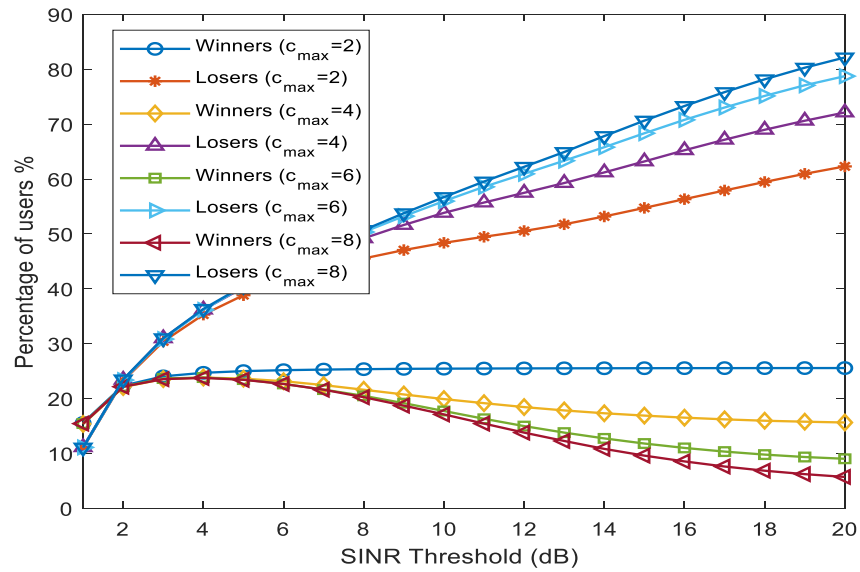


Figure 3.13: Number of winners and losers in the SINR approach when the maximum cluster size is limited to 2, 4, 6, and 8.

Figure 3.14 shows the number of winners for the proposed approach when c_{max} changes from 2 to 8. Figure 3.14 shows that the number of winners increases from 25.6% to 29% when c_{max} increases from 2 to 8. This shows that there are 3.4% of UEs who cannot achieve a rate gain higher than 2 when $c_{max} = 2$; however, allowing these UEs to be served by 8 BSs enables them to achieve a rate gain higher than 8.

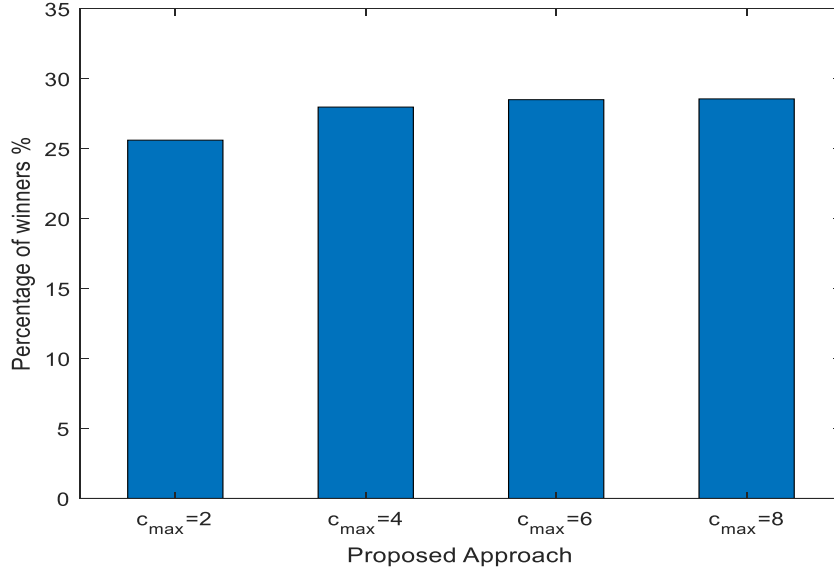


Figure 3.14: Percentage of winners in the proposed approach when the maximum cluster size c_{max} is limited to 2, 4, 6, and 8.

3.5.2 Impact of BS Densification

It is important to study the impact of increasing the number of BSs when CoMP is implemented. The aim is to understand whether CoMP is more beneficial or less beneficial in dense networks, or whether increasing the number of BSs has no impact on the performance of JT-CoMP. The performance of user-centric JT-CoMP under different BS densities is evaluated in this section.

Comparing the PLD, RSS, SINR, and the proposed user-centric approaches, Figures 3.15 to 3.18 show the impact of BS densification on the number of winners and losers when the density of pico and femto BSs are $\lambda_{pm} = 16$ BSs/km² and $\lambda_{fm} = 32$ BSs/km², $\lambda_{pm} = 24$ BSs/km² and $\lambda_{fm} = 48$ BSs/km², $\lambda_{pm} = 32$ BSs/km² and $\lambda_{fm} = 64$ BSs/km². Including 8 macro BSs/km², this is equivalent to a total BS density (macro, pico, and femto) of 56 BSs/km² (sparse), 80 BSs/km² (medium), 104 BSs/km² (dense). From Figures 3.15 to 3.17, it can be seen that the number of CoMP UEs (number of winners and losers) increases as the number of BSs increases. For example, when the PLD threshold is 10 dB, Figure 3.15 shows that the percentage of CoMP UEs increases from 61.63% to 63.7% when the BS density increases from 56 BSs/km² to 104 BSs/km². This is because increasing the number of BSs forces some non-CoMP UEs to operate in two ways CoMP mode as the average received powers by these UEs from

their second strongest BSs become stronger due to the shorter distance between the non-CoMP UE and its second strongest BS. This also applies to some CoMP UEs that would operate with higher cluster sizes since their average received powers by the their third, fourth, ... c_{max} BSs become stronger as well. In other words, this increase in the number of two ways CoMP UEs and the increase in the cluster size happen because the requirements in (3.5), (3.6), and (3.7) become easier to satisfy as the number of BSs increases. All UEs that are forced to operate in CoMP mode due to BS densification and all UEs that would operate with higher cluster size due to the same reason must satisfy the winner condition where their rate gain must be higher than their cluster size. It is clear from Figures 3.15 to 3.17 that as the number of BSs increases most of these UEs fail to satisfy the winner condition which will increase the number of losers and decrease the number of winners. To illustrate this with an example, if a UE operates in two ways CoMP when the BS density is sparse, increasing the BS density can force this UE to operate in three ways CoMP as the average received power from the third strongest BS is strong enough to allow this BS cooperate. Although this UE met the winner condition when it operated with two ways CoMP, it might not be able to meet the winner condition when it operates in three ways CoMP.

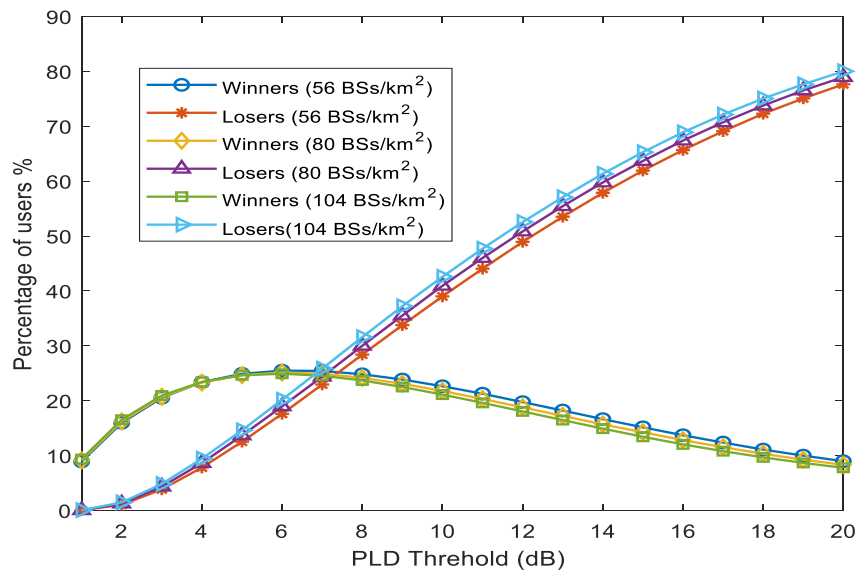


Figure 3.15: Percentage of winners and losers in the PLD approach for sparse (56 BSs/km²), medium (80 BSs/km²), and dense (104 BSs/km²) deployment.

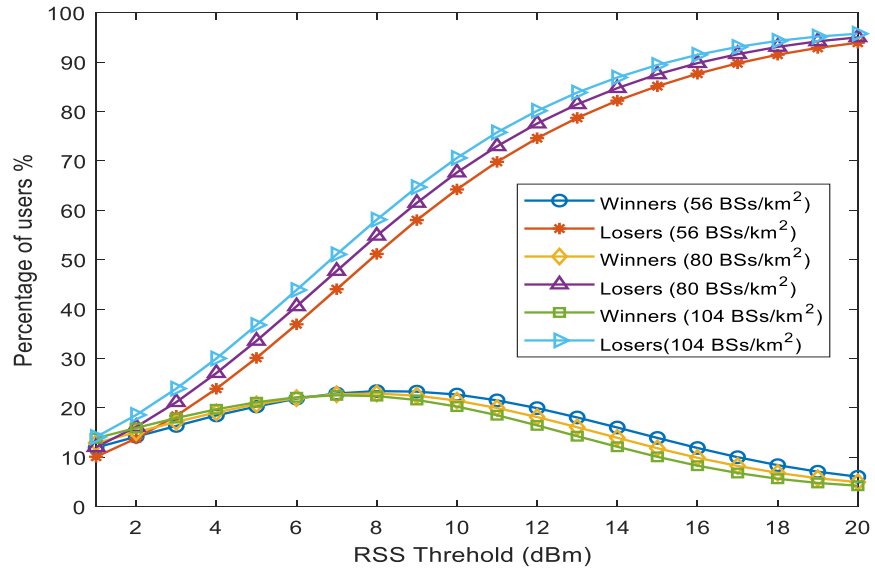


Figure 3.16: Percentage of winners and losers in the RSS approach for sparse (56 BSs/km²), medium (80 BSs/km²), and dense (104 BSs/km²) deployment.

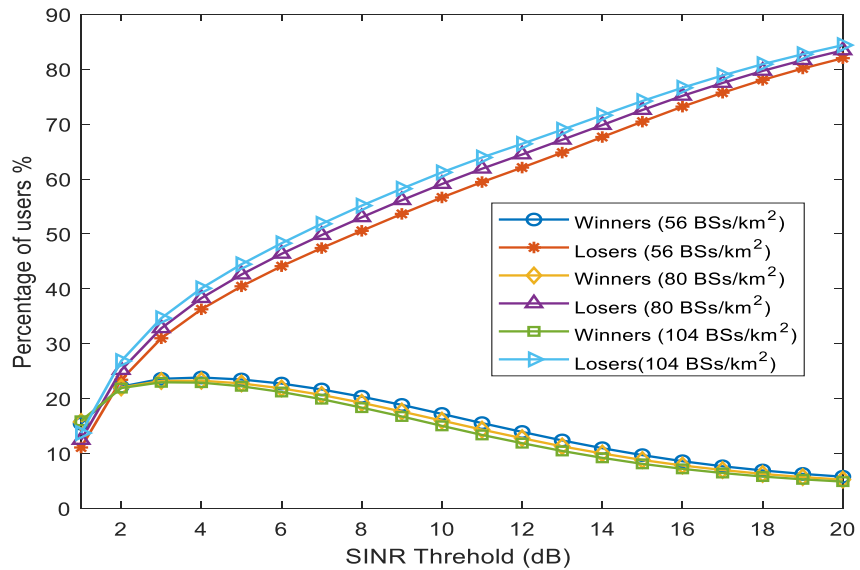


Figure 3.17: Percentage of winners and losers in the SINR approach for sparse (56 BSs/km²), medium (80 BSs/km²), and dense (104 BSs/km²) deployment.

Figure 3.18 shows the percentage of winners when the proposed approach is implemented for sparse, medium and dense deployments. As Figure 3.18 shows, the performance of JT-CoMP in terms of the percentage of winners is not affected by the density of BSs. Figures 3.15 to 3.17 have shown the opposite because the PLD, RSS, and SINR approaches decide the mode of operation (CoMP or no CoMP) based on thresholds that would allow different percentage of UEs (based on the density of BSs)

to operate in CoMP mode even if these UEs do not balance between SINR gain and loss of bandwidth.

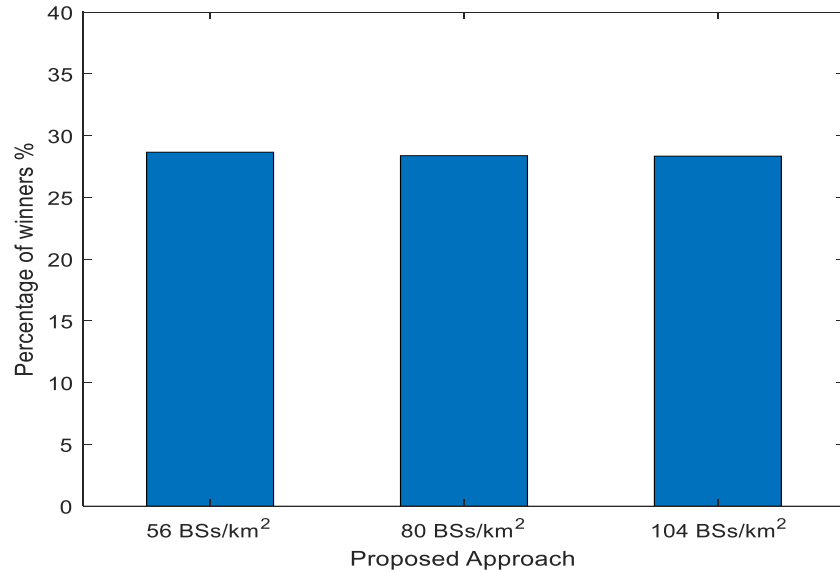


Figure 3.18: Percentage of winners in the proposed approach for sparse (56 BSs/km²), medium (80 BSs/km²), and dense (104 BSs/km²) deployment.

3.5.3 Impact of Spatial Modelling of SC BSs

Although pure PPP networks might have some BSs that are close to each other due to the absence of a minimum separation distance between any two BSs, it is interesting to study this type of distribution in JT-CoMP networks as it can represent the highest level of overlapping regions. It is also interesting to compare the performance of JT-CoMP in pure PPP networks and in repulsive PPP networks where a minimum separation distance δ is applied. In addition, it is important to study the impact of different minimum separation distances.

Figure 3.19 shows the performance of the PLD in terms of the number of winners and losers when SC BSs are spatially distributed according to pure PPP and repulsive PPP. In repulsive PPP, the minimum separation distances for pico and femto BSs is set to $\delta_p = 10$ m and $\delta_f = 5$ m, $\delta_p = 20$ m and $\delta_f = 10$ m, $\delta_p = 30$ m and $\delta_f = 15$ m, and $\delta_p = 40$ m and $\delta_f = 20$ m. As Figure 3.19 shows, the performance of JT-CoMP in terms of the number of winners and losers in pure PPP and repulsive PPP is exactly the same. This is also true for the RSS, SINR, and the proposed approach. Figures that compare the performance of the RSS, SINR, and the proposed approach are not shown

since the performance of these approaches in pure PPP and repulsive PPP is exactly the same.

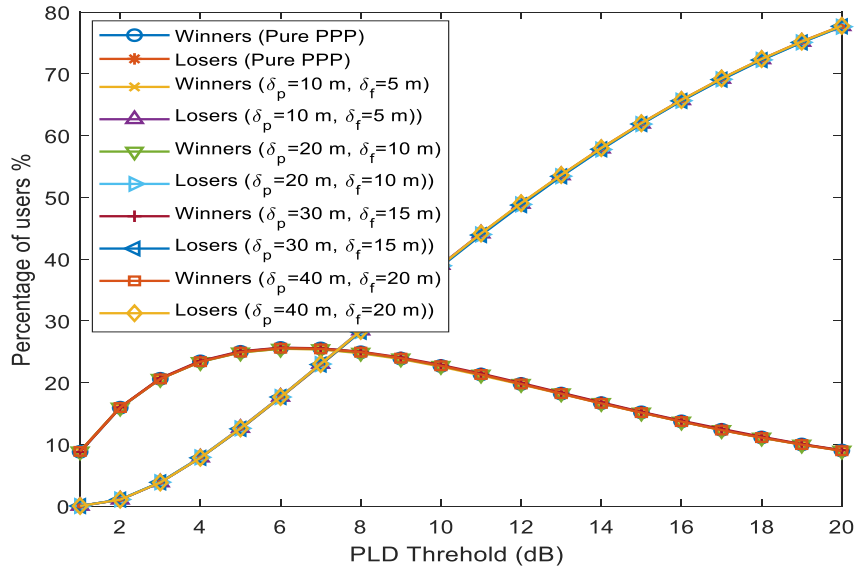


Figure 3.19: The performance of JT-CoMP in pure PPP networks compared repulsive PPP networks with when the PLD approach is implemented.

3.6 Conclusion

User-centric JT-CoMP clustering where a UE can be served by multiple BSs simultaneously is one of the main technologies that shifts the current wireless architecture from cell-centric to cell-less. In user-centric JT-CoMP clustering, a user can be associated with BSs even if this user is not geographically located within their cell coverage. User-centric clustering is a promising approach to identify UEs that could benefit from JT-CoMP and restrict UEs that achieve marginal SINR gain from operating in CoMP mode. This identification is important in order to efficiently utilise the system's bandwidth as allowing UEs with marginal SINR gain would waste radio resources. A new user-centric clustering approach that balances between the SINR gain and loss of radio resources is proposed. In the proposed approach, a UE operates in a CoMP mode only if its rate gain is sufficient enough to compensate for the loss of bandwidth. To validate the effectiveness of the proposed user-centric clustering approach, it has been compared with three common and existing user-centric clustering approaches namely, PLD, RSS, and SINR. Results have shown the effectiveness of the proposed UC approach in restricting any UE from operating in CoMP mode if it would waste the bandwidth. When the maximum cluster size is limited to 8, the best

performance in terms of including the users that obtain a rate gain higher than their cluster is achieved when the PLD, RSS, and SINR thresholds are 6 dB, -57 dBm, and 3 dB, respectively. At these thresholds, the percentage of winners are 25.69%, 23.5%, and 23.75% when the PLD, RSS, and SINR approaches are implemented, respectively. However, these thresholds include 18%, 50%, and 31% of losers. The number of winners and losers in the proposed approach are 29% and 0%. The results also show that all the UC clustering approaches outperform no CoMP in terms of outage probability. The percentage of UEs that achieves SINR higher than 0 dB has increased from 73% with no CoMP to 100%, 93%, 100% and 91% when the PLD, RSS, SINR, and proposed approach are implemented.

The impact of limiting the maximum cluster size has been investigated. The results have shown that increasing the maximum cluster size from 2 to 8 degrades the system performance when the PLD and SINR thresholds goes above 8 dB and 3 dB while the RSS goes below -57 dBm. On the contrary, the proposed approach has shown that increasing the maximum cluster size from 2 to 8 slightly increases the number of UEs that could benefit from JT-CoMP. The impact of BS densification on the performance of JT-CoMP has been studied. According to the results, it has been observed that JT-CoMP performs slightly worse in dense networks when the PLD, RSS, and SINR approaches are applied. The proposed approach has shown that the density of BSs has no impact on the performance of JT-CoMP. Simulation results have shown that the performance of JT-CoMP is identical regardless of the spatial distribution of SC BSs. Overall, the proposed approach has shown that it can perform better than the traditional UC clustering approaches. In addition, the proposed approach is not negatively influenced by the maximum cluster size or the density of BSs, unlike the traditional schemes. The strength and effectiveness shown by user-centric JT-CoMP clustering in the simulation results, particularly the proposed user-centric clustering approach, can play a significant role in mitigating inter-cell interference in a 5G cell-less architecture.

Although user-centric JT-CoMP clustering has shown its effectiveness in enhancing the outage probability, it is essential to take radio resource management into account. In this chapter, this has been partially performed by evaluating the number of winners and losers when JT-CoMP is implemented. Nevertheless, the number of winners and losers does not provide a complete insight into the performance of JT-CoMP since it does not

take the load of each BS into account. As a result, joint user-centric clustering and radio resource allocation that takes the load of each BS into account is considered in the next chapter in order to robustly evaluate the performance of JT-CoMP in 5G HetNets.

CHAPTER 4

Joint Multi-Cell Resource Allocation and User-centric Clustering in JT-CoMP

Contents

4.1	Introduction	77
4.2	System Model	79
4.3	Set Definitions of CoMP and non-CoMP Users Per Base Station.....	79
4.4	Multi-cell Radio Resource Management	81
4.4.1	Challenges of Resource Allocation in User-Centric JT-CoMP	83
4.4.2	Resource Matching Approach	84
4.4.3	Bandwidth Allocation	86
4.4.4	Bandwidth Underutilisation Problem	87
4.4.5	Impact of JT-CoMP on Base Station Loading.....	91
4.5	Performance Comparison.....	93
4.6	Conclusion	104

4.1 Introduction

Most of the research in the state-of-the-art has tackled user-centric clustering and radio resource allocation separately. Nonetheless, it is crucial to jointly consider multi-cell resource allocation and user-centric clustering in order to comprehensively evaluate the performance of JT-CoMP. In addition, this joint consideration of user-centric clustering and multi-cell resource assignment is an essential path towards the development and realisation of a 5G cell-less architecture. In this chapter, joint user-centric JT-CoMP clustering and multi-cell resource allocation are developed in two steps where user-centric clusters are constructed as a first step and according to the clustering results obtained, resources are assigned. The first step involves the formation

of clusters for all users based on the user-centric clustering algorithms presented in Chapter 3. The second step requires development of an effective multi-cell radio resource allocation scheme that can address the challenges and restrictions of allocating resources from multiple base stations. One of the main challenges in multi-cell resource allocation in JT-CoMP is the radio resource mismatching problem between cooperating base stations that happens due to load imbalance. Another challenge is the bandwidth underutilisation problem that occurs when all the users associated with a small cell base station operate in a JT-CoMP mode.

The main contributions of this chapter can be summarised as follows:

- 1) A novel radio resource management scheme that can support multi-cell scheduling in JT-CoMP. The proposed resource allocation scheme solves the JT-CoMP mismatching resources problem where one base station has a higher number of PRBs for the CoMP region than a cooperating base station by letting the two cooperating base stations negotiate and agree on the number of PRBs that they can provide for their CoMP region. It also mathematically develops a new scheme that divides the total available bandwidth among CoMP and non-CoMP regions.
- 2) A novel hybrid approach that allows cell-edge users to operate in JT-CoMP and no CoMP simultaneously. A hybrid user can operate in a no CoMP mode on certain PRBs while at the same time it operates in a JT-CoMP mode on other PRBs. The purpose of the development of this approach is to solve the bandwidth underutilisation problem; thus, improving the overall user throughput as well as the cell-edge throughput.
- 3) Evaluation of the effect of assigning different portions of bandwidth to CoMP users on the performance in terms of the overall throughput and cell-edge throughput.

The organisation of this chapter is as follows. In Section 4.2, the system model is presented. Section 4.3 provides mathematical definitions of the set of CoMP and non-CoMP users per base station based on set theory. Section 4.4 presents multi-cell radio resource management in JT-CoMP. Firstly, it starts by presenting the challenges of resource allocation in user-centric JT-CoMP. Then, it explains the concept of the proposed resource matching approach. Based on this approach, a multi-cell bandwidth

allocation scheme is developed. Section 4.4 also describes the bandwidth underutilisation problem in JT-CoMP 5G HetNets and proposes a hybrid approach that can address this problem. Section 4.5 compares the performance of the traditional JT-CoMP and the hybrid approach. Finally, conclusions are drawn in Section 4.6.

4.2 System Model

The system model in this chapter follows the system model presented in Chapter 3 with one exception. The exception is that the maximum user-centric cluster size in this chapter is limited to 2. This limitation is because allowing more than two base stations to cooperate would require a very large SINR gain to achieve a rate gain that can compensate for the loss of bandwidth, as shown in Figure 3.2. Moreover, as this chapter will show, the load unevenness problem imposes further restrictions on benefiting from 3 ways CoMP or higher.

The performance metric in this chapter is the achievable throughput. The achievable throughput is calculated based on Shannon's equation as follows:

$$T = B \log_2(1 + SINR) \quad (4.1)$$

where B is the total bandwidth.

4.3 Set Definitions of CoMP and non-CoMP Users Per Base Station

In JT-CoMP, each base station can have non-CoMP and CoMP users associated with it. Non-CoMP users are the users associated with the base station that provides the strongest received power and their cluster size is one. CoMP users of base station i are the users belonging to base station i which can provide the strongest received power or the second strongest received power. To develop a multi-cell radio resource allocation scheme, it is important to define the set of CoMP and non-CoMP users of each base station. Moreover, it is crucial to define the overlapping regions that each base station has to support. Set theory is utilised to mathematically define the set of non-CoMP users, CoMP users, as well as the overlapping regions of each base station.

The set of non-CoMP users of base station i can be defined as follows:

$$\mathcal{N}_i = \left\{ k \in \mathbb{R}^2 \mid x_1 = BS\ i \ \& \ |C_k| = 1 \right\} \quad (4.2)$$

where $|C_k|$ is the user-centric cluster size of user k .

The set of CoMP users receiving strongest and second strongest power from base stations i and j in CoMP region p , respectively is defined as follows:

$$\mathcal{V}_{ijp} = \left\{ k \in \mathbb{R}^2 \mid x_1 = BS\ i \ \& \ x_2 = BS\ j \right\} \quad (4.3)$$

The following defines the set of CoMP users receiving strongest and second strongest power from base stations j and i in CoMP region p , respectively:

$$\mathcal{W}_{ijp} = \left\{ k \in \mathbb{R}^2 \mid x_2 = BS\ i \ \& \ x_1 = BS\ j \right\} \quad (4.4)$$

Using (4.3) and (4.4), the set of all CoMP UEs associated with base station i in its CoMP region p is:

$$\mathcal{D}_{ip} = \mathcal{V}_{ijp} \cup \mathcal{W}_{ijp} \quad (4.5)$$

The set of base stations that cooperate with base station i is defined as follows:

$$\mathcal{P}_i = \left\{ BS\ j \in \mathcal{J} \mid |\mathcal{D}_{ip}| > 0, j \neq i \right\} \quad (4.6)$$

Using (4.5) and (4.6), the set of all CoMP UEs associated with base station i can be written as follows:

$$\mathcal{Q}_i = \cup_{p \in \mathcal{P}_i} \mathcal{D}_{ip} \quad (4.7)$$

Finally, the set of non-CoMP and CoMP UEs associated with base station i can be written as follows:

$$\mathcal{A}_i = \mathcal{N}_i \cup \mathcal{Q}_i \quad (4.8)$$

Figure 4.1 provides an example that shows the CoMP and non-CoMP users of a certain base station. As shown in the example, BS 1 has two non-CoMP users and three CoMP users. In Figure 4.1, stars represent the set of users v_{12} who receive the strongest and second strongest received power from BSs 1 and 2, respectively while triangles

represent the set of users w_{12} who receive the strongest and second strongest received power from BSs 2 and 1, respectively. Both v_{12} and w_{12} belong to BS 1 as its CoMP users.

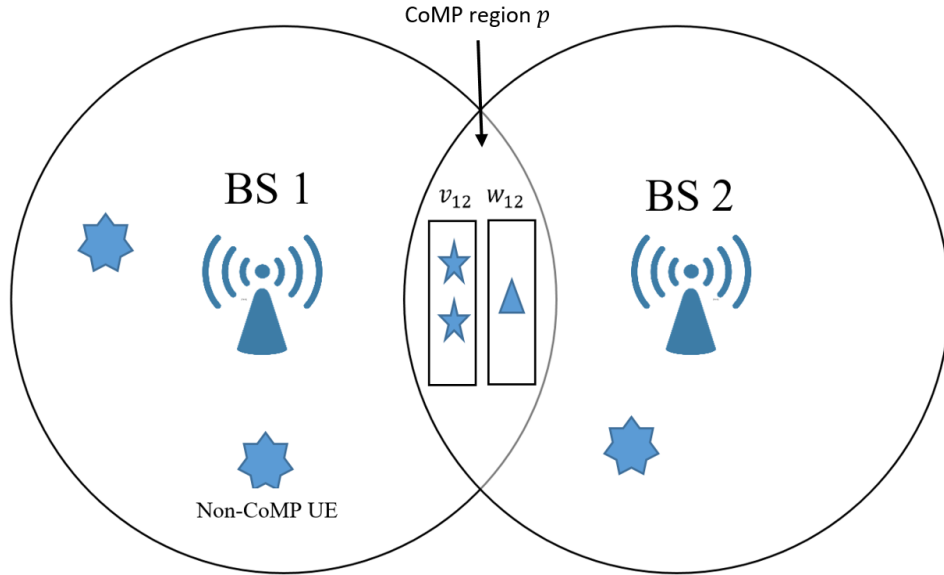


Figure 4.1: An example illustrating the set of CoMP and non-CoMP UEs of a base station.

4.4 Multi-cell Radio Resource Management

In a JT-CoMP system, it is important to exploit a radio resource management scheme that can satisfy not only CoMP users but also non-CoMP users. Effective schemes are not available up to now. The whole bandwidth of each base station is assigned to its CoMP and non-CoMP users and the amount of bandwidth each user obtains is dependent on the number of users associated with each base station. Assigning a high proportion of radio resources for CoMP users will boost their throughput; however, this will decrease the number of the available radio resources for non-CoMP users causing their throughput to significantly drop. Also, assigning a high proportion of resources for non-CoMP users will enhance their throughput but clearly the throughput of CoMP users will decrease. Thus, developing a radio resource assignment technique for JT-CoMP is required to balance resource assignment between CoMP and non-CoMP users. One approach that attempts to provide this balance is to assign CoMP users half of the radio resources that a non-CoMP user would be assigned. This approach is referred as half bandwidth assignment. Figure 4.2 provides an example that explains half bandwidth assignment. In this example, for BS 1 the total bandwidth

is divided between UE 1, UE 3, and UE 4. Assuming that BS 1 has 100 PRBs, this amount of PRBs is first divided between all CoMP users (UE 3 and UE 4) and all non-CoMP users (UE 1). Since UE 3 and UE 4 are CoMP users, the amount of bandwidth they obtain should be equal to the amount of bandwidth allocated to each non-CoMP user. This allows treatment of both UE 3 and UE 4 as only one user. As a consequence, the 100 PRBs is divided by two (UE 1 as one entity while UE 3 and UE 4 as another entity). Based on this assignment, UE 1 is allocated 50 PRBs and both UE 3 and UE 4 are allocated 50 PRBs. The 50 PRBs for UE 3 and UE 4 is further divided between them equally where each user obtains 25 PRBs. The final assignment of radio resources becomes 50 PRBs for UE 1, 25 PRBs for UE 3, and 25 PRBs for UE 4. This shows that each CoMP user (UE 3 or UE 4) is assigned half of the radio resources that non-CoMP users (UE 1) obtain. When more than one user is present in the non-CoMP region, the same assignment is performed providing non-CoMP users with full bandwidth and CoMP users with half bandwidth and allocating resources accordingly. Similar bandwidth allocation is performed for BS 2. This half bandwidth assignment is considered quite fair for two reasons. The first is that it is anticipated that the SINR of CoMP users will significantly increase while the second is that a PRB that is allocated to a CoMP user by one of its cooperating base stations (strongest base station) cannot be reused by any other base station in its cluster (the second strongest base station). Although half bandwidth assignment appears to be reasonably fair, there is currently no proof that it is an optimal assignment. Therefore, it is important to investigate assigning different portions of bandwidth for CoMP users. For example, a CoMP user can be assigned the same (full bandwidth) or twice (double bandwidth) the amount of PRBs that a non-CoMP user would obtain.

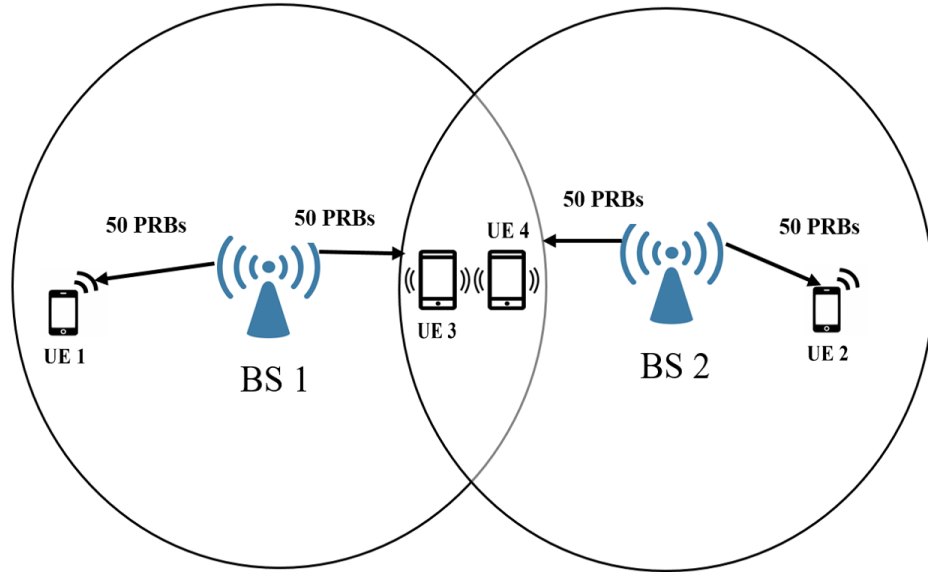


Figure 4.2: An example of half bandwidth assignment.

4.4.1 Challenges of Resource Allocation in User-Centric JT-CoMP

Radio resource management for JT-CoMP is a challenging task since it involves assigning radio resources from multiple base stations. This multi-cell assignment induces four resource allocation restrictions in user-centric JT-CoMP:

- 1) A PRB that is reserved for a UE by one base station of its cluster cannot be reused by any other base station in the same cluster. This restricts the usage of the same resource block from the cooperating base station to serve another user.
- 2) All base stations that form a UE's cluster must reserve an identical number of PRBs for this UE, in order for JT-CoMP to operate. This reduces the frequency reuse to a factor of c where c is the cluster size. For example, if all users are allowed to operate with JT-CoMP and the maximum cluster size is set to 5, then the frequency reuse reduces to 5. This problem can be reduced by allowing only a certain percentage of users to operate in CoMP mode; those that are likely to benefit most.
- 3) Due to load unevenness and the different numbers of CoMP regions a base station may have, one base station may have fewer radio resources to support a specific CoMP region while the other cooperating base stations supporting the same CoMP region have more radio resources. This resource mismatch clearly

restricts the radio resources that can be used to support CoMP users. This problem must be addressed to enable all users that are located in the CoMP region to be supported.

- 4) The load imbalance among different tiers causes some small cell base stations to be associated with CoMP UEs only. In this case, such base stations might not fully utilise their bandwidth as their bandwidth utilisation depends on their cooperating base stations. To address this issue, a hybrid approach is proposed where a user that decides to operate in a CoMP mode based on the user-centric clustering algorithms presented in Chapter 3 can operate in CoMP and non-CoMP modes simultaneously.

4.4.2 Resource Matching Approach

This part focuses on addressing the resource mismatching problem that occurs when allocating resources from multiple base stations. An example that illustrates how the different loads of each base station and different CoMP regions of each base station cause a mismatch in the number of PRBs that two cooperating base stations can provide for their CoMP region is shown in Figure 4.3. Figure 4.3 shows that BS 1 and BS 2 have different loads (numbers of users) and different CoMP regions, thus the bandwidth that BS 1 can provide for its overlapping region with BS 2 is different from the bandwidth that BS 2 can provide for the same region. For CoMP region 1, the example shows that BS 1 is able to provide 40 PRBs while BS 2 can only provide 25 PRBs. This resource mismatching problem in the number of PRBs that can be provided by two cooperating base stations for their CoMP region must be considered when implementing JT-CoMP.

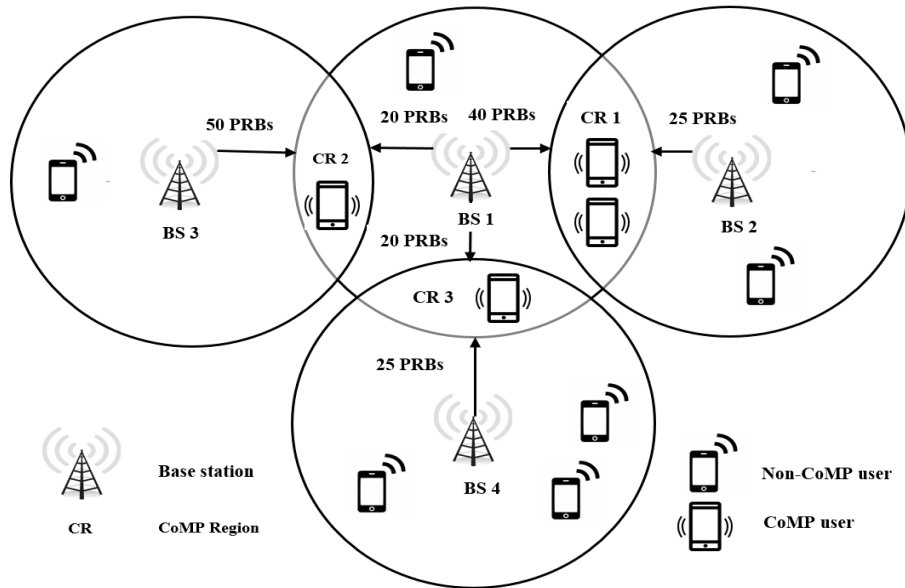


Figure 4.3: An example of resource mismatching for CoMP regions.

To solve this mismatching problem, a resource matching approach is proposed where both base stations need to negotiate and agree on the amount of bandwidth that each base station should provide. Since one base station may have a smaller number of available PRBs than its cooperating base station, both base stations should agree to provide a bandwidth that is equal to the minimum affordable bandwidth of both base stations. This is mathematically explained in Algorithm 4.1 that is presented later in Section 4.4.3 from step 8 to step 15. This strategy will ensure that the two cooperating base stations have perfect matching in terms of the offered bandwidth allowing them to reserve identical PRBs to support their CoMP region. Due to this proposed allocation, the base station that offers a larger bandwidth will be left with a portion of bandwidth that is not used to support the CoMP region. To efficiently utilise this unused portion of bandwidth, this bandwidth is allocated to non-CoMP users that belong to the base station with higher available bandwidth. To further illustrate this concept, an example is provided in Figure 4.4. In Figure 4.4, BS 1 and BS 2 are two cooperating base stations that jointly transmit data to some particular users located in their overlapping region. BS 1 communicates with BS 2 informing it that it has 40 available PRBs. Also, BS 2 sends a message to BS 1 informing that it has 25 PRBs. Each base station then agrees to provide the minimum offered bandwidth of BS 1 and BS 2. In this particular example, BS 1 and BS 2 agree to provide 25 PRBs each. Since BS 1 will be left with 15 unused PRBs (40 PRBs - 25 PRB), it allocates those PRBs for its non-CoMP users.

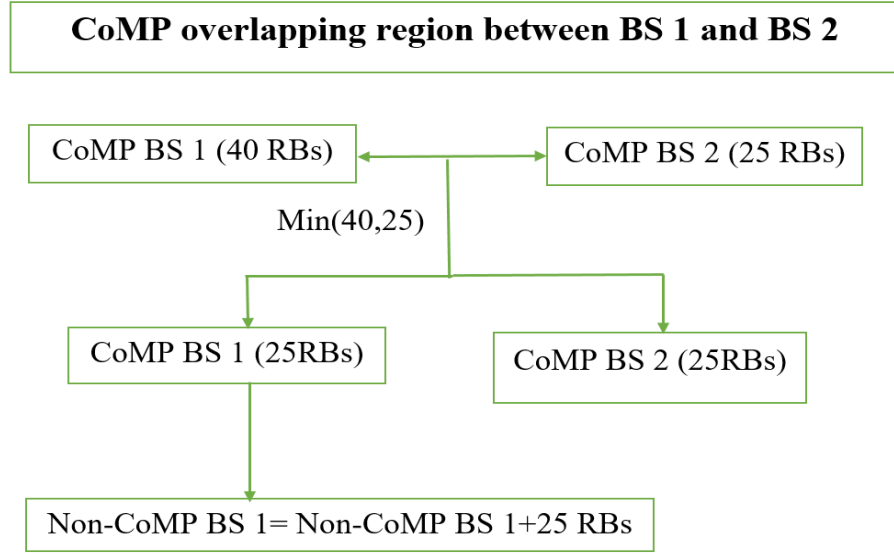


Figure 4.4: An example solved by the proposed resource matching approach

4.4.3 Bandwidth Allocation

This part develops mathematical expressions that divide the total bandwidth into CoMP and non-CoMP bandwidths in order to support both CoMP and non-CoMP UEs. When CoMP is implemented, each base station can have non-CoMP and CoMP users. Non-CoMP UEs are typically UEs that are located in the cell-centre area whereas CoMP users are the UEs that are inside the overlapping areas. The overlapping area can be identified by using the user-centric clustering algorithms presented in Chapter 3.

The following explains how each base station can identify its CoMP and non-CoMP UEs. Each base station considers all UEs in its overlapping regions as its CoMP users without taking into account if this base station is the strongest or second strongest base station. Also, each base station considers the remaining UEs that are located outside the overlapping regions as its non-CoMP UEs.

The total bandwidth of base station i is divided into non-CoMP bandwidth $B_i^{non-CoMP}$ and CoMP bandwidth B_i^{CoMP} as follows:

$$B_i^{non-CoMP} = \frac{B_i}{(|\mathcal{N}_i| + (b|\mathcal{Q}_i|))} \quad (4.9)$$

$$B_i^{CoMP} = BS_i - BS_i^{non-CoMP} \quad (4.10)$$

where B_i is the total available bandwidth and b is the proportion of resources a CoMP UE would be assigned when it operates in CoMP mode compared to those it obtains with no CoMP. For instance, with $b = 0.5$ (half bandwidth assignment), if a UE that operates with no CoMP is allocated 8 PRBs, it would be assigned 4 PRBs if it chooses to operate in CoMP mode. B_i^{CoMP} is the CoMP bandwidth of base station i that should support all the CoMP regions that base station i is involved in. Thus, B_i^{CoMP} is further split into $|\mathcal{P}_i|$ portions where $|\mathcal{P}_i|$ is the number of CoMP regions of base station i . The following expresses how the CoMP bandwidth of base station i is divided among its CoMP regions:

$$B_{ip}^{CoMP} = BS_i^{CoMP} \frac{|\mathcal{D}_{ip}|}{|\mathcal{Q}_i|} \quad (4.11)$$

Algorithm 4.1 illustrates the proposed multi-cell bandwidth allocation that can support JT-CoMP networks.

Algorithm 4.1 Multi-cell bandwidth allocation

```

1: for all  $m \in \mathcal{M}$  do
2: Calculate the non-CoMP bandwidth based on (4.9)
3: Calculate the CoMP bandwidth based on (4.10)
4:   for all  $l \in \mathcal{L}^m$ 
5: Calculate  $B_{ml}^{CoMP}$  based on (4.11)
6:   end for
7:end for
8: for all  $m \in \mathcal{M}$  do
9:   for all  $l \in \mathcal{L}^m$ 
10:     $B_{ml}^{CoMP} = \min(B_{ml}^{CoMP}, B_{V_l^{m_l}}^{CoMP})$ 
11:    if  $B_{ml}^{CoMP} > B_{V_l^{m_l}}^{CoMP}$  then
12:       $B_m^{non-CoMP} = B_m^{non-CoMP} + (B_{ml}^{CoMP} - B_{V_l^{m_l}}^{CoMP})$ 
13:    end if
14:   end for
15: end for

```

4.4.4 Bandwidth Underutilisation Problem

One of the problems that is faced when JT-CoMP is implemented in 5G HetNets is when a base station, particularly a small cell base station, has only CoMP UEs associated with it. In a HetNets non-CoMP system, small cells are lightly loaded due to their low transmission power [109]. When JT-CoMP is applied, the users associated with a small cell base station are split into non-CoMP and CoMP users. In some cases such as when all users of a small cell base station are located at the cell-edge or when

the requirement to operate in a CoMP mode can be easily satisfied due to high PLD and SINR thresholds or low RSS threshold, all users that are associated with a small cell base station become CoMP UEs. A base station with only CoMP UEs might not be able to fully utilise its available bandwidth as its bandwidth utilisation is dependent on the CoMP bandwidth of its set of cooperating base stations. In other words, a base station with only CoMP UEs might be restricted from fully utilising its bandwidth since it cannot provide a bandwidth higher than the bandwidth of any of its cooperating base stations. This is because there must be a bandwidth matching even though this base station has an excess of bandwidth due to the absence of non-CoMP UEs and the fewer number of CoMP UEs compared with its overlapping base stations. This bandwidth underutilisation problem becomes severe if the base station with CoMP UEs only is cooperating with a base station that is highly loaded. That is because a heavily loaded base station would have a low amount of bandwidth to support a CoMP overlapping region while the cooperating small cell base station has a high amount of bandwidth. A good example of this is an overlapping region between a small cell base station and a heavily loaded macro base station. To further illustrate the bandwidth underutilisation problem, Figure 4.5 shows an example when all the users of a small cell base station are served by JT-CoMP. Figures 4.4 (a) shows an overlapping region between a small cell base station that has CoMP UEs only and a heavily loaded macro base station. Due to the heavy load of the macro base station (45 non-CoMP UEs and 5 CoMP UEs), assuming full bandwidth assignment, the macro base station would be able to provide only 10 PRBs to support the overlapping region. As the small cell base station has only one CoMP UE and it does not have any non-CoMP UEs, it is able to support the overlapping region with its full bandwidth, i.e., 100 PRBs. This resource mismatching leaves the small cell base station with 90 PRBs that cannot be utilised. These 90 PRBs could have been utilised and assigned to non-CoMP UEs as proposed in Algorithm 4.1; however, this is not valid in this case due to the absence of non-CoMP UEs. Figure 4.5 (b) shows a CoMP overlapping region between a small cell base station and another small cell base station. The light load of small cell BS 1 and small cell BS 2 allows them to provide the overlapping region with 100 PRBs and 50 PRBs, respectively. This shows that the overlapping region is better supported in this case compared with the case in Figure 4.5(a). Nevertheless, there would still be 50 PRBs that are not utilised.

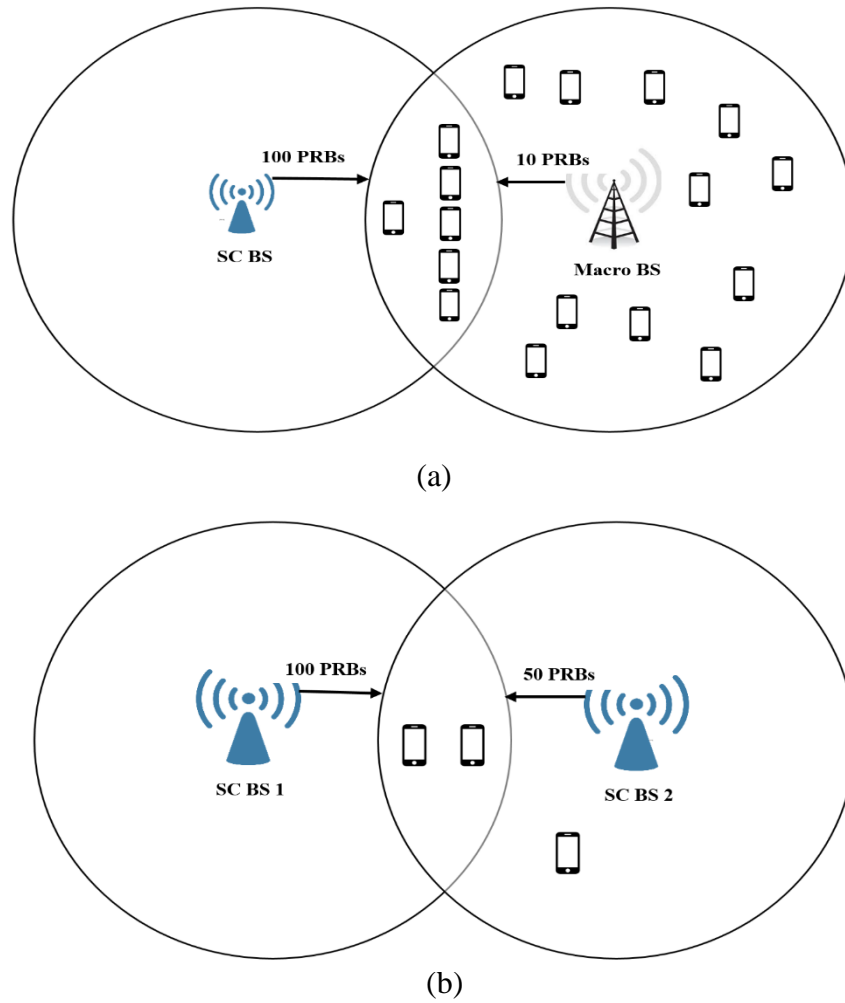


Figure 4.5: The bandwidth underutilisation problem. An overlapping region with a heavily loaded macro base station and a small cell base station is shown in (a) while (b) shows an overlapping region with two small cell base stations where the bandwidth underutilisation problem is less severe.

To address this bandwidth underutilisation problem, a new multi-cell hybrid resource allocation scheme is proposed where a UE that decides based on (3.5), (3.6), (3.7), or (3.10) to operate in CoMP mode can be served by JT-CoMP and no CoMP simultaneously. This hybrid UE can be served by the two strongest base stations on certain PRBs while at the same time the strongest base station can serve this UE on different PRBs. Unlike the proposed multi-cell resource allocation scheme in Algorithm 4.1 where the bandwidth of a base station that cannot support an overlapping region due to resource matching is assigned to its non-CoMP users, this hybrid approach allocates this bandwidth to the set of CoMP UEs of this base station that are located in this overlapping region. Based on this hybrid approach, in an overlapping region, a base

station might be left with some unutilised bandwidth if it has no CoMP UEs who receive the strongest power from this base station but it has some CoMP UEs who receive the second strongest power from this base station. To address this issue, the unutilised bandwidth is assigned to its non-CoMP UEs. Implementing this hybrid scheme can help to address the bandwidth underutilisation problem since small cell base stations can utilise any underspent bandwidth to serve hybrid UEs in no CoMP mode.

Figure 4.6 shows an example that illustrates the concept of the proposed hybrid approach. In Figure 4.6, a hybrid user (UE 1) can be served simultaneously by BSs 1 and 2 (multipoint transmission) on 10 identical PRBs and by BS 1 on another 30 PRBs in no CoMP mode.

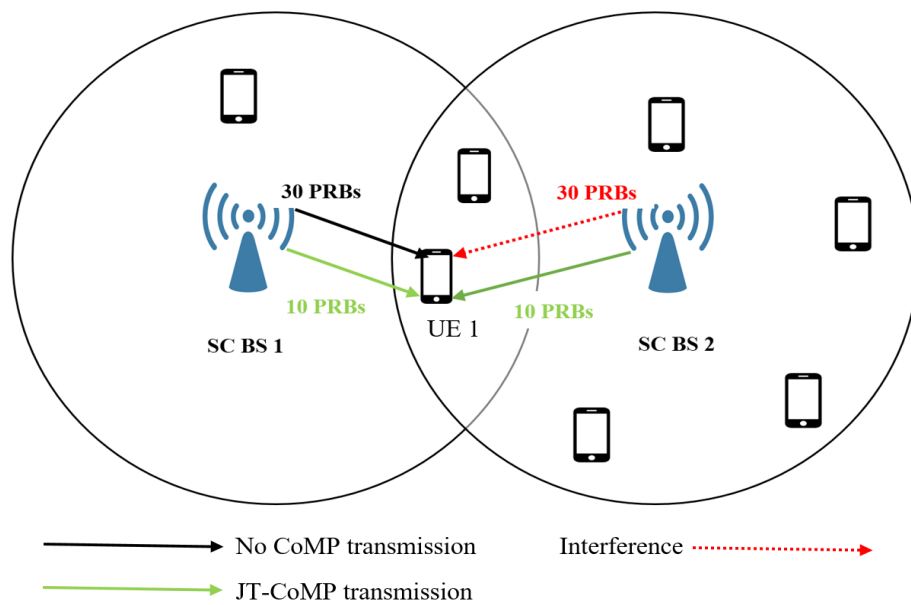


Figure 4.6: The proposed hybrid approach where a hybrid user (UE 1) can be served by no CoMP and JT-CoMP simultaneously.

The pseudo-code for the proposed multi-cell hybrid resource allocation approach is presented in Algorithm 4.2. The hybrid approach follows the traditional JT-CoMP scheme in terms of calculating the non-CoMP bandwidth per base station, CoMP bandwidth per base station, and CoMP bandwidth per overlapping area according to (4.9), (4.10), and (4.11), respectively. Moreover, the hybrid approach implements the proposed resource matching approach. As a consequence, steps 1 to 10 in both Algorithm 4.1 and Algorithm 4.2 are identical.

Algorithm 4.2 Hybrid Multi-cell bandwidth allocation

```
1: Perform steps 1 to 10 in Algorithm 4.1
2:  if  $B_{ml}^{CoMP} > B_{V_l^{m_l}}^{CoMP}$  then
3:   if  $|V_{ml}| = 0$ 
4:     $B_m^{non-CoMP} = B_m^{non-CoMP} + (B_{ml}^{CoMP} - B_{V_l^{m_l}}^{CoMP})$ 
5:   else
6:     $B_{ml}^{non-CoMP} = B_{ml}^{CoMP} - B_{V_l^{m_l}}^{CoMP}$ 
7:   end if
8:  end if
9: end for
10: end for
```

4.4.5 Impact of JT-CoMP on Base Station Loading

The load per base station increases when JT-CoMP is implemented since each base station will serve not only the UEs it provides with the strongest received power as it does with no CoMP but it will also serve the UEs it provides with the second strongest received power. Figure 4.7 provides an example where it is shown how JT-CoMP increases the load per base station. To illustrate the influence of JT-CoMP on the base station loading, some potential load distributions are presented in Figure 4.7. In Figure 4.7(a), BS 1 and BS 2 have 6 and 4 UEs with no CoMP, respectively. When CoMP is applied, the load of BS 1 becomes 7 UEs since the UE that is served by BS 2 with no CoMP operates now in CoMP mode and it needs to be served jointly by BS 1 and BS 2. Similarly, the load of BS 2 will increase from 4 UEs with no CoMP to 7 UEs with CoMP. It is clear that JT-CoMP has a direct impact on the base station loading. Considering a full bandwidth assignment where a CoMP UE obtains the same amount of bandwidth as a non-CoMP UE and also considering the proposed resource matching approach described in Section 4.4.2, the non-CoMP UEs of BS 1 will obtain slightly fewer PRBs since there is only one extra UE that needs to be served by BS 1. Although BS 2 needs help from BS 1 to jointly serve one of its UEs, BS 1 will require BS 2 to jointly serve 3 of its UEs. As a result, the non-CoMP UEs of BS 2 will be left with fewer radio resources. This scenario shows that both non-CoMP UEs of BS 1 and BS 2 need to sacrifice a certain amount of bandwidth in order to improve the throughput performance of the CoMP UEs. Figure 4.7(b) shows the same scenario of load distribution as in Figure 4.7(a) except that BS 1 has only one non-CoMP user. Since BS 1 can support a higher bandwidth for the CoMP region as it has fewer non-CoMP UEs compared with BS 2, it will have to match the bandwidth provided by BS 2 to support the CoMP region. After resource matching, the CoMP bandwidth that BS 1 did not utilise will be reallocated to the non-CoMP UE of BS 1 in the case that Algorithm 4.1 is

implemented. The non-CoMP user of BS 1 will achieve significantly higher throughput compared with that with no CoMP. In Figure 4.7(c), BS 2 can provide higher bandwidth for the CoMP region

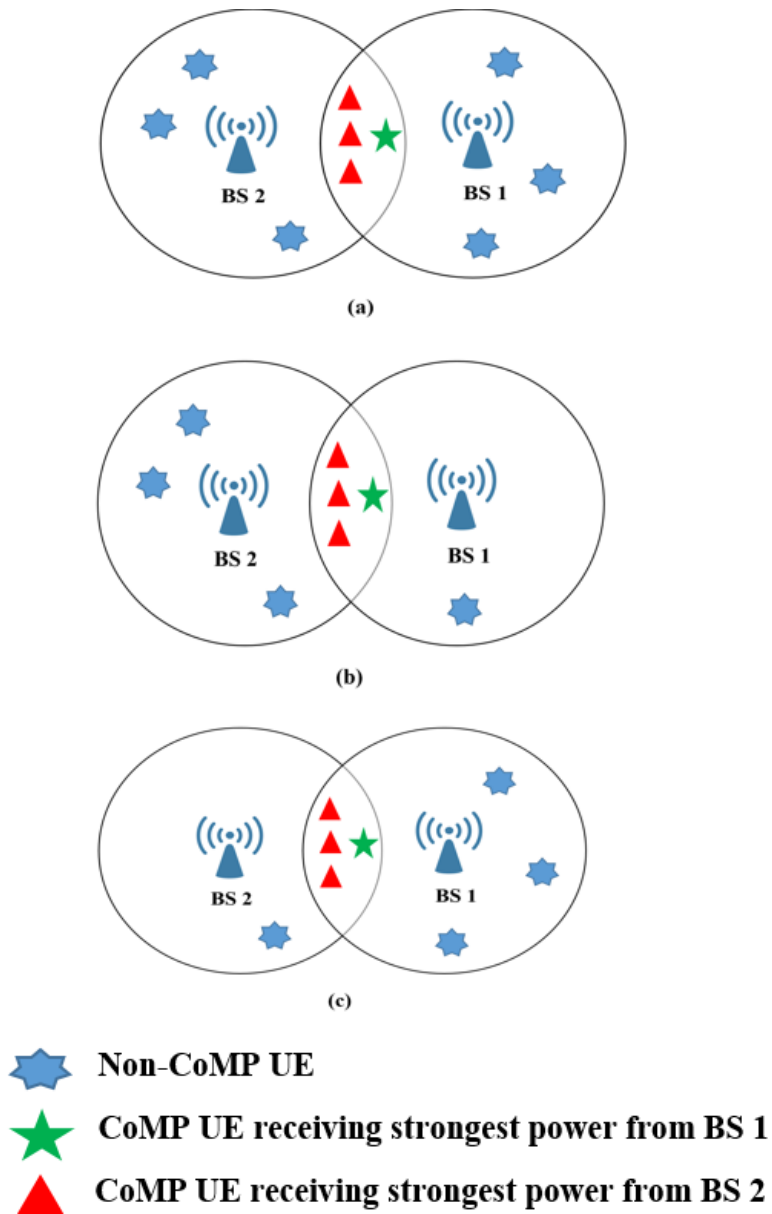


Figure 4.7: Some potential load distributions in JT-CoMP.

as it has fewer non-CoMP UEs compared with BS 1. Although BS 2 will reallocate the unused amount of CoMP bandwidth to its non-CoMP UE, this UE still achieves higher throughput with no CoMP as the unused CoMP bandwidth allocated for this UE is not large. In other words, the amount of bandwidth this UE is assigned when CoMP is

implemented is less than the bandwidth it obtains with no CoMP, even if it still obtains a bandwidth bonus via the resource matching approach.

4.5 Performance Comparison

The simulation parameters used in this chapter are the same parameters used in Chapter 3. This includes the pathloss model, shadowing, simulation area, transmission power of macro, pico, and femto base stations, and noise floor. When the traditional JT-CoMP and the hybrid approach are implemented, the maximum user-centric cluster size is set to 2. There are two main reasons to limit the number of cooperating base stations to 2. First, as shown in Figure 3.2, allowing more than two base stations to cooperate requires an extremely high SINR gain in order to compensate for the bandwidth loss. From Figure 3.2, if a user achieves a 5 dB SINR with no CoMP, it must achieve at least 18.5 dB when it operates with three ways CoMP in order to compensate for the bandwidth loss. This SINR gain is clearly hard to achieve. Another reason for not allowing three or more base stations to cooperate is because of the load unevenness that happens due to load imbalance among base stations. This load unevenness problem reduces the available bandwidth for CoMP users as all cooperating base stations except the base station with the minimum CoMP bandwidth cannot use their full CoMP bandwidth to support their overlapping CoMP region. The base station with the minimum CoMP bandwidth clearly restricts the benefit available from JT-CoMP. In the case of a maximum user-centric cluster size of 2 and a significant load imbalance among cooperating base stations, a CoMP user might perform better if it were to operate in non-CoMP mode. Obviously, allowing more than two base stations to cooperate increases the load unevenness level which further restricts cooperating base stations from supporting their CoMP regions. Macro base stations are distributed according to a hexagonal deployment with inter-site distance of 500 m while pico and femto base stations are modelled by repulsive PPP with a repulsion distance of $\delta_p = 20$ m and $\delta_f = 10$ m, respectively. The density of pico base stations λ_{pm} and femto base stations λ_{fm} is 16 base stations/km², and 32 base stations/km², respectively. Users are distributed based on an independent PPP with a density of 560 UE/km². The performance of the four user-centric clustering approaches presented in Chapter 3 are compared. In Chapter 3, a 6 dB PLD, an RSS of -57 dBm, and an SINR of 3 dB have shown better performance compared with other thresholds. Thus, this chapter sets the

thresholds of PLD, RSS, and SINR to 6 dB, -57 dBm, and 3 dB, respectively. The performance of no CoMP, traditional JT-CoMP and the hybrid approach are compared in terms of overall user throughput, cell-edge throughput and macro-cell-edge throughput. Cell-edge users are defined as the 5th percentile of the distribution of user SINR with no CoMP and their throughput is defined as the cell-edge throughput. This definition may include a few users with extremely poor SINR due to heavy shadowing although they are not physically located in the cell-edge area. The macro-cell-edge throughput is defined as the 5th percentile no CoMP user throughput. It is expected that most of the macro-cell-edge users belong to macro base stations due to the heavy load. However, there might be a few macro-cell-edge users who are associated with small cell base stations.

Figure 4.8 shows the outage probability with and without JT-CoMP when the maximum user-centric cluster size c_{max} is limited to 2. In this figure, c_{max} is limited to 2, unlike Figure 3.10 where c_{max} is limited to 8. Comparing Figures 3.10 and 4.7, it is obvious that better outage probability is achieved when c_{max} is 8. This is because increasing c_{max} from 2 to 8 would allow some UEs to be served by more than 2 base stations, thus converting the third, fourth, and c_{max} most dominant interfering signals into useful signals. As Figures 3.10 and 4.7 show, the percentage of UEs that achieve higher than 0 dB is reduced from 100%, 93%, 100% and 91% to 94%, 91%, 94%, and 88% for the PLD, RSS, SINR, and proposed UCCA approach, respectively when c_{max} changes from 8 to 2.

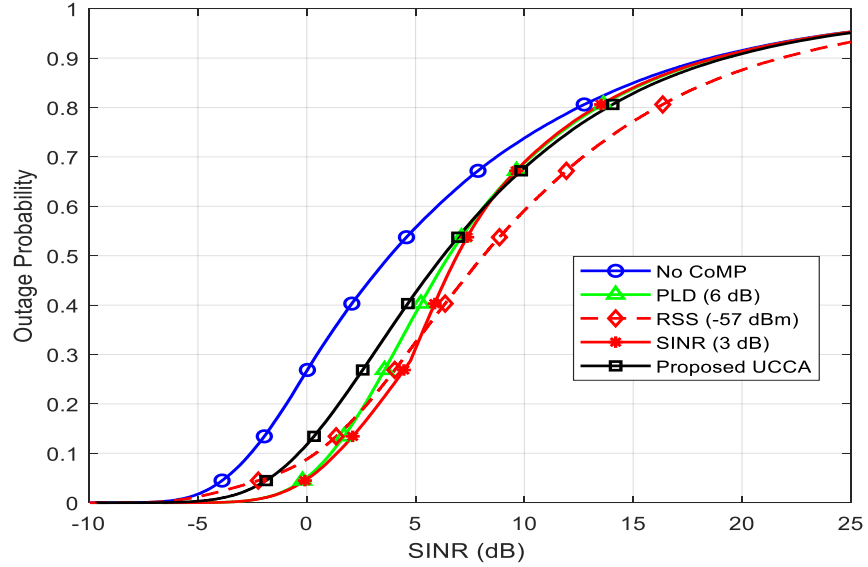


Figure 4.8: Outage probability with no CoMP and with the PLD (6 dB), RSS (-57 dBm), SINR (3 dB), and the proposed UCCA approaches when $c_{max} = 2$.

To evaluate the performance of JT-CoMP in HetNets, Figure 4.9 shows the CDF of the overall user throughput when $b = 1$, i.e., full bandwidth assignment. From the figure, no CoMP clearly outperforms all the user-centric JT-CoMP approaches. The worst performance is achieved by the RSS approach followed by the SINR, PLD, and proposed UCCA approach. In a no CoMP system, the percentage of users that achieve higher than 1 Mbps is 39%. When JT-CoMP is applied, this percentage reduces to 30%, 28%, 28%, and 35% when the PLD, RSS, SINR, and proposed UCCA JT-CoMP approaches are implemented, respectively. The poor performance achieved by JT-CoMP is because of the bandwidth underutilisation problem explained in Section 4.4.4. When $b = 0.5$ (half bandwidth assignment) and $b = 2$ (double bandwidth assignment), no CoMP also outperforms JT-CoMP. The results are not shown for the two cases of $b = 0.5$ and $b = 1$ to avoid repeating showing results that draw the same conclusion. Moreover, the impact of assigning different portions of bandwidth for CoMP users is going to be investigated.

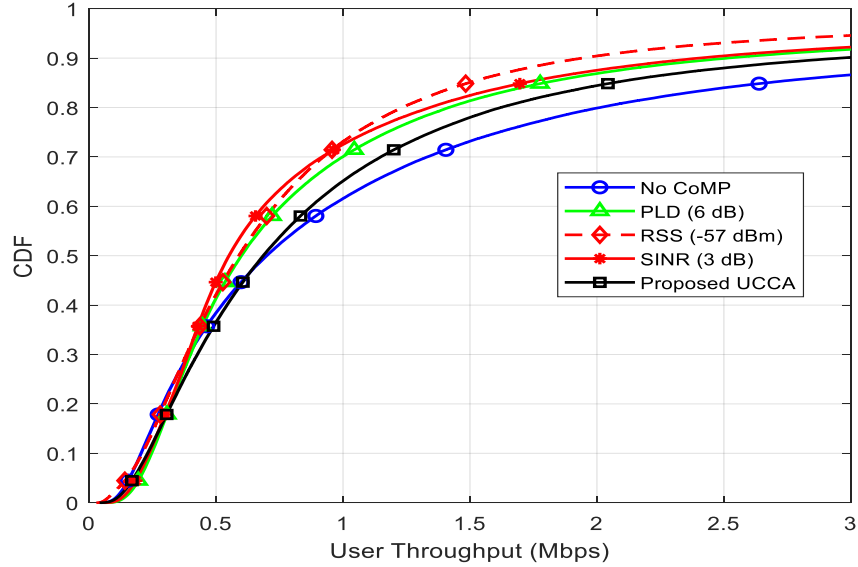


Figure 4.9: User throughput with and without JT-CoMP. In JT-CoMP, full bandwidth assignment is considered.

Figure 4.10 compares the CDF of the throughput of cell-edge users when $b = 1$ with no CoMP and with JT-CoMP. As Figure 4.10 shows, all user-centric JT-CoMP clustering approaches except the RSS approach can provide significant throughput gain for cell-edge users compared with no CoMP. The best performance is achieved by the proposed UCCA followed by the PLD and SINR approaches. The poor performance of RSS is because most of the cell-edge users are not served by JT-CoMP when the RSS clustering approach is implemented. Since the RSS approach relies on the average received power and due to the high and low transmission powers of macro base stations and small cell base stations, respectively, most of the users that operate in JT-CoMP are associated with macro base stations even if they are not physically located in the cell-edge area. Also, most of the cell-edge users of small cell base stations operate in a no CoMP mode as it is hard for them to satisfy the RSS threshold requirement in (3.6). As a result, macro users with high SINR benefit from the SINR gain as well as the full bandwidth assignment at the expense of the small cell cell-edge users who operate in no CoMP mode. This clearly shows that the RSS approach is not effective in HetNets although it has shown the best performance in terms of outage probability as illustrated in Figures 3.10 and 4.7. Comparing no CoMP and JT-CoMP, Figure 4.10 illustrates that 77%, 74%, and 84% of the cell-edge users obtain better throughput when

the PLD, SINR, and proposed UCCA are implemented, respectively. This significant cell-edge throughput improvement is achieved because the cell-edge users are assigned full bandwidth. Since a CoMP UE is assigned a bandwidth that it would obtain if it operated with no CoMP, the cell-edge throughput improvement comes from the SINR gain. Assuming perfect resource matching and load balance, this full bandwidth assignment should improve the throughput of all cell-edge users. However, due to the resource mismatching problem, a cell-edge CoMP UE with slight SINR gain may perform better with no CoMP as shown in Figure 4.10. From Figures 4.9 and 4.10, the benefits of the proposed UCCA approach is that it can significantly improve the cell-edge throughput without affecting the overall throughput, unlike the compared existing user-centric schemes. The limitation of this approach is that it does not provide the best performance in terms of outage probability as shown in Figure 4.8. The proposed approach can be applied in systems where fairness among users is crucial

To evaluate the performance and effectiveness of the proposed hybrid approach, it is compared with no CoMP and with the traditional JT-CoMP scheme in terms of overall user throughput and cell-edge throughput. In this comparison, users in both the traditional JT-CoMP and the proposed hybrid approach first form their own clusters based on the best two user-centric clustering algorithms which are the PLD and proposed UCCA approach. As illustrated in Figures 4.8 and 4.9, the proposed UCCA and the PLD perform better than the RSS and SINR approaches. Based on the clustering results, radio resources are assigned based on Algorithm 4.1 for the traditional JT-CoMP scheme while in the hybrid approach, radio resources are allocated according to Algorithm 4.2. Considering the PLD and the proposed UCCA approach, Figure 4.10 compares the performance of no CoMP, the traditional JT-CoMP scheme and the hybrid

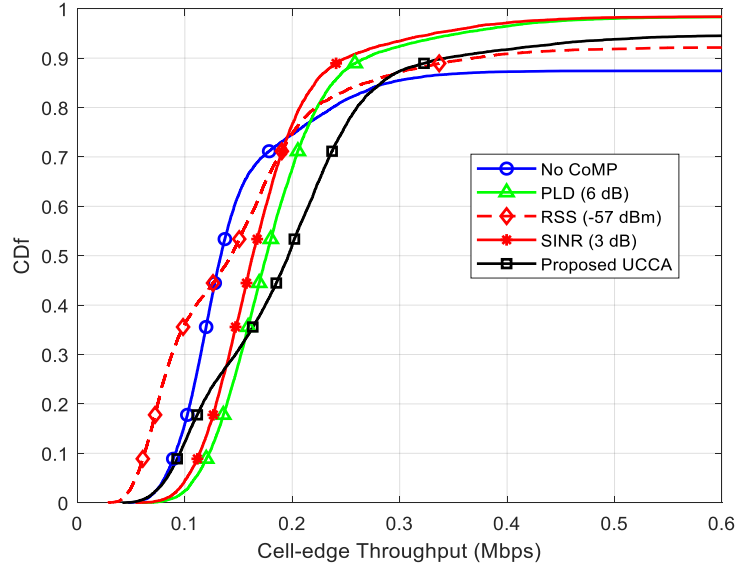


Figure 4.10: Cell-edge throughput with and without JT-CoMP. In JT-CoMP, full bandwidth assignment is considered

scheme in terms of the overall user throughput when $b = 1$. Figure 4.11 shows that the hybrid approach outperforms the traditional JT-CoMP approach in terms of the overall user throughput. Also, the performance of the hybrid approach, particularly when the proposed UCCA is implemented, is comparable to no CoMP. From Figure 4.11, the percentage of users that achieve higher than 1 Mbps is 38%, 30%, 35%, 35%, and 38% when no CoMP, JT-CoMP with PLD, hybrid approach with PLD, JT-CoMP with the proposed UCCA algorithm, hybrid approach with the proposed UCCA algorithm are implemented, respectively. The poor performance achieved by the traditional JT-CoMP is due to the bandwidth underutilisation problem where some small cell base stations cannot fully utilise their bandwidth. The hybrid approach achieves good performance because it efficiently utilises the bandwidth and it also benefits from the SINR gain.

Considering a full bandwidth assignment ($b = 1$) and the PLD and the proposed UCCA as user-centric clustering approaches, Figure 4.12 shows the CDF of cell-edge throughput when no CoMP, the traditional JT-CoMP, and the hybrid approach are implemented. As Figure 4.12 illustrates, both the traditional JT-CoMP and the hybrid approach provide significant throughput improvement for cell-edge users. The figure also shows that users at the edge achieve better throughput when the hybrid approach is applied compared with the traditional JT-CoMP. From Figure 4.12, the percentage of cell-edge users that achieves higher than 0.2 Mbps with no CoMP is 26%. The

traditional JT-CoMP approach increases this percentage to 29% and 47% when the PLD and proposed UCCA approaches are implemented, respectively. The hybrid approach increases this percentage further to 47% and 55% when the PLD and the proposed UCCA clustering approaches are used to form the cluster of each cell-edge user, respectively. The reason that the hybrid approach outperforms the traditional JT-CoMP approach is because, in the hybrid approach, the unutilised bandwidth due to resource matching can be used to serve cell-edge users in a non-CoMP mode. This is not valid in the traditional JT-CoMP approach as cell-edge users in an overlapping area are not capable of operating in a non-CoMP mode to use the unutilised bandwidth.

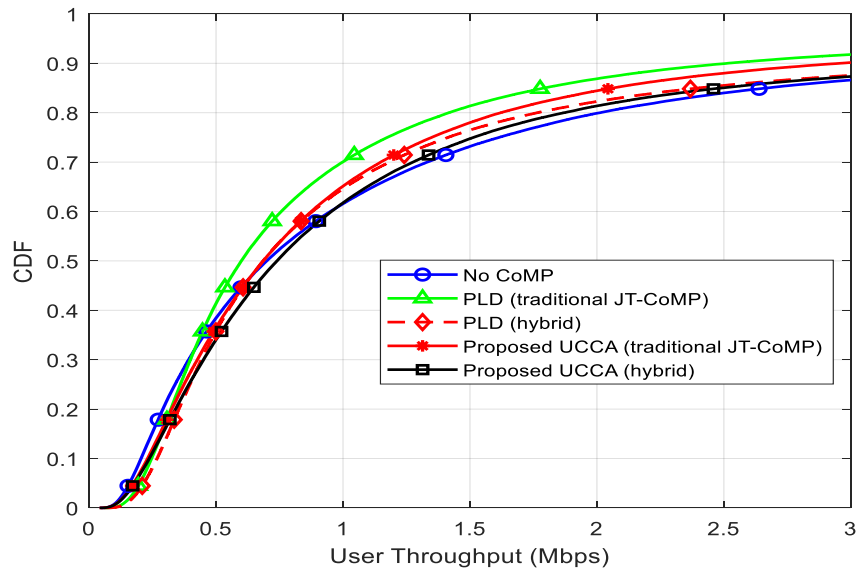


Figure 4.11: A comparison between no CoMP, the traditional JT-CoMP and the hybrid approach in terms of overall user throughput. In the traditional JT-CoMP and the hybrid approach, full bandwidth assignment is considered.

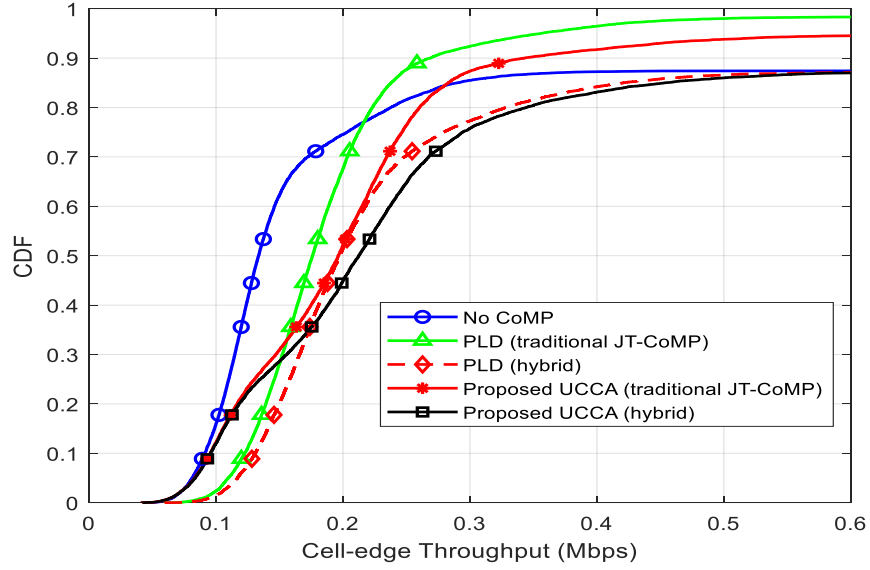


Figure 4.12: A comparison between no CoMP, the traditional JT-CoMP and the hybrid approach in terms of cell-edge throughput. In the traditional JT-CoMP and the hybrid approach, full bandwidth assignment is considered.

It is crucial to investigate the performance of the overall user throughput and cell-edge throughput when different portions of bandwidth is assigned for users that operate in a CoMP mode. The impact of assigning half bandwidth, full bandwidth, and double bandwidth is evaluated when the hybrid approach is implemented and users form their own clusters of base stations based on the proposed UCCA. The proposed UCCA scheme is used as user-centric clustering approach as it has shown its effectiveness in Figures 4.10 and 4.11 in improving both the overall throughput and cell-edge throughput. Figure 4.13 shows the CDF of the overall user throughput with no CoMP, half bandwidth, full bandwidth, and double bandwidth assignments. It can be seen that half bandwidth assignment performs better than no CoMP. Also, the performance of full bandwidth assignment is comparable to no CoMP. The worst performance is achieved when double bandwidth is considered. The poor performance of double bandwidth is because allocating a high proportion of bandwidth to hybrid users reduces the amount of bandwidth for non-CoMP users. Due to double bandwidth assignment, some non-CoMP users with high SINR obtain less radio resources resulting in a low throughput. In the case of half bandwidth assignment, the amount of bandwidth a non-CoMP user obtains is almost the same amount of bandwidth it obtains when it operates with no CoMP; thus, no significant throughput reduction occurs. In addition, CoMP users can achieve some throughput gain which helps to improve the overall user throughput. When full

bandwidth assignment is considered, the throughput of cell-edge users is improved due to the SINR gain; however, the throughput of non-CoMP is slightly decreased since they are assigned slightly less bandwidth compared with no CoMP. This behaviour is shown in Figure 4.13 where full bandwidth assignment outperforms no CoMP region in the low throughput region (0.1 to 0.9 Mbps) while no CoMP performs slightly better than full bandwidth assignment in terms of the percentage of users who achieve higher than 0.9 Mbps. According to Figure 4.13, 38%, 41%, 38%, and 35% of users achieve a throughput higher than 1 Mbps when no CoMP, half bandwidth, full bandwidth, and double bandwidth are considered, respectively.

Figure 4.14 shows the cell-edge throughput for no CoMP, half bandwidth, full bandwidth, and double bandwidth. As shown in Figure 4.14, increasing the CoMP bandwidth from half bandwidth to double bandwidth assignment can significantly improve the cell-edge throughput. The percentage of users that obtain higher than 0.2 Mbps increases from 23% with no CoMP to 24%, 54%, and 71% when half, full, double

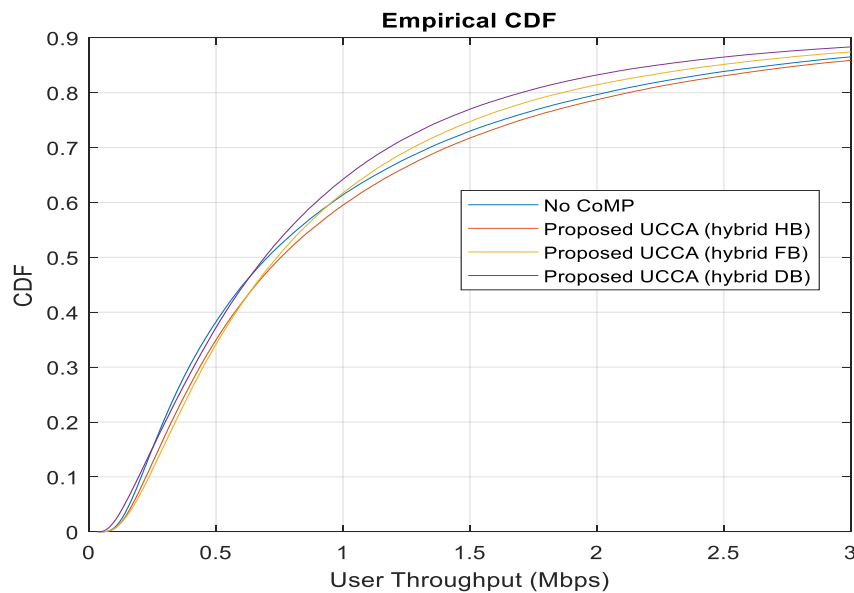


Figure 4.13: A comparison of assigning half bandwidth, full bandwidth, and double bandwidth for CoMP users in terms of user throughput when the hybrid approach is implemented.

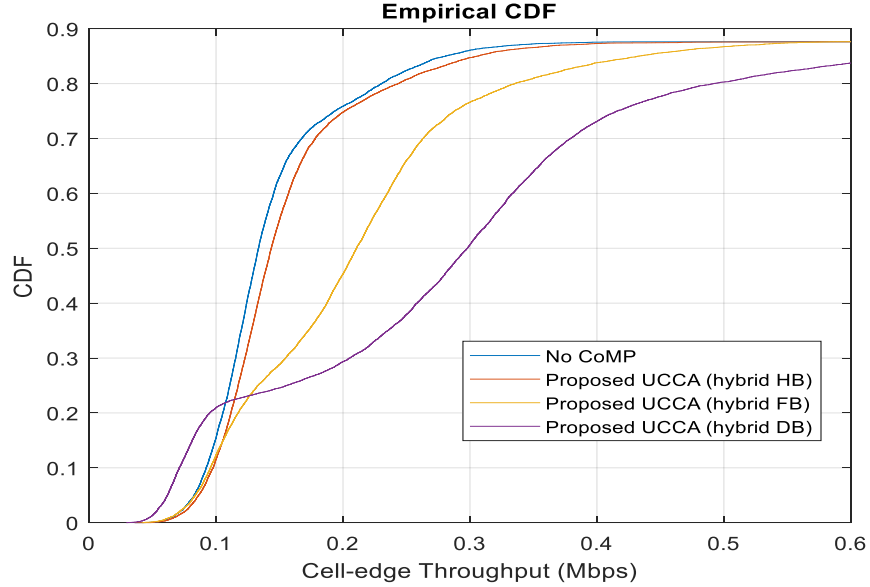


Figure 4.14: A comparison of assigning half bandwidth, full bandwidth, and double bandwidth for CoMP users in terms of cell-edge throughput when the hybrid approach is implemented.

bandwidth assignments are considered. It is also obvious that half bandwidth assignment is not an effective allocation scheme in improving the cell-edge throughput as its performance is almost as poor as no CoMP. The only good aspect of half bandwidth assignment is that it does not degrade the overall throughput as can be seen from Figure 4.13. Full bandwidth assignment shows significant cell-edge throughput without severely affecting the overall throughput. Although double bandwidth assignment performs better than half and full bandwidth assignment in terms of cell-edge throughput, this improvement comes at the expense of the overall user throughput as shown in Figure 4.13. Comparing no CoMP and double bandwidth assignment, it is shown that there are some users that perform better when they operate with no CoMP compared with double bandwidth assignment scheme. These are non-CoMP users with poor SINR who could not meet the requirement in (3.10) in order to become hybrid users. Since these non-CoMP users have the same SINR level in both no CoMP and a CoMP system, their throughput degradation is due to obtaining less amount of radio resources.

It is interesting to investigate the impact of implementing CoMP on the users that achieve the lowest throughput. In a single-tier network, these users are the cell-edge users. However, in HetNets, these users are not necessarily the users located at the cell-edge area. Users in HetNets can achieve low throughput due to two reasons: low SINR

and low amount of assigned bandwidth due to a heavy load on its associated base station. Due to the heavy load on macro base stations, it is expected that cell-edge users of macro base stations are the users that achieve the lowest throughput. Considering full bandwidth assignment, Figure 4.15 shows the CDF of the 5% percentile of users with the lowest throughput when they operate with no CoMP. As Figure 4.15 shows, both traditional JT-CoMP and the hybrid approach can significantly enhance the macro-cell-edge throughput. In the no CoMP system, no macro-cell-edge user can achieve higher than 0.2 Mbps. This is because the macro-cell-edge users suffer from high levels of interference. In addition, they are allocated a low amount of PRBs due to the heavy load on macro base stations. The percentage of macro-cell-edge users that achieve a throughput higher than 0.2 Mbps increases from 0% with no CoMP to 35% and 42% when the traditional PLD JT-CoMP and the traditional JT-CoMP with the proposed UCCA are implemented, respectively. This significant improvement is due to the high SINR gain and the full bandwidth assignment. From Figure 4.15, it is clear that the performance of the hybrid approach is slightly better than the traditional JT-CoMP approach. The hybrid approach provides slight improvement because its main aim is to solve the bandwidth underutilisation problem of small cell base stations and help the users associated with small cell base stations to significantly improve their throughput as shown in Figures 4.10 and 4.11. The throughput improvement of the macro-cell-edge-users comes from the SINR gain and not from the hybrid approach. This slight improvement confirms that most of the users with the lowest throughput are macro users located at the cell-edge. Another observation from Figure 4.15 is that the PLD approach performs better than the proposed UCCA approach for the poorest users, when the CDF is below about 50%. This is because some macro-cell-edge users operate in JT-CoMP when the PLD approach is implemented while the same set of users operates in no CoMP mode when the proposed UCCA approach is applied as they cannot meet the requirement in (3.10). Due to this reason, these users achieve better throughput in the case of the PLD approach as they can benefit from the SINR gain and the full bandwidth assignment. However, this throughput improvement comes at the expense of the overall throughput as can be seen from Figure 4.11.

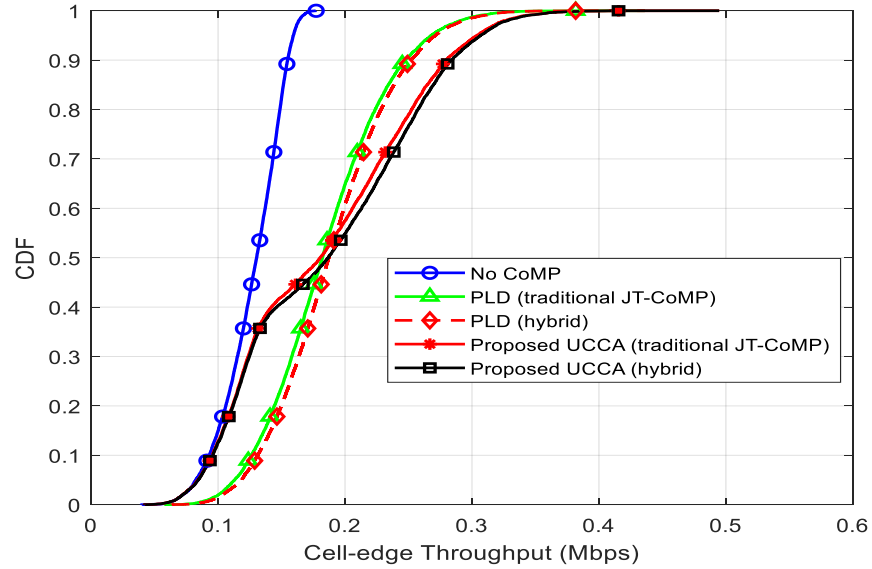


Figure 4.15: Macro-cell-edge throughput with and without CoMP. Full bandwidth assignment is considered when the JT-CoMP and the hybrid approach are implemented.

4.6 Conclusion

It is essential to jointly consider user-centric clustering and multi-cell radio resource allocation in order to provide a complete and comprehensive evaluation on the performance of JT-CoMP. Joint user-centric clustering and resource allocation are performed in two phases. In the first phase, the cluster of each user is identified by the user-centric algorithms presented in Chapter 3. Based on the obtained clustering results, resources from multiple base stations are assigned. Multi-cell radio resource allocation in JT-CoMP HetNets faces two main challenges. The first challenge is the resource mismatching that occurs due to the load unevenness among cooperating base stations. This resource mismatching problem has been addressed by letting two cooperating base stations agree on the number of PRBs that each base station can provide. Another challenge is the bandwidth underutilisation problem where some small cell base stations might have unutilised bandwidth due to the absence of non-CoMP users and the inability to support its CoMP regions as it has to follow the resource matching approach. This problem happens because of the load imbalance between different base stations. To address this problem, a hybrid approach has been proposed where a cell-edge user can operate in both CoMP and non-CoMP modes simultaneously.

The traditional JT-CoMP approach has shown poor performance in terms of the overall user throughput due to the bandwidth underutilisation problem. The bandwidth

underutilisation problem has been mitigated by implementing the proposed hybrid approach. According to the results, the hybrid approach has shown its effectiveness in improving the cell-edge throughput without reducing the overall throughput, unlike the traditional JT-CoMP scheme. The proposed hybrid scheme is a promising solution to reduce inter-cluster interference in HetNets; however, users are required to operate in non-CoMP mode and CoMP simultaneously which increases the complexity level particularly in terms of multi-cell resource allocation. The increased multi-cell resource allocation complexity can be reduced by designing a cell-less architecture that can manage radio resources centrally. The impact of allocating different amounts of bandwidth to CoMP UEs has been investigated. The results have demonstrated that half bandwidth assignment can improve the overall user throughput; nevertheless, its cell-edge throughput is almost as poor as no CoMP. The double bandwidth assignment has shown significant cell-edge throughput but at the expense of the overall users. As results have shown, the implementation of double bandwidth assignment is not a suitable allocation scheme as it significantly degrades the overall system performance. The results have shown that it is better to implement full bandwidth assignment as it can significantly enhance the cell-edge throughput while the overall throughput is not degraded. Considering full bandwidth assignment and the proposed UCCA approach, the percentage of bottom 5% users that achieve higher than 0.2 Mbps is increased from 26% with no CoMP to 47% and 55% when the traditional JT-CoMP and the proposed hybrid approach are implemented respectively. Another observation of implementing both the traditional JT-CoMP and the hybrid approach is that both schemes can significantly help to improve the throughput of users that obtain low throughput due to the heavy load on macro base stations when they operate with no CoMP. The percentage of low throughput users that achieve higher than 0.2 Mbps increases from 0% with no CoMP to 44% and 42%, when the hybrid and conventional JT-CoMP approaches are applied, respectively.

Although user-centric clustering has shown promising performance particularly in improving cell-edge throughput, this type of clustering increases the complexity and overheads as UEs can select their own set of base stations with no limit. To reduce this complexity and overheads, base stations are first grouped into base station clusters and then each UE forms its own set of cooperative base stations that belong to the same cluster. Deploying this approach does not only help to reduce the complexity and

overheads caused by user-centric clustering but it also leads to a cell-less architecture that promises to provide better coverage and higher throughput particularly for cell-edge users. The next chapter utilises the developed resource matching approach as well as the hybrid approach to form a cell-less architecture where users can be served by multiple base stations that belong to the same base station cluster.

CHAPTER 5

5G Cell-less Architecture

Contents

5.1	Introduction	107
5.2	System Model	108
5.2.1	Performance Metrics	111
5.3	Performance Evaluation	111
5.3.1	Impact of CPU Densification.....	116
5.3.2	Impact of Different Cluster-edge Distances	119
5.4	Conclusion	125

5.1 Introduction

The implementation of user-centric JT-CoMP clustering in a cell-centric architecture as in Chapter 3 and 4 has shown significant improvements in terms of outage probability, overall user throughput and bottom 5% throughput. Nonetheless, a cell-centric implementation increases the level of complexity and overheads as there is no limit on the set of cooperating base stations that a user can choose. This cell-centric problem motivates design of a cell-less architecture where complexity and overheads can be reduced. In addition, designing a cell-less architecture can aid in reducing inter-cell interference that has always been a major concern in cell-centric wireless architectures. In a cell-less architecture, a number of macro and small cell base stations are geographically distributed over an area where each base station is associated with its nearest CPU and each user can be jointly served by multiple base stations that are connected to the same CPU.

The main contributions of this chapter are as follows:

- 1) Development of a novel cell-less architecture that allows macro base stations located at the edge of a cluster to be connected to multiple CPUs.

- 2) A comparison between the zero forcing technique and the developed hybrid approach that utilises the proposed resource matching scheme in a cell-less architecture.
- 3) Evaluating the performance of a cell-less architecture under different CPU densities and different cluster-edge distances.

The organisation of the rest of this chapter is as follows. Section 5.2 presents the system model. Section 5.3 compares the performance of cell-centric and cell-less architectures. It also investigates the performance of a cell-less architecture when different CPU densities and cluster-edge distances are considered. Section 5.4 concludes the work presented in this chapter.

5.2 System Model

Similar to Chapters 3 and 4, a three tier downlink heterogeneous network that consists of M macro base stations, P pico base stations and F femto base stations is considered in this chapter. The area is divided into several regions where each region has one CPU. A CPU can be collocated with one of the macro base stations. Each base station is connected to its nearest CPU via front-haul connections. The technology that provides front-haul connections between base stations and CPUs and any limitations this technology might have is out of scope. As in [74], it is assumed that front-haul connections have unlimited bandwidth. Let \mathcal{A} denote the set of all base stations in the area, \mathcal{S} denotes the set of CPUs, \mathcal{D} and \mathcal{Z} denote the set of base stations and users that belong to cluster s , respectively and \mathcal{U} represents the set of users associated with base station m . The system model is shown in Figure 5.1. Two main cases are investigated: cell-centric and a cell-less architecture. In the cell-less design, two different models are considered: the hybrid approach developed in Chapter 4 (CLH) and zero forcing (CLZF).

In CLH, user-centric JT-CoMP clustering is implemented where a user can be served by the two strongest base stations irrespective of their tier as long as these two base stations are connected to the same CPU. Similar to the work in [40], each user measures the average received power from its neighbouring base stations and reports the power levels to its serving base station, i.e., its strongest base station. Then, the serving base stations sends the signal levels to its associated CPU. The CPU uses this power

level information to assign users their own cluster of base stations for cooperation. In this approach, the SINR of user k is calculated as follows:

$$SINR_k = \frac{\sum_{j \in \mathcal{C}_k} P_i^{Tx} |g_{kj}|^2}{\sum_{i \in \mathcal{A}/\mathcal{C}_k} P_i^{Tx} |g_{ki}|^2 + \sigma^2} \quad (5.1)$$

The equation in (5.1) is similar to (3.1) except that the set of cooperating base stations in (5.1) is limited to base stations that belong to the same CPU.

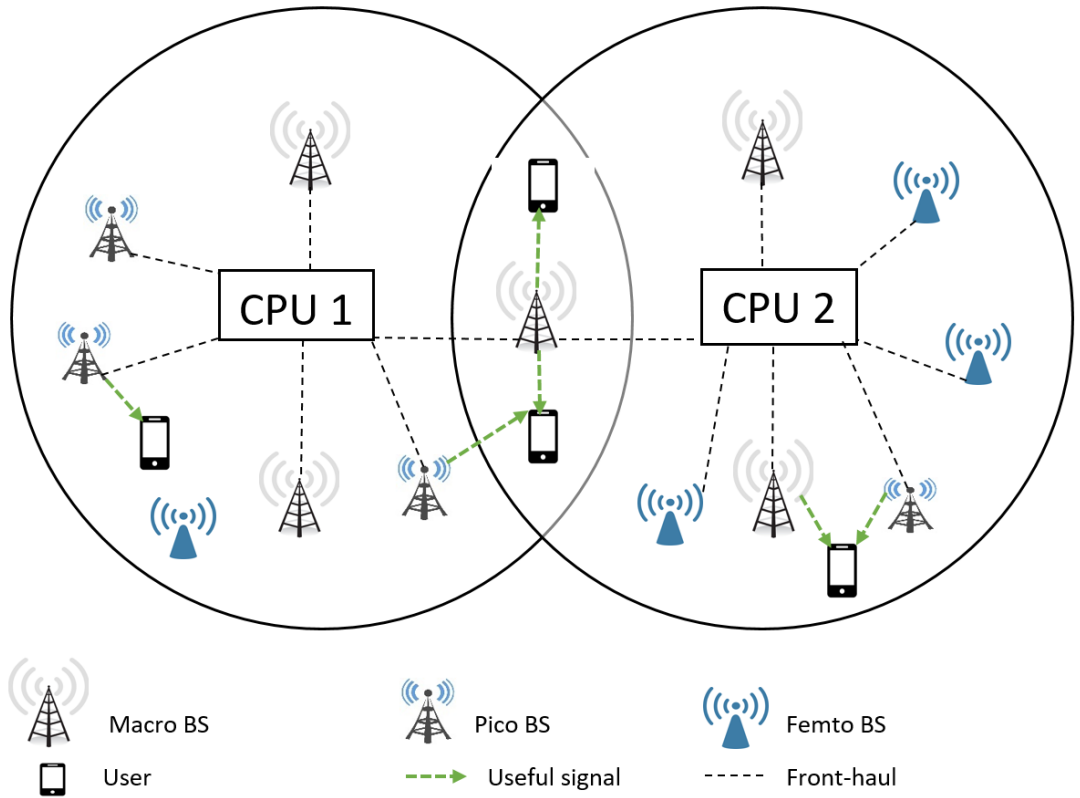


Figure 5.1: System model

In the case of CLZF, perfect CSI knowledge is assumed. The implementation of ZF precoding can completely eliminate intra-cluster interference [40, 110]. The received signal at user k can be calculated as follows:

$$\mathbf{y} = \mathbf{H}\mathbf{W}\mathbf{x} + \mathbf{n} \quad (5.2)$$

where \mathbf{x} is the transmitted signal and \mathbf{n} is the noise power.

Channel vectors for user k are expressed as follows:

$$\mathbf{h}_k = [h_{k1} \ h_{k2} \ \dots \ h_{kc_{max}}] \quad (5.3)$$

where $\mathbf{H} = [\mathbf{h}_1 \ \mathbf{h}_2 \ \dots \ \mathbf{h}_K]^T$

The expression of beaming vectors for user k is as follows:

$$\mathbf{w}_k = [w_{1k} \ w_{2k} \ \dots \ w_{c_{maxk}}]^T \quad (5.4)$$

where $\mathbf{W} = [\mathbf{w}_1 \ \mathbf{w}_2 \ \dots \ \mathbf{w}_K]$

The received signal at a user k can be expressed as:

$$y_k = \mathbf{h}_k^{C_k} \mathbf{w}_k^{C_k} x_k + \sum_{i \in \mathcal{Z}/k} \mathbf{h}_k^{C_k} \mathbf{w}_i^{C_k} x_i + \sum_{j \in \mathcal{K}/\mathcal{Z}} \mathbf{h}_k^{A/C_k} \mathbf{w}_j^{A/C_k} x_j + n_k \quad (5.5)$$

The first term in (5.5) represents the desired signal received by user k , intra-cluster and inter-cluster interference are represented by the second and third terms of (5.5), respectively, and n_k represents the noise power.

The SINR received by user k can be written as follows [40]:

$$SINR_k = \frac{|\mathbf{h}_k^{C_k} \mathbf{w}_k^{C_k} x_k|^2}{|\sum_{i \in \mathcal{Z}/k} \mathbf{h}_k^{C_k} \mathbf{w}_i^{C_k} x_i|^2 + |\sum_{j \in \mathcal{K}/\mathcal{Z}} \mathbf{h}_k^{A/C_k} \mathbf{w}_j^{A/C_k} x_j|^2 + \sigma_k^2} \quad (5.6)$$

Assuming perfect channel knowledge and implementing zero forcing precoding, intra-cluster interference cancels out. As a result, (5.6) becomes in the following form [40]:

$$SINR_k = \frac{\sum_{i \in \mathcal{C}_k} P_i^{Tx} |h_{ki}|^2}{\sum_{j \in \mathcal{A}/\mathcal{C}_k} P_j^{Tx} |h_{kj}|^2 + \sigma_k^2} \quad (5.7)$$

Traditionally, each base station is allowed to be connected to one CPU only as in cell-free architectures. The drawback of this traditional approach is the cluster edge effect that gives rise to inter-cluster interference. A user that is associated with a cluster-edge base station can suffer from high interference that comes from base stations that belong to neighbouring clusters. In the case of JT-CoMP in a cell-centric architecture, this user can be served jointly by the cluster-edge base station and another base station that belongs to a neighbouring cluster. However, in a cell-less architecture, this is prohibitive since the set of cooperating base stations of a user must belong to the same cluster. This limitation in a cell-less architecture is to reduce the complexity and

overheads; however, it clearly creates inter-cluster interference that needs to be addressed.

To reduce inter-cell interference in a cell-less architecture, a new cell-less approach is proposed where a macro base station that is located at the cluster-edge of a CPU can be connected to its x nearest CPUs. These base stations are referred as cluster-edge base stations and they are identified based on their distances from their nearest CPUs. A cluster-edge base station BS_i^{edge} can be mathematically defined as follows:

$$BS_i^{edge} = \begin{cases} 1, & \text{if } d(\mathbf{b}_i, \mathbf{c}_1) - d(\mathbf{b}_i, \mathbf{c}_2) < e \\ 0, & \text{if } d(\mathbf{b}_i, \mathbf{c}_1) - d(\mathbf{b}_i, \mathbf{c}_2) > e \end{cases} \quad (5.8)$$

where $d(\mathbf{b}_i, \mathbf{c}_1)$ and $d(\mathbf{b}_i, \mathbf{c}_2)$ are the distances between base station i and its closest and second closest CPUs respectively, and e is the cluster edge distance that can determine the size of the overlapping cluster edge area. A high e value allows more base stations to be associated with multiple clusters compared with a low e .

Allowing base stations at the edge to connect to multiple CPUs has been proposed in cell-free networks in [74]. However, the work in [74] did not investigate the performance of cell-free networks in terms of outage probability, user throughput, and bottom 5% throughput. Moreover, it did not consider radio resource management.

5.2.1 Performance Metrics

The performance metrics considered in this chapter are the outage probability and the achievable throughput as defined in (3.2) and (4.1), respectively.

5.3 Performance Evaluation

The simulation parameters in this chapter are the same parameters used in Chapter 3. Macro base stations are distributed in an area of 6 km x 6 km hexagonally with an inter-site distance of 500 m. This macro inter-site distance is equivalent to 10 macro base stations/km². CPUs are distributed in the same area with a density of one CPU/km². According to this macro and CPU densities, one CPU can accommodate 10 macro base stations. To investigate the impact of CPU densification on the performance of a cell-less architecture, sparse (one CPU/km²), medium (two CPUs/km²), and dense (three CPUs/km²) deployment of CPUs are considered. Similar

to Chapter 3 and 4, the spatial modelling of pico and femto base stations are based on repulsive PPP with densities of 16 and 32 base stations/km² and repulsion distances of 20 m and 10 m, respectively. Also, users are randomly distributed based on another independent PPP over the same area with a density of 560 UE/km². Similar to Chapter 4, when the CLH is implemented, the maximum cluster size c_{max} is limited to 2.

The performance of cell-centric and cell-less architectures is compared in terms of outage probability, overall user throughput, and bottom 5% throughput. Figure 5.2 shows the outage probability of both cell-centric and cell-less architectures. In the cell-less architecture, two cases are considered: single CPU association and double CPU association. In single CPU association a base station is connected to only one CPU whereas base stations in double CPU association can be connected to their two nearest CPUs if they satisfy the requirement in (5.8). CLH and CLZF are denoted as CLH1 and CLZF1 in the case of a single CPU association and CLH2 and CLZF2 when double CPU association is considered. From Figure 5.2, it is clear that a cell-less architecture with a single CPU association represented by CLH1 and CLZF1 outperforms the cell-centric design in terms of outage probability. The percentage of users that achieve higher than 0 dB increases from 74% when the cell-centric approach is implemented to 83% and 93% when a cell-less architecture is formed by CLH1 and CLZF1, respectively. Comparing a hybrid cell-centric approach and a hybrid cell-less approach (CLH1), the hybrid cell-centric approach in Chapter 4 performs slightly better than CLH1 as shown in Figures 4.7 and 5.2 due to restricting cooperation to be within a cluster in the case of CLH1. From Figures 4.7 and 5.2, the percentage of users that achieve higher than 0 dB is 88% and 83% when the cell-centric hybrid approach and CLH1 are implemented, respectively. In Figure 4.7 where the hybrid approach in a cell-centric design is implemented, a user associates with the two strongest base stations with no limit on choosing the cooperative base stations. In CLH1, users at the edge of a cluster associate with the strongest base stations; however, these users might not be associated with the second strongest base stations as their second strongest base stations may belong to another cluster. In this case, the second strongest base stations act as a strong source of interference that results in decreased SINR levels. As illustrated in Figure 5.2, the implementation of CLZF1 has shown superior performance compared with the cell-centric approach and the CLH1 due to its strength in cancelling all intra-

cluster interference and not only the strongest intra-cluster source of interference as in CLH1. Nonetheless, CLZF1 still suffers from inter-cluster interference.

To reduce inter-cluster interference due to the edge effect in a cell-less architecture, the double CPU association approach is implemented where cluster-edge macro base stations are connected to their nearest two CPUs. Figure 5.2 also compares the performance of a cell-less architecture with a single CPU association with a cell-less architecture that implements double CPU association. As Figure 5.2 demonstrates, the outage probability performance of CLH2 is almost the same as CLH1. This is because users still receive interference from base stations at the edge even if they are associated with multiple CPUs. The only difference between the single and double CPU association in the CLH scheme is that a few users that are served by the third, fourth or x^{th} strongest base station in the case of a single CPU scheme can be served by their second strongest base station if this base station is connected to its second nearest CPU. The power level difference between the second strongest base station and the third, fourth, or x^{th} strongest base station can be low which results in marginal difference in the performance. In the case where CLZF2 is implemented, a significant SINR gain is obtained. From Figure 5.2, the percentage of users that achieve higher than 0 dB is 97% in the case of CLZF2. This significant improvement is because allowing cluster-edge macro base stations to be connected to two CPUs eliminates the inter-cluster interference caused by them. This in turns enhance the SINR levels of users located at the edge of clusters. It is clear that macro base stations at the edge have a significant impact on the performance of cell-less architectures mainly due to their high transmission power.

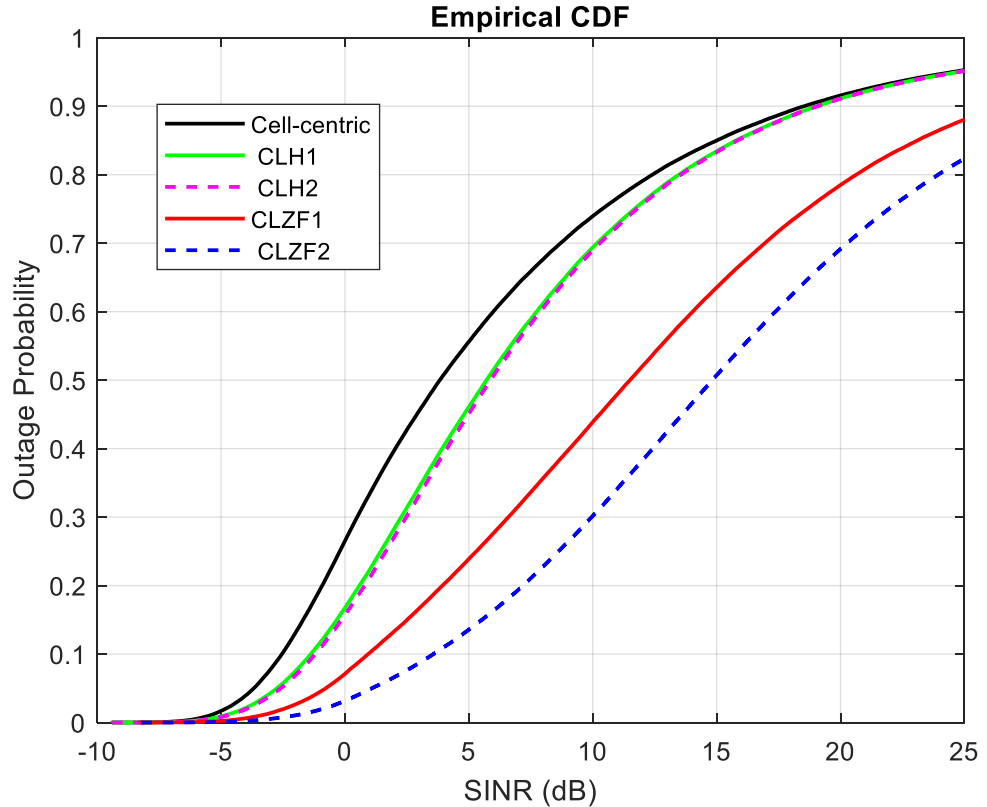


Figure 5.2: Outage probability with the cell-centric approach, the hybrid cell-less scheme (CLH1 and CLH2), and the cell-less zero forcing scheme (CLZF1 and CLZF2).

Figure 5.3 compares the performance of cell-less and cell-centric architectures in terms of overall user throughput. The implementation of CLH in a cell-less architecture slightly decreases the user throughput compared to its implementation in a cell-centric architecture as in Figure 4.8. The slight user throughput degradation in CLH is due to restricting cluster-edge users from associating to their second strongest base stations that are located in neighbouring clusters. The results also show that implementing double CPU association in CLH does not improve the system performance because, as explained in the previous paragraph, the power level difference between the second strongest base station and the third, fourth, or x^{th} strongest base station is not high. Figure 5.3 shows that CLZF has superior performance in terms of user throughput compared with the cell-centric and CLH schemes. From Figure 5.3, the percentage of users that obtain a throughput more than 1 Mbps increases from 39% and 39% when cell-centric and CLH1 are implemented to 64% when CLZF1 is applied. It is also clear that the implementation of CLZF2 that allows cluster-edge macro base stations to be connected to 2 CPUs can further improve the overall user throughput. The percentage of users achieving throughput higher than 1 Mbps increases from 64% to 76% when

CLZF1 and CLZF2 are implemented, respectively. The significant throughput improvement achieved by CLZF1 is due to the strength of zero forcing in eliminating intra-cluster interference which helps to improve the SINR levels and increase the throughput. As expected, CLZF2 outperforms CLZF1 since CLZF2 allows macro base stations to connect to two CPUs which leads to significant reduction in terms of inter-cluster interference whereas inter-cluster interference is not mitigated in CLZF1.

Figure 5.4 shows the throughput of the bottom 5% users when cell-less and centric approaches are implemented. It is obvious from Figure 5.4 that a cell-less design can enhance the throughput of the bottom 5% of users compared with cell-centric implementation. Although CLH performs better than cell-centric, its bottom 5% throughput gain is marginal compared with CLZF. The superiority of the CLZF approach is due to the elimination of intra-cluster interference and tackling inter-cluster interference where the bottom 5% users do not suffer from the cell-edge effect as in the cell-centric architecture.

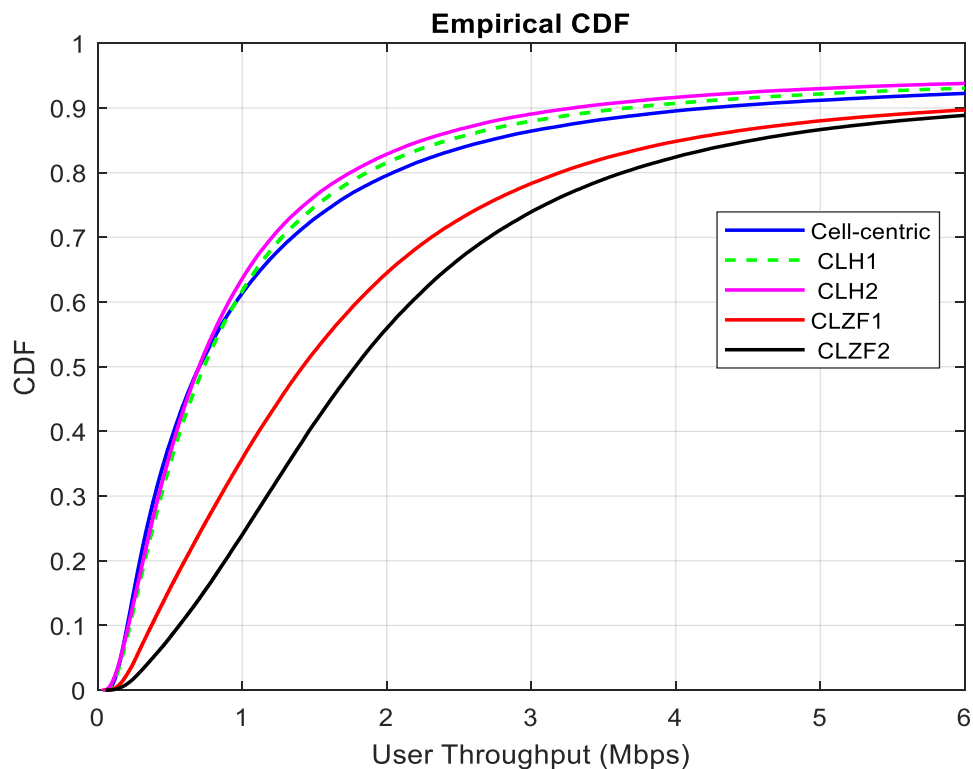


Figure 5.3: User throughput with the cell-centric approach, the hybrid cell-less scheme (CLH1 and CLH2), and the cell-less zero forcing scheme (CLZF1 and CLZF2).

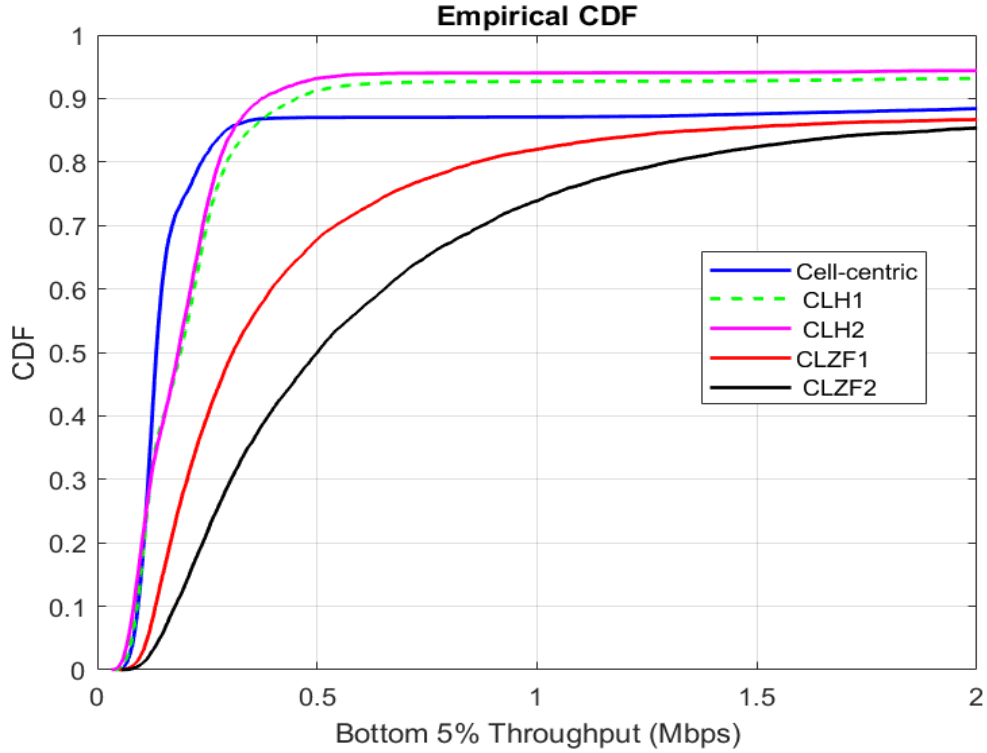
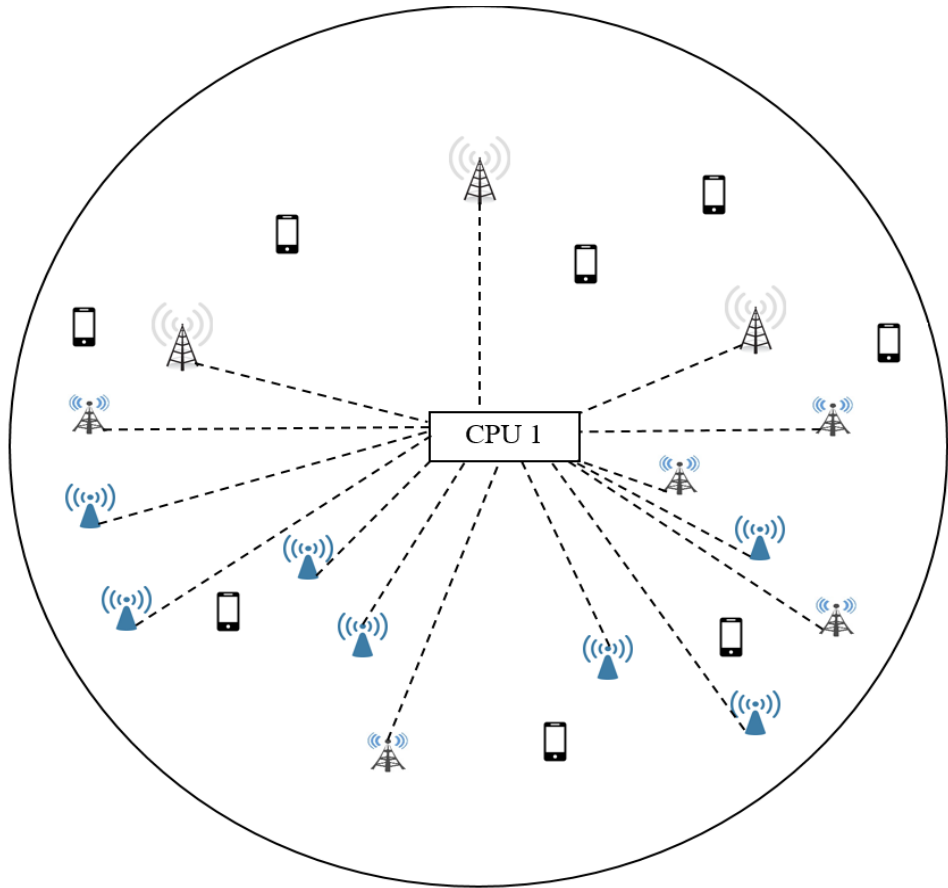


Figure 5.4: Bottom 5% throughput with the cell-centric approach, the hybrid cell-less scheme (CLH1 and CLH2), and the cell-less zero forcing scheme (CLZF1 and CLZF2).

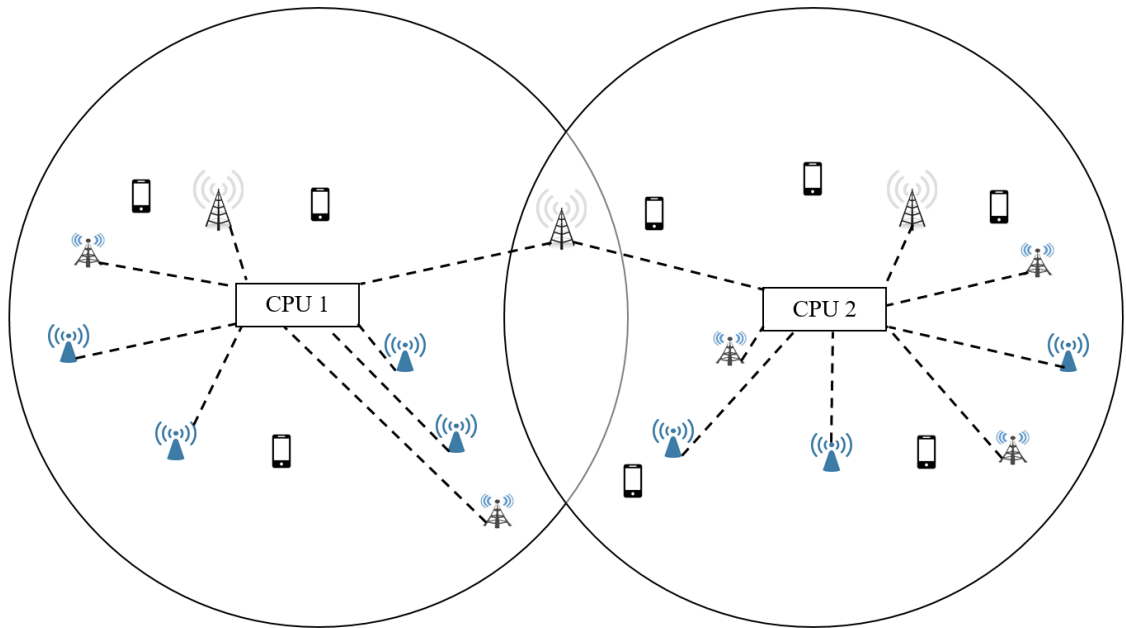
The percentage of users achieving higher than 0.2 Mbps is increased from 26% with cell-centric implementation to 44%, 44%, 71% and 86% when CLH1, CLH2, CLZF1 and CLZF2 are applied, respectively.

5.3.1 Impact of CPU Densification

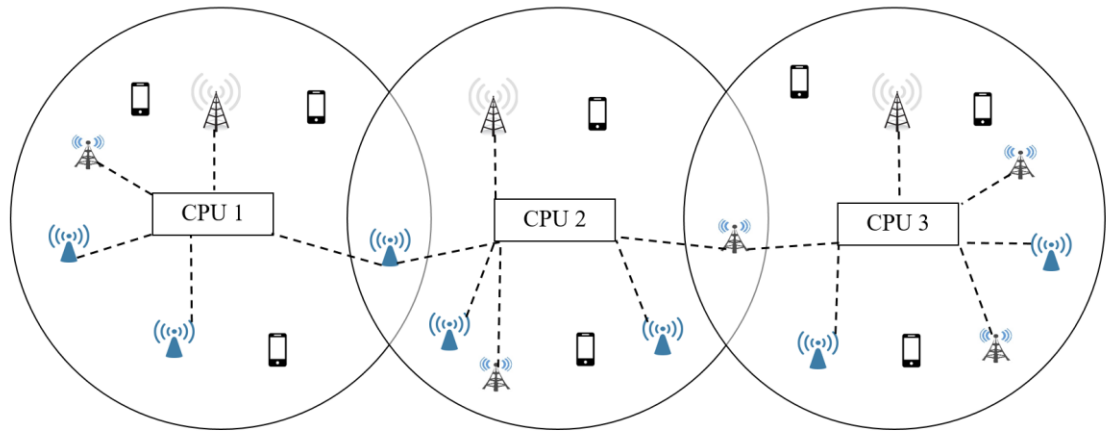
Dense deployment of CPUs in a small area may limit the benefits of a cell-less architecture as it can increase inter-cluster interference due to the increased level of the edge effect. On the other hand, the existence of a few CPUs in a large area may lead to increased delay as in C-RAN networks. Therefore, it is essential to investigate the impact of decreasing or increasing the number of CPUs per unit area on the performance of the cell-less architecture. Figure 5.5 provides an example of CPU densification.



(a) One CPU/km²



(b) Two CPUs/km²



(c) Three CPUs/ km²

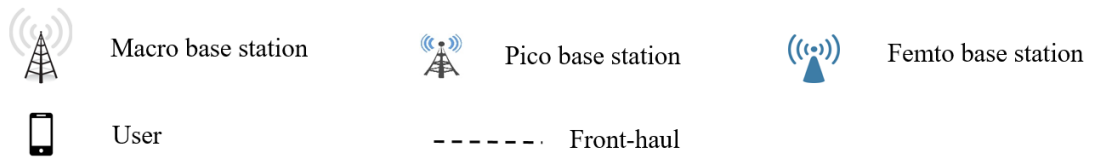


Figure 5.5: An example of CPU densification in cell-less architectures.

Figure 5.6 compares the performance of a double CPU cell-less architecture in terms of outage probability when the CPU densities are set to one CPU/km², two CPUs/km², and three CPUs/km². The main benefit of CPU densification is to reduce the processing on a single CPU in a given area since each CPU would have a lower number of users associated with it compared with sparse CPU implementation. This can significantly help to avoid delays. From Figure 5.6, it is clear that decreasing CPU density improves the outage probability performance. When the CPU density decreases from three CPUs/km² to one CPU/km², the percentage of users that obtain an SINR higher than 0 dB increases from 81% to 84% and from 91% to 97% when CLH2 and CLZF2 are implemented, respectively. Figure 5.6 shows that the performance of CLH2 is slightly affected by CPU densification. In the case of CLZF2, significant improvement is achieved when the CPU density decreases from three CPUs/km² to one CPU/km² as a sparse deployment of CPUs would allow a higher number of base stations to be connected to one CPU which helps to eliminate higher amount of inter-cluster interference. In other words, the edge effect in sparse CPU deployment is not as strong as dense CPU deployment.

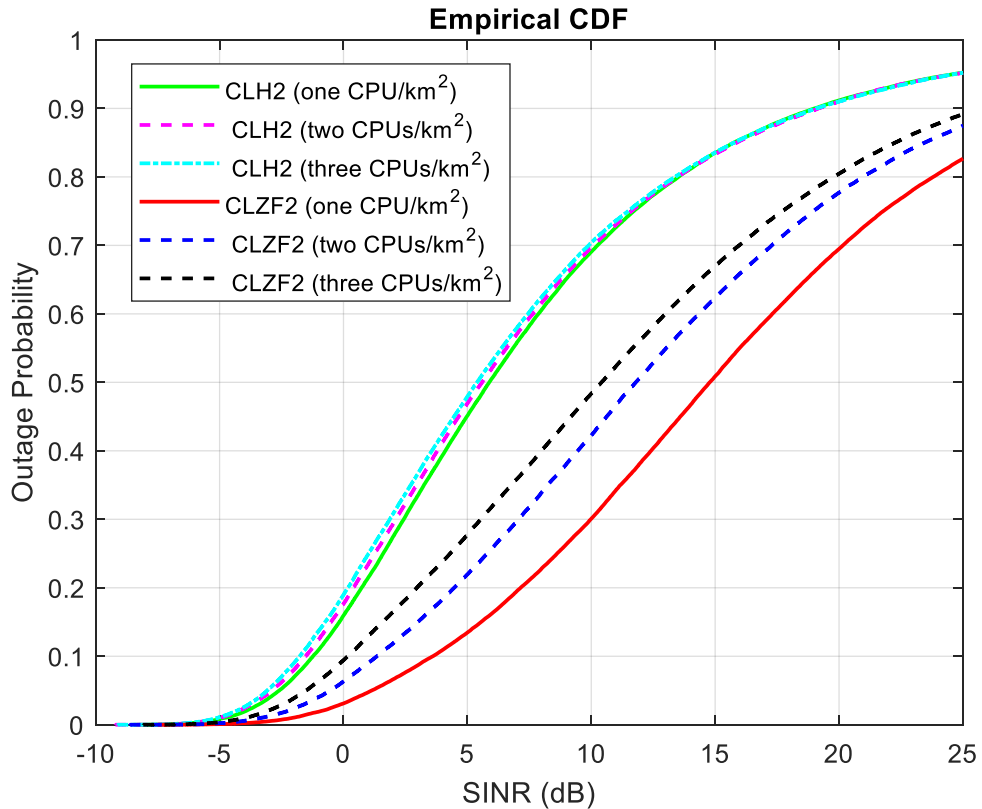


Figure 5.6: The impact of CPU densification on the outage probability performance.

5.3.2 Impact of Different Cluster-edge Distances

Cluster-edge base stations have been identified based on their distance from their nearest CPUs. A high cluster-edge distance would permit many base stations to be connected to multiple CPUs even though these base stations may provide negligible improvement. On the contrary, a low cluster-edge distance may prevent some base stations that act as strong source of inter-cluster interference from connecting to multiple CPUs. Thus, it is crucial to investigate the performance of a cell-less architecture under different cluster-edge distances.

Figure 5.7 illustrates the outage probability performance of a cell-less architecture when the cluster-edge distance is varied from 0 m to 1000 m. A cluster-edge distance of 0 m represents a cell-less architecture with a single CPU association. When the cluster-edge distance is 50 m only base stations at the edge of the cluster are connected to 2 CPUs. A cluster edge-distance of 350 m would also allow base stations that are far

away from the cluster edge to be associated with multiple CPUs. A cluster-edge distance of 1000 m would permit all base stations to be connected to 2 CPUs. According to the results shown in Figure 5.7, increasing the cluster-edge distance can significantly improve the SINR levels of users. Implementing CLZF, the percentage of users that obtain an SINR higher than 0 dB increases from 93% when the cluster-edge distance is 0 m (single CPU association) to 97%, 97%, and 99% when the cluster-edge distance is set to 50 m, 350 m, and 1000 m, respectively. This shows that cluster-edge base stations cause harmful interference to users at the cluster edge and eliminating this interference can significantly improve the link quality of edge users. The results in Figure 5.7 with a cluster-edge distance of 1000 m shows that macro base stations located closer to CPUs can still cause severe inference to users located at neighbouring clusters. However, allowing all macro base stations to be connected to two CPUs increases the complexity level.

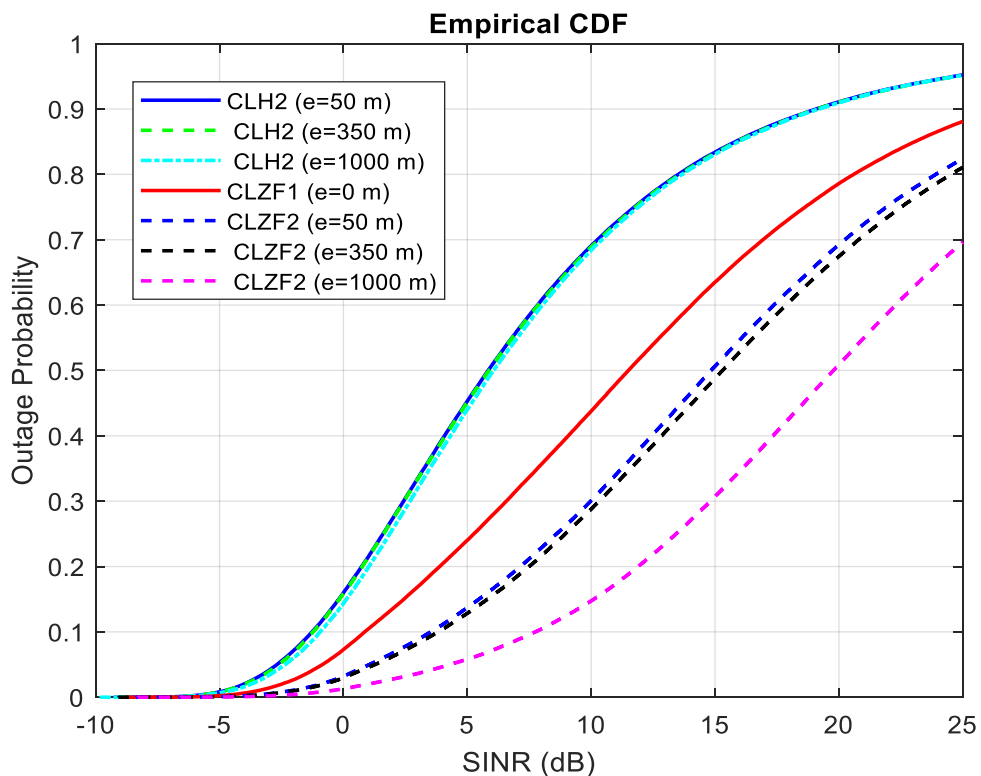
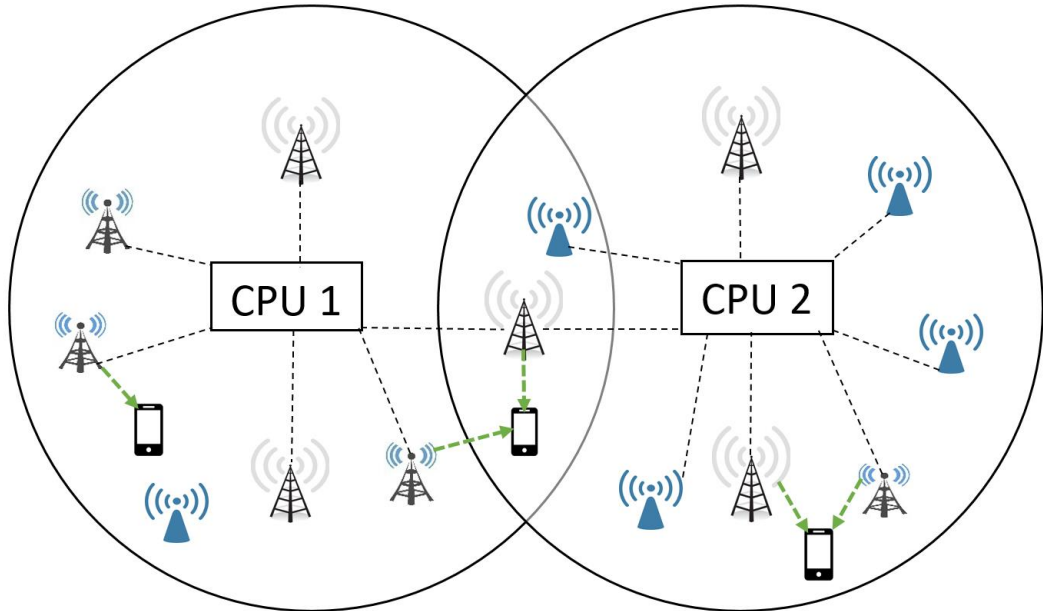


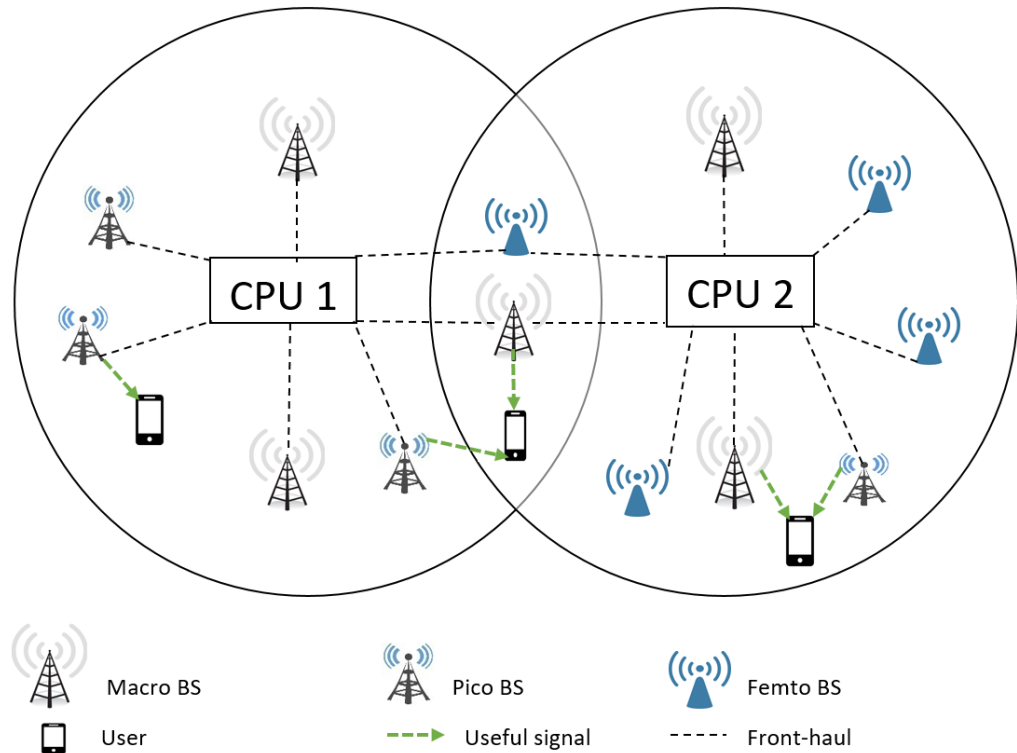
Figure 5.7: The impact of different cluster-edge distances on the performance of the outage probability.

The results in Figures 5.2 to 5.7 did not consider allowing small cell base stations to be associated multiple CPUs. Nonetheless, it is crucial to study the impact of connecting small cells to 2 CPUs on the performance of a cell-less architecture. Figure 5.8(a)

provides an example where only macro base stations are connected with two CPUs while Figure 5.8(b) shows the cases when both macro and small cell base stations at the edge are associated with two CPUs.



(a) An example where only macro base stations located at the edge are allowed to be connected to their two nearest CPUs.



(b) An example where both macro and small cell base stations located at the edge are associated with two CPUs.

Figure 5.8: Two different cases of double CPU association.

Figure 5.9 compares the outage probability when only small cells are allowed to connect to two CPUs with the case of single CPU association. This comparison can show the impact of allowing small cell base stations to associate with multiple CPUs on the performance of a cell-less architecture. Figure 5.9 also compares the performance when only small cell base stations are connected with two CPUs with another scheme that allows only macro base stations to associate with two CPUs. From Figure 5.9, it is clear that allowing small cells to connect to their second nearest CPU achieves marginal SINR gain. This marginal SINR improvement is due to the low transmission power of small cells where the interference they create to their neighbouring clusters is not strong. Thus, eliminating weak interfering signals coming from small cells at the edge does not significantly help to reduce inter-cluster interference.

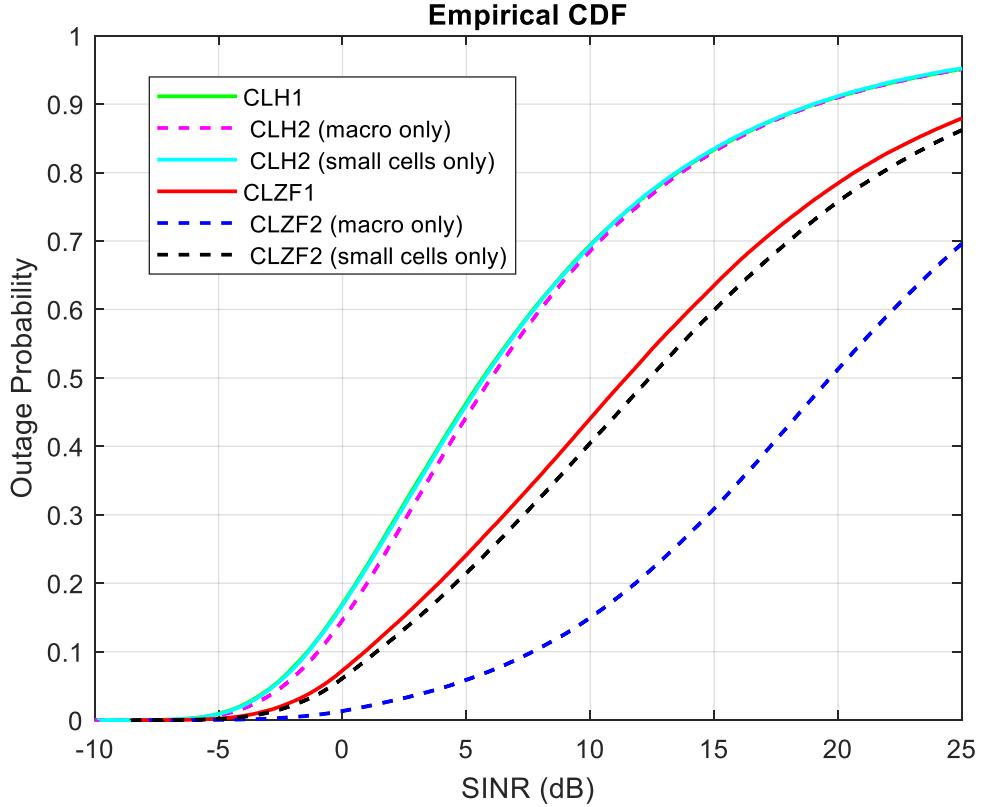


Figure 5.9: The impact of allowing small cell base stations to connect to two CPUs.

5.3.3 Complexity of Zero Forcing

Zero forcing is a promising approach that can tackle intra-cluster interference; however, implementing this scheme may require high computational complexity [111]. The zero forcing equation in (5.5) which includes the desired signal, intra-cluster and inter-cluster interference requires matrix inversions as well as matrix-matrix multiplications. Although efficient implementation of these two operations can be achieved in hardware, performing such operations for high-dimensional matrices in a very short period can be challenging [112]. The computational complexity of the zero forcing scheme is derived in [112] where multiplications and divisions are considered while additions and subtractions are ignored due to their easy implementation in hardware.

Considering two matrices $\mathbf{E} \in \mathbb{C}^{B_1 \times B_2}$ and $\mathbf{Y} \in \mathbb{C}^{B_2 \times B_3}$ and utilising Hermitian symmetry, the number of required multiplications to perform $\mathbf{E}\mathbf{E}^H$ is $\frac{B_1^2 B_2}{2} + \frac{B_1 B_2}{2}$ [112]. Due to its efficient hardware implementation, the \mathbf{LDL}^H decomposition approach can be implemented to compute the inverse of one matrix when it is multiplied by another

matrix, i.e., $\mathbf{E}^{-1}\mathbf{Y}$ [113] where \mathbf{L} is a lower triangular matrix and \mathbf{D} is a diagonal matrix. To compute the \mathbf{LDL}^H decomposition of matrix \mathbf{E} , $\frac{B_1^3 - B_1}{3}$ multiplications are required. From equation (5.5) which requires matrix inversions and matrix-matrix multiplications, the computational complexity of zero forcing becomes $\frac{3Z^2D}{2} + \frac{ZD}{2} + \frac{Z^3 - Z}{3}$ [112] where Z is the number of users and D is the number of base stations.

Figure 5.10 shows the complexity of zero forcing when the number of users Z varies from 1 to 30. It compares four different cases based on the number of base stations: $D = 40$, $D = 60$, $D = 80$, and $D = 100$. As Figure 5.10 illustrates, the complexity increases as the number of users increase. Considering $D = 40$, the number of complex multiplications increases from 6.53×10^3 to 6.35×10^4 when the number of users are 10 and 30, respectively. For the same number of users, Figure 5.10 shows that the higher the number of base stations, the higher the complexity. For instance,

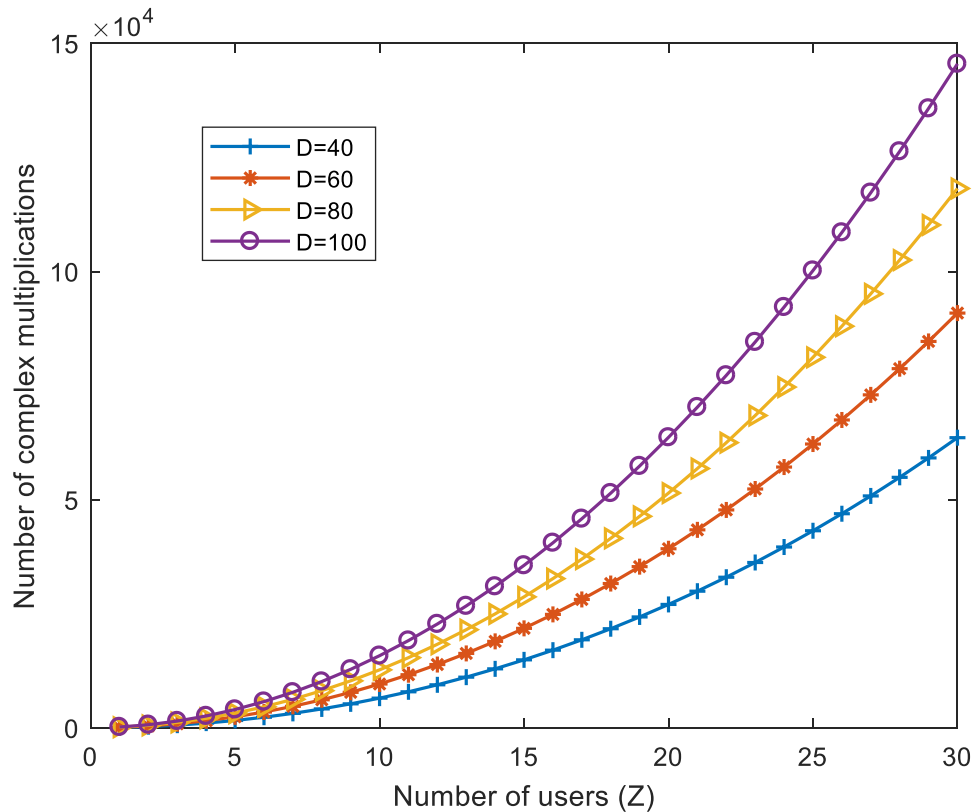


Figure 5.10: Complexity of the zero forcing scheme when different number of users and different number of base stations are considered.

when the number of users are 30, the number of required complex multiplications increases from 6.35×10^4 to 1.45×10^5 when the number of base stations increases from 40 to 100. The zero forcing scheme has shown significant improvements in terms of user throughput and bottom 5% throughput as shown in Figures 5.3 and 5.4; however, these improvements comes at the expense of high complexity particularly with the use of a large number of base stations as seen in Figure 5.10. Developing a new variant of zero forcing with reduced complexity and faster processing are two possible ways to address the complexity issue of zero forcing in the future.

5.4 Conclusion

This chapter has focused on developing and evaluating the performance of a cell-less architecture that aims to provide equal services to all users. The traditional cell-less architecture suffers from inter-cluster interference which has been addressed by allowing macro base stations located at a cluster edge to be connected to multiple CPUs. The performance of a cell-less architecture has been compared with the conventional cell-centric approach in terms of outage probability, overall throughput, and bottom 5% throughput. Two different cases are investigated in a cell-less design: zero forcing technique and the hybrid approach. The results have shown that the best performance in terms of outage probability, overall throughput, and bottom 5% throughput is achieved by a cell-less architecture with zero forcing, followed by the cell-less hybrid approach and the cell-centric approach. Although a cell-less architecture with a single CPU association has shown superior performance, it still suffers from inter-cluster interference. As the results have shown, inter-cluster interference is mainly caused by macro base stations due to their high transmission power. This inter-cluster interference has been mitigated by allowing macro base stations located at the edge of a cluster to be associated with their nearest two CPUs. This double CPU association approach has shown significant enhancement in terms of improving the SINR levels compared with a single CPU association when zero forcing is applied. However, the results have demonstrated that double CPU association is not an effective approach when implementing CLH because allowing macro base stations to be connected to multiple CPUs does not eliminate the intra-cluster interference. Implementing double CPU association in CLH only allows a few users to be connected to their second strongest base station instead of their third, fourth, or x^{th} strongest base station where the power

level difference between them might be low resulting in a marginal impact on the overall performance. The percentage of users that achieve higher than 0 dB is 74%, 83%, and 84%, 93%, and 97% when the cell-centric, CLH1, CLH2, CLZF1, and CLZF2 schemes are implemented.

The performance of a cell-less architecture under different CPU densities and cluster-edge distances has been investigated. The results have shown that it is better to have a low CPU density such as one CPU/km² in order to help mitigate inter-cluster interference. Also, the results have demonstrated that increasing the cluster-edge distance allows more base stations to be connected to multiple CPUs which results in better outage performance. Nonetheless, this improvement comes at the expense of complexity.

This chapter has also studied the impact of allowing small cell base stations to be associated with multiple CPUs. Due to the low transmission power of small cell base stations, this approach is not effective in tackling inter-cluster interference in cell-less architectures. Implementing this approach would just increase the level of complexity without providing noticeable improvements.

Overall, cell-less architecture with zero forcing is a promising approach that has shown great performance in terms of outage probability, user throughput, and bottom 5% throughput. However, its implementation increases the complexity. As a result, it is essential to study the trade-off between the system performance and the implementation complexity. The cell-less hybrid approach has also shown significant improvements especially for the bottom 5% users without the knowledge of perfect CSI as in the zero forcing scheme.

CHAPTER 6

Conclusions and Future Work

Contents

6.1	Conclusions	127
6.2	Novel Contributions	131
6.2.1	User-centric JT-CoMP Clustering Approach	131
6.2.2	Resource Matching Approach	131
6.2.3	Multi-cell Radio Resource Management	132
6.2.4	JT-CoMP-No CoMP Hybrid Approach	133
6.2.5	Development of a Novel Cell-less Architecture	133
6.3	Future Work	134
6.3.1	Load Balancing in Cell-less Architectures	134
6.3.2	Energy Efficient Cell-less Architectures	134
6.3.3	Cell-less Millimetre Wave Systems.....	134
6.3.4	Multi-objective Cell-less Architecture.....	135
6.3.5	Cell-less Architecture: a Stochastic Geometry Approach	135

6.1 Conclusions

This thesis has illustrated that future wireless networks could implement cell-less architectures as a way to overcome the limitations of cell-centric approaches. The focus of this thesis has been on investigating how such cell-less architectures can better mitigate the conventional inter-cell interference in cell-centric approaches and as a result provide improved and uniform services to all users. Cell-less architectures have been shown to provide significant performance improvements in terms of outage probability, overall throughput, and bottom 5% throughput compared with the

conventional cell-centric approach. This major enhancement is achieved due to the ability of cell-less architectures to utilise interference mitigation techniques such as JT-CoMP and zero forcing in order to tackle inter-cell interference which is a major concern in cell-centric designs.

As described in Chapter 1, the research presented in this thesis has been guided by the following hypothesis:

Exploiting a cell-less architecture that utilises promising technologies such as joint transmission coordinated multipoint and zero forcing can play an essential role towards meeting the 5G requirements in terms of improving the system capacity.

Background knowledge and literature related to the scope of this thesis has been presented in Chapter 2. This has mainly focused on interference management in 5G heterogeneous networks particularly on user-centric JT-CoMP. It also presented the architectures of four different types of radio access networks: cell-centric, C-RAN, cell-free, and cell-less. Finally, spatial modelling of macro and small cell base stations was discussed.

Chapter 3 investigated the performance of user-centric JT-CoMP clustering as it is one of the main elements of a cell-less design. A novel user-centric clustering algorithm is proposed and its effectiveness is compared against existing algorithms under different scenarios such as different maximum cluster size and different density of base station assumptions. The proposed algorithm has shown that it can better balance between SINR gain and wastage of radio resources. In addition, it has shown that its performance is not affected by the maximum cluster size and the number of base stations per unit area, unlike the conventional user-centric algorithms. Overall, according to the results of Chapter 3, JT-CoMP user-centric clustering is a promising approach to mitigate inter-cell interference and increase the SINR levels. However, to completely evaluate the performance of JT-CoMP, it is important to take radio resource management into account.

In Chapter 4, joint user-centric JT-CoMP clustering and radio resource management is considered. JT-CoMP multi-cell resource allocation faces two main challenges: resource mismatching and bandwidth underutilisation. Resource mismatching happens due to the different loads of each base station, and it is addressed

by a proposed resource matching approach where cooperating base stations negotiate on the amount of bandwidth they can offer for their overlapping regions. The second challenge is the bandwidth underutilisation problem that occurs when some small cell base stations have only CoMP users resulting in some underspent bandwidth that cannot be utilised as these base stations need to follow the resource matching approach. To tackle this problem, a hybrid approach that allows users at the edge to operate in no CoMP and CoMP modes simultaneously is proposed. Results have demonstrated that the traditional JT-CoMP approach in heterogeneous networks exhibits poor performance because of the bandwidth underutilisation problem. The hybrid approach has shown significant improvement particularly in terms of cell-edge throughput as it can benefit from the SINR gain provided by CoMP and it can deal with the bandwidth underutilisation problem. This chapter also investigated the performance of JT-CoMP when allocating different portions of bandwidth to CoMP users. In JT-CoMP networks, it is essential to efficiently allocate radio resources in a way that satisfies both CoMP and non-CoMP users. Allocating a high portion of bandwidth to CoMP users would enhance their throughput; however, this improvement might come at the expense of non-CoMP users' throughput. Half, full, and double bandwidth assignment schemes where CoMP users are allocated half, the same, and twice the bandwidth a non-CoMP user would obtain have been studied. The results have shown that half bandwidth allocation is only good in improving the overall user throughput; however, it is unable to improve the cell-edge throughput. Although double bandwidth assignment has demonstrated significant enhancement in terms of cell-edge throughput, it is also not a suitable scheme as the overall user throughput is significantly decreased. The best allocation scheme is found to be full bandwidth assignment as it can provide significant cell-edge throughput improvement without reducing the overall user throughput. The user-centric approach used in this chapter can increase complexity and overheads since any base station in the network is allowed to be involved in the cooperation set of a served user.

Chapter 5 focuses on developing and investigating the performance of a cell-less architecture that implements zero forcing and the hybrid approach while allowing edge base stations to be associated with multiple CPUs. The design of a cell-less architecture is developed where macro base stations located at the edge of a cluster are allowed to be associated with multiple CPUs and users form their own set of cooperating base stations

in a user-centric fashion. The performance of a cell-less architecture is evaluated under two different cases: zero forcing implementation and the hybrid approach developed in Chapter 4. In addition, the performance of a cell-less architecture is compared with the traditional cell-centric approach. Results have shown that the cell-less architecture in the two considered scenarios outperform the cell-centric approach in terms of outage probability and the achievable throughput. Comparing the ZF approach and the hybrid approach, ZF achieves better SINR and throughput as it can cancel the intra-cluster interference and not only the most dominant intra-cluster interfering signal as in the hybrid approach. Although a cell-less architecture has shown significant improvement in terms of outage probability and throughput gain, it still suffers from inter-cluster interference. To tackle inter-cell interference, macro base stations located at the edge of a base station cluster are connected to the two nearest CPUs. This double CPU association has demonstrated its effectiveness in mitigating inter-cluster interference. The performance of a cell-less architecture has been investigated when different CPU densities and different cluster-edge distances are considered. The obtained results have demonstrated that increasing the number of CPUs per unit area degrades the system performance due to the increased edge effect. Therefore, it is important not to densify CPUs in order to efficiently tackle inter-cluster interference. A low CPU density of one CPU/km² significantly improves performance in tackling inter-cluster interference. Moreover, the results have shown that allowing all base stations to connect to multiple CPUs can significantly improve the SINR levels, however, this approach can lead to increased complexity. To reduce this complexity, base stations at the edge are only allowed to associate with their two nearest CPUs which can also provide significant SINR gain that is slightly lower than the gain achieved when all base stations are connected to two CPUs. Finally, Chapter 5 investigated the case when small cell base stations are allowed to associate with multiple CPUs. According to the results, this approach does not help to address inter-cluster interference due to the low transmission power of small cell base stations. Overall, a cell-less architecture with zero forcing implementation can provide significant gain in terms of outage probability, user throughput, and bottom 5% throughput which helps to provide good services to all users. Nevertheless, the implementation of this approach increases the complexity level. The implementation of the hybrid approach in a cell-less architecture has also shown promising performance particularly for the bottom 5% users without requiring perfect CSI as in zero forcing.

6.2 Novel Contributions

This research has proposed novel contributions that aim to develop a cell-less architecture that can be implemented in future wireless networks. The following presents the original contributions of this thesis in detail.

6.2.1 User-centric JT-CoMP Clustering Approach

A novel user-centric JT-CoMP clustering approach that can balance between the SINR gain and the loss of radio resources has been proposed in Chapter 3. The proposed algorithm allows a user to operate in JT-CoMP mode only if the JT-CoMP rate of this user is above a certain threshold. To validate the effectiveness of the proposed algorithm, its performance is compared with three well-known user-centric algorithms, namely, PLD, RSS, and SINR. The results in Chapter 3 have shown that the proposed approach outperforms all compared algorithms in terms of providing an effective balance between the SINR improvement and wastage of bandwidth. The superiority of the proposed user-centric clustering approach over the conventional approaches is that it can identify the users who can benefit from JT-CoMP without wasting bandwidth whereas the traditional user-centric algorithms may allow some users to operate in JT-CoMP even if their SINR gain does not compensate for the bandwidth loss. In addition, unlike the traditional user-centric algorithms, its performance is not influenced by the density of base stations and the maximum user-centric cluster size. Part of this work has directly contributed to the 5Gaura project. The complete scheme of this contribution has been submitted to the *Wireless Personal Communications* journal to be considered for publication (under review).

6.2.2 Resource Matching Approach

The conventional JT-CoMP approach faces a resource mismatching problem where cooperating base stations may have different amount of bandwidth to support their overlapping region. This problem occurs due to load imbalance. The state-of-the-art has assumed that cooperating base stations can perfectly provide the same amount of bandwidth for their CoMP region which is not practical due to different loads at each base station. A resource mismatching approach is proposed to solve the aforementioned problem. In the proposed scheme, cooperating base stations negotiate and agree on the

amount of radio resources that they can offer for their overlapping region. As some base stations may have lower amount of bandwidth, cooperating base stations should allocate the minimum affordable bandwidth for the CoMP region. This leaves base stations with higher bandwidth with a portion of underspent bandwidth that cannot be used to support CoMP users. To fully utilise the available bandwidth, the unused CoMP bandwidth of a base station is allocated to its non-CoMP users. This contribution has been submitted to the *Wireless Personal Communications* journal to be considered for publication (under review).

6.2.3 Multi-cell Radio Resource Management

A joint multi-cell radio resource allocation and user-centric clustering scheme that can support efficient implementation of JT-CoMP is proposed. This joint scheme is performed in two steps. The first step constructs the user-centric clusters and based on the clustering results, radio resources are allocated. The proposed multi-cell approach provides mathematical expressions that allows flexible assignment of bandwidth for CoMP and non-CoMP users which can help to improve the overall and cell-edge throughput. The performance of the proposed multi-cell scheme is evaluated in Chapter 4 with different amounts of bandwidths given to CoMP users such as full and half bandwidth assignment. The literature has mainly focused on user-centric clustering and multi-cell allocation separately. The work in [50] has provided two different bandwidth allocation schemes, i.e., half and full bandwidth assignments, for HAP systems. These schemes are different from the work presented in this thesis as they are developed based on the maximum affordable bandwidth for CoMP regions and not on the minimum. Part of this contribution has been published in [58] in *EURASIP Journal on Wireless Communications and Networking*. Also, the multi-cell approach has been published in [57] in *IEEE 29th Annual International Symposium on Personal, Indoor and Mobile Radio Communications (PIMRC)*, and in [54] in *2018 15th International Symposium on Wireless Communication Systems (ISWCS)*.

6.2.4 JT-CoMP-No CoMP Hybrid Approach

A hybrid approach where a cell-edge user in heterogeneous networks can be jointly served by no CoMP and JT-CoMP is proposed. A user located at the edge can be served by multiple base stations in JT-CoMP mode on certain radio resources while at the same time it can be served by its strongest base station on different radio resources. In the traditional JT-CoMP scheme, a user at the edge is only allowed to operate in CoMP mode which leaves some bandwidth underutilised. The development of this hybrid approach is needed to overcome the problem of bandwidth underutilisation that happens because of the light load of small cell base stations. The performance of the hybrid approach was compared with the traditional JT-CoMP scheme in Chapter 4 and the results have shown the superiority of the hybrid approach in terms of the overall user throughput as well as the bottom 5% throughput. This contribution is to be submitted to Transactions on Emerging Telecommunications Technologies journal to be considered for publication.

6.2.5 Development of a Novel Cell-less Architecture

A cell-less architecture that allows macro base stations located at the edge of a base station cluster to be associated with multiple CPUs is proposed. This allows to reduce inter-cluster interference which is a major concern in cell-less architectures. In addition, users are served only by a subset of base stations that promise to provide significant received power. Traditionally, base stations are associated with only a single CPU and a user is served by all base stations. The work in [74] has also proposed to allow base stations at the edge to connect to multiple CPUs in cell-free networks; however, it did not investigate the system performance in terms of outage probability and throughput. Moreover, it did not consider radio resource management. The authors also considered a single tier network and not heterogeneous networks as in this thesis. The performance of a cell-less architecture has been evaluated in two different scenarios: zero forcing implementation and the hybrid approach. In addition, the performance of a cell-less architecture under different cluster-edge distances and different CPU densities is studied. This contribution is to be submitted to IEEE Transactions on Mobile Computing journal to be considered for publication.

6.3 Future Work

This section provides some recommendations for future work to further improve the performance of cell-less architectures. The following presents some potential research directions to extend the ideas presented in this thesis.

6.3.1 Load Balancing in Cell-less Architectures

In cell-less architecture user association approaches, most users are associated with macro base stations due to their high transmission power even if they have a shorter distance to small cells, e.g. pico or femto base stations. This traditional association approach causes a load imbalance with the macro base stations being overloaded while small cell base stations are lightly loaded. Biased user association proposed by 3GPP can be implemented in cell-less architectures to offload users from macro base stations to small cell base stations. It would be interesting to apply different biasing approaches such as the 3GPP per base station biasing or per-tier biasing. In per base station biasing each base station is assigned a unique biasing value while in per-tier biasing all small cell base stations in each tier are assigned a common bias value. The implementation of biasing can cause some users located at the edge of a CPU to shift from their original cluster to a neighbouring cluster which results in a different performance. Evolutionary algorithms such as particle swarm optimisation or genetic algorithm can be used to generate per base station biasing.

6.3.2 Energy Efficient Cell-less Architectures

Energy efficiency in cell-less architectures has not been well investigated yet in the literature. It is important to know how good energy efficiency in cell-less architectures is. Moreover, it is critical to develop precoding techniques that can improve the performance of energy efficiency.

6.3.3 Cell-less Millimetre Wave Systems

This thesis has focused on the performance of sub-6 GHz in a cell-less architecture. It would be interesting to evaluate the performance of cell-less when millimetre waves (mmwaves) are exploited on the access network. Channel estimation and precoding are

some potential directions that need to be studied. Also, it be interesting to evaluate the cell-less mmwaves systems with fronthaul constraints.

6.3.4 Multi-objective Cell-less Architecture

An interesting future direction that can better represent practical deployment of cell-less networks is to consider multi-objective optimisation that takes into account a number of metrics such as energy efficiency and spectral efficiency and also considers some limitations such as load conditions and fronthaul constraints. Multi-objective methods such as the weight sum approach can be utilised to formulate multiple objective functions into a single objective function. It is worth investigating the trade-off that exist between different objectives and find an optimal balance between the considered metrics.

6.3.5 Cell-less Architecture: a Stochastic Geometry Approach

Stochastic geometry as a powerful mathematical tool has shown its effectiveness in providing tractable and accurate models to analyse the performance of cell-centric networks. Stochastic geometry can be utilised in a cell-less architecture and analyse its performance in terms of different metrics such as outage probability and energy efficiency.

Glossary

4G	4 th Generation
5G	5 th Generation
5G-NR	5G New Radio
ABS	Almost Blank Sub-frame
BBU	Baseband Unit
CB	Coordinated Beamforming
CPU	Central Processing Unit
C-RAN	Cloud Radio Access Network
CRE	Cell Range Expansion
CS	Coordinated Scheduling
CSI	Channel State Information
eICIC	Enhanced Inter-cell Interference Coordination
HAP	High Altitude Platform
HetNet	Heterogeneous Network
JT-CoMP	Coordinated Multipoint Joint Transmission
LTE	Long-term Evolution
MHPP	Matern Hard-core Point Process
Mmwave	Millimetre Wave
PLD	Power Level Difference
PPP	Poisson Point Process

PRB	Physical Resource Block
RRH	Remote Radio Head
SINR	Signal-to-Interference-Noise-Ratio
SIR	Signal-to-Interference Ratio
ZF	Zero Forcing

References

- [1] Q. C. Li, H. Niu, A. T. Papathanassiou, and G. Wu, "5G network capacity: Key elements and technologies," *IEEE Vehicular Technology Magazine*, vol. 9, no. 1, pp. 71-78, 2014.
- [2] B. Bangerter, S. Talwar, R. Arefi, and K. Stewart, "Networks and devices for the 5G era," *IEEE Communications Magazine*, vol. 52, no. 2, pp. 90-96, 2014.
- [3] A. Damnjanovic *et al.*, "A survey on 3GPP heterogeneous networks," *IEEE Wireless communications*, vol. 18, no. 3, pp. 10-21, 2011.
- [4] V. Chandrasekhar, J. G. Andrews, and A. Gatherer, "Femtocell networks: a survey," *IEEE Communications magazine*, vol. 46, no. 9, pp. 59-67, 2008.
- [5] N. Bhushan *et al.*, "Network densification: the dominant theme for wireless evolution into 5G," *IEEE Communications Magazine*, vol. 52, no. 2, pp. 82-89, 2014.
- [6] J. G. Andrews, H. Claussen, M. Dohler, S. Rangan, and M. C. Reed, "Femtocells: Past, present, and future," *IEEE Journal on Selected Areas in communications*, vol. 30, no. 3, pp. 497-508, 2012.
- [7] A. Checko *et al.*, "Cloud RAN for mobile networks—A technology overview," *IEEE Communications surveys & tutorials*, vol. 17, no. 1, pp. 405-426, 2014.
- [8] E. Hossain, M. Rasti, H. Tabassum, and A. Abdelnasser, "Evolution toward 5G multi-tier cellular wireless networks: An interference management perspective," *IEEE Wireless Communications*, vol. 21, no. 3, pp. 118-127, 2014.
- [9] G. RP-100383, "New work item proposal: Enhanced ICIC for nonCA Based Deployments of Heterogeneous Networks for LTE," in *CMCC*, 2010, Vienna, Austria, 2010.
- [10] J. Zheng, J. Li, N. Wang, and X. Yang, "Joint load balancing of downlink and uplink for eICIC in heterogeneous network," *IEEE Transactions on Vehicular Technology*, vol. 66, no. 7, pp. 6388-6398, 2016.
- [11] A. Liu, V. K. Lau, L. Ruan, J. Chen, and D. Xiao, "Hierarchical radio resource optimization for heterogeneous networks with enhanced inter-cell interference coordination (eICIC)," *IEEE Transactions on Signal Processing*, vol. 62, no. 7, pp. 1684-1693, 2014.
- [12] S. Deb, P. Monogioudis, J. Miernik, and J. P. Seymour, "Algorithms for enhanced inter-cell interference coordination (eICIC) in LTE HetNets," *IEEE/ACM transactions on networking*, vol. 22, no. 1, pp. 137-150, 2013.
- [13] J. Li, X. Wang, Z. Li, H. Wang, and L. Li, "Energy Efficiency Optimization Based on eICIC for Wireless Heterogeneous Networks," *IEEE Internet of Things Journal*, vol. 6, no. 6, pp. 10166-10176, 2019.
- [14] S. Vasudevan, R. N. Pupala, and K. Sivanesan, "Dynamic eICIC—A proactive strategy for improving spectral efficiencies of heterogeneous LTE cellular networks by leveraging user mobility and traffic dynamics," *IEEE Transactions on Wireless Communications*, vol. 12, no. 10, pp. 4956-4969, 2013.
- [15] W. Tang, R. Zhang, Y. Liu, and S. Feng, "Joint resource allocation for eICIC in heterogeneous networks," in *2014 IEEE Global Communications Conference*, 2014, pp. 2011-2016: IEEE.
- [16] Y. Wang and K. I. Pedersen, "Performance analysis of enhanced inter-cell interference coordination in LTE-Advanced heterogeneous networks," in *2012 IEEE 75th Vehicular Technology Conference (VTC Spring)*, 2012, pp. 1-5: IEEE.

- [17] Y. Wang, B. Soret, and K. I. Pedersen, "Sensitivity study of optimal eICIC configurations in different heterogeneous network scenarios," in *2012 IEEE International Conference on Communications (ICC)*, 2012, pp. 6792-6796: IEEE.
- [18] C.-N. Lee, J.-H. Lin, C.-F. Wu, M.-F. Lee, and F.-M. Yeh, "A dynamic CRE and ABS scheme for enhancing network capacity in LTE-advanced heterogeneous networks," *Wireless Networks*, vol. 25, no. 6, pp. 3307-3322, 2019.
- [19] G. T. 36.819, "Coordinated Multi-Point Operation for LTE Physical Layer Aspects," 2013.
- [20] 3GPP-TR-36.741, "Study on further enhancements to coordinated multipoint (CoMP) operation for LTE," Mar. 2017.
- [21] 3GPP-RP-170750, "New WID: Further enhancements to Coordinated Multi-Point (CoMP) Operation for LTE," Mar. 2017.
- [22] Q. Cui *et al.*, "Evolution of limited-feedback CoMP systems from 4G to 5G: CoMP features and limited-feedback approaches," *IEEE vehicular technology magazine*, vol. 9, no. 3, pp. 94-103, 2014.
- [23] S. Basso, H. Farooq, M. A. Imran, and A. Imran, "Coordinated multi-point clustering schemes: A survey," *IEEE Communications Surveys & Tutorials*, vol. 19, no. 2, pp. 743-764, 2017.
- [24] 3GPP, "Technical specification group radio access network; coordinated multi-point operation for LTE physical layer aspects (release 11)," 2011.
- [25] R. Tanbourgi, S. Singh, J. G. Andrews, and F. K. Jondral, "A tractable model for noncoherent joint-transmission base station cooperation," *IEEE Transactions on Wireless Communications*, vol. 13, no. 9, pp. 4959-4973, 2014.
- [26] E. Dahlman, S. Parkvall, and J. Skold, *4G: LTE/LTE-advanced for mobile broadband*. Academic press, 2013.
- [27] J. Lee *et al.*, "Coordinated multipoint transmission and reception in LTE-advanced systems," *IEEE Communications Magazine*, vol. 50, no. 11, pp. 44-50, 2012.
- [28] F. Qamar, K. B. Dimyati, M. N. Hindia, K. A. B. Noordin, and A. M. Al-Samman, "A comprehensive review on coordinated multi-point operation for LTE-A," *Computer Networks*, vol. 123, pp. 19-37, 2017.
- [29] F. Zheng, M. Wu, and H. Lu, "Coordinated multi-point transmission and reception for LTE-advanced," in *2009 5th International Conference on Wireless Communications, Networking and Mobile Computing*, 2009, pp. 1-4: IEEE.
- [30] Y.-N. R. Li, J. Li, W. Li, Y. Xue, and H. Wu, "CoMP and interference coordination in heterogeneous network for LTE-advanced," in *2012 IEEE Globecom Workshops*, 2012, pp. 1107-1111: IEEE.
- [31] P. Marsch and G. P. Fettweis, *Coordinated Multi-Point in Mobile Communications: from theory to practice*. Cambridge University Press, 2011.
- [32] G. Cili, H. Yanikomeroglu, and F. R. Yu, "Cell switch off technique combined with coordinated multi-point (CoMP) transmission for energy efficiency in beyond-LTE cellular networks," in *Communications (ICC), 2012 IEEE International Conference on*, 2012, pp. 5931-5935: IEEE.
- [33] S. S. Ali and N. Saxena, "A novel static clustering approach for CoMP," in *2012 7th International Conference on Computing and Convergence Technology (ICCT)*, 2012, pp. 757-762: IEEE.

- [34] H. Shimodaira, G. K. Tran, K. Sakaguchi, K. Araki, S. Nanba, and S. Konishi, "Diamond Cellular Network—Optimal Combination of Small Power Basestations and CoMP Cellular Networks—," *IEICE Transactions on Communications*, vol. 99, no. 4, pp. 917-927, 2016.
- [35] P. Marsch and G. Fettweis, "Static clustering for cooperative multi-point (CoMP) in mobile communications," in *2011 IEEE International Conference on Communications (ICC)*, 2011, pp. 1-6: IEEE.
- [36] K. Huang and J. G. Andrews, "A stochastic-geometry approach to coverage in cellular networks with multi-cell cooperation," in *2011 IEEE Global Telecommunications Conference-GLOBECOM 2011*, 2011, pp. 1-5: IEEE.
- [37] S. Akoum and R. W. Heath, "Multi-cell coordination: A stochastic geometry approach," in *2012 IEEE 13th International Workshop on Signal Processing Advances in Wireless Communications (SPAWC)*, 2012, pp. 16-20: IEEE.
- [38] P. Marsch, M. Grieger, and G. Fettweis, "Large scale field trial results on different uplink coordinated multi-point (CoMP) concepts in an urban environment," in *2011 IEEE Wireless Communications and Networking Conference*, 2011, pp. 1858-1863: IEEE.
- [39] J. Holfeld, E. Fischer, and G. Fettweis, "Field trial results for CoMP downlink transmissions in cellular systems," in *2011 International ITG Workshop on Smart Antennas*, 2011, pp. 1-7: IEEE.
- [40] S. Basso, M. Jaber, M. A. Imran, and P. Xiao, "Load aware self-organising user-centric dynamic CoMP clustering for 5G networks," *IEEE Access*, vol. 4, pp. 2895-2906, 2016.
- [41] H. S. Kang and D. K. Kim, "User-centric overlapped clustering based on anchor-based precoding in cellular networks," *IEEE Communications Letters*, vol. 20, no. 3, pp. 542-545, 2016.
- [42] V. Garcia, Y. Zhou, and J. Shi, "Coordinated multipoint transmission in dense cellular networks with user-centric adaptive clustering," *IEEE Transactions on Wireless Communications*, vol. 13, no. 8, pp. 4297-4308, 2014.
- [43] A. H. Sakr and E. Hossain, "Location-aware cross-tier coordinated multipoint transmission in two-tier cellular networks," *IEEE Transactions on Wireless Communications*, vol. 13, no. 11, pp. 6311-6325, 2014.
- [44] W. Nie, F.-C. Zheng, X. Wang, W. Zhang, and S. Jin, "User-centric cross-tier base station clustering and cooperation in heterogeneous networks: Rate improvement and energy saving," *IEEE Journal on Selected Areas in Communications*, vol. 34, no. 5, pp. 1192-1206, 2016.
- [45] A. Jahid, M. S. Islam, M. S. Hossain, M. E. Hossain, M. K. H. Monju, and M. F. Hossain, "Toward Energy Efficiency Aware Renewable Energy Management in Green Cellular Networks With Joint Coordination," *IEEE Access*, vol. 7, pp. 75782-75797, 2019.
- [46] L. Liu, Y. Zhou, W. Zhuang, J. Yuan, and L. Tian, "Tractable coverage analysis for hexagonal macrocell-based heterogeneous UDNs with adaptive interference-aware CoMP," *IEEE Transactions on Wireless Communications*, vol. 18, no. 1, pp. 503-517, 2018.
- [47] K. Feng and M. Haenggi, "A Location-Dependent Base Station Cooperation Scheme for Cellular Networks," *IEEE Transactions on Communications*, 2019.
- [48] X. Yu, Q. Cui, and M. Haenggi, "Coherent Joint Transmission in Downlink Heterogeneous Cellular Networks," *IEEE Wireless Communications Letters*, vol. 7, no. 2, pp. 274-277, 2018.

- [49] G. Nigam, P. Minero, and M. Haenggi, "Coordinated multipoint joint transmission in heterogeneous networks," *IEEE Transactions on Communications*, vol. 62, no. 11, pp. 4134-4146, 2014.
- [50] M. D. Zakaria, D. Grace, P. D. Mitchell, T. M. Shami, and N. Morozs, "Exploiting User-Centric Joint Transmission–Coordinated Multipoint With a High Altitude Platform System Architecture," *IEEE Access*, vol. 7, pp. 38957-38972, 2019.
- [51] M. D. Zakaria, D. Grace, P. D. Mitchell, and T. M. Shami, "User-centric JT-CoMP for high altitude platforms," in *2018 26th International Conference on Software, Telecommunications and Computer Networks (SoftCOM)*, 2018, pp. 1-6: IEEE.
- [52] L. Liu, Y. Zhou, V. Garcia, L. Tian, and J. Shi, "Load aware joint CoMP clustering and inter-cell resource scheduling in heterogeneous ultra dense cellular networks," *IEEE Trans. Veh. Technol.*, vol. 67, no. 3, pp. 2741-2755, 2017.
- [53] Y. Lin, R. Zhang, C. Li, L. Yang, and L. Hanzo, "Graph-Based Joint User-Centric Overlapped Clustering and Resource Allocation in Ultradense Networks," *IEEE Transactions on Vehicular Technology*, vol. 67, no. 5, pp. 4440-4453, 2018.
- [54] T. M. Shami, D. Grace, A. Burr, and M. D. Zakaria, "Radio resource management for user-centric JT-CoMP," in *2018 15th International Symposium on Wireless Communication Systems (ISWCS)*, 2018, pp. 1-5: IEEE.
- [55] Y. Lin, R. Zhang, C. Li, L. Yang, and L. Hanzo, "Graph-based joint user-centric overlapped clustering and resource allocation in ultradense networks," *IEEE Transactions on Vehicular Technology*, vol. 67, no. 5, pp. 4440-4453, 2017.
- [56] W. Bai, Y. Li, T. Yao, and H. Zhang, "Performance Analysis of Dynamic Re-Clustering and Resource Allocation in Ultra Dense Network," *IEEE Access*, vol. 6, pp. 60891-60899, 2018.
- [57] T. M. Shami, D. Grace, A. Burr, and M. D. Zakaria, "User-centric JT-CoMP clustering in a 5G cell-less architecture," in *2018 IEEE 29th Annual International Symposium on Personal, Indoor and Mobile Radio Communications (PIMRC)*, 2018, pp. 177-181: IEEE.
- [58] T. M. Shami, D. Grace, A. Burr, and J. S. Vardakas, "Load balancing and control with interference mitigation in 5G heterogeneous networks," *EURASIP Journal on Wireless Communications and Networking*, vol. 2019, no. 1, p. 177, 2019.
- [59] J. D. Gibson, *Mobile communications handbook*. CRC press, 2012.
- [60] A. Goldsmith, *Wireless communications*. Cambridge university press, 2005.
- [61] G. T. v1.0.0, "Evolved Universal Terrestrial Radio Access (E-UTRA); Further advancements for E-UTRA Physical layer aspects," 2009.
- [62] S. Ghassemzadeh, L. Greenstein, A. Kavcic, T. Sveinsson, and V. Tarokh, "UWB indoor path loss model for residential and commercial buildings," in *2003 IEEE 58th Vehicular Technology Conference. VTC 2003-Fall (IEEE Cat. No. 03CH37484)*, 2003, vol. 5, pp. 3115-3119: IEEE.
- [63] V. Erceg *et al.*, "An empirically based path loss model for wireless channels in suburban environments," *IEEE Journal on selected areas in communications*, vol. 17, no. 7, pp. 1205-1211, 1999.
- [64] J. Walrand and P. P. Varaiya, *High-performance communication networks*. Morgan Kaufmann, 2000.

- [65] A. Lozano, R. W. Heath, and J. G. Andrews, "Fundamental limits of cooperation," *IEEE transactions on information theory*, vol. 59, no. 9, pp. 5213-5226, 2013.
- [66] Y. Lin, L. Shao, Z. Zhu, Q. Wang, and R. K. Sabhikhi, "Wireless network cloud: Architecture and system requirements," *IBM Journal of Research and Development*, vol. 54, no. 1, pp. 4: 1-4: 12, 2010.
- [67] C. Mobile, "C-RAN: the road towards green RAN," *White paper, ver*, vol. 2, pp. 1-10, 2011.
- [68] K. Wang, K. Yang, and C. S. Magurawalage, "Joint energy minimization and resource allocation in C-RAN with mobile cloud," *IEEE Transactions on Cloud Computing*, vol. 6, no. 3, pp. 760-770, 2016.
- [69] C. Pan, M. Elkashlan, J. Wang, J. Yuan, and L. Hanzo, "User-centric C-RAN architecture for ultra-dense 5G networks: Challenges and methodologies," *IEEE Communications Magazine*, vol. 56, no. 6, pp. 14-20, 2018.
- [70] P. Luong, F. Gagnon, C. Despins, and L.-N. Tran, "Optimal joint remote radio head selection and beamforming design for limited fronthaul C-RAN," *IEEE Transactions on Signal Processing*, vol. 65, no. 21, pp. 5605-5620, 2017.
- [71] J. Tang, B. Shim, and T. Q. Quek, "Service multiplexing and revenue maximization in sliced C-RAN incorporated with URLLC and multicast eMBB," *IEEE Journal on Selected Areas in Communications*, vol. 37, no. 4, pp. 881-895, 2019.
- [72] F. Tian, P. Zhang, and Z. Yan, "A survey on C-RAN security," *IEEE Access*, vol. 5, pp. 13372-13386, 2017.
- [73] I. Chih-Lin, J. Huang, R. Duan, C. Cui, J. X. Jiang, and L. Li, "Recent progress on C-RAN centralization and cloudification," *IEEE Access*, vol. 2, pp. 1030-1039, 2014.
- [74] A. Burr, M. Bashar, and D. Maryopi, "Ultra-dense Radio Access Networks for Smart Cities: Cloud-RAN, Fog-RAN and "cell-free" Massive MIMO," *arXiv preprint arXiv:1811.11077*, 2018.
- [75] R. Wang, H. Hu, and X. Yang, "Potentials and challenges of C-RAN supporting multi-RATs toward 5G mobile networks," *IEEE Access*, vol. 2, pp. 1187-1195, 2014.
- [76] H. Q. Ngo, A. Ashikhmin, H. Yang, E. G. Larsson, and T. L. Marzetta, "Cell-free massive MIMO versus small cells," *IEEE Transactions on Wireless Communications*, vol. 16, no. 3, pp. 1834-1850, 2017.
- [77] G. Interdonato, E. Björnson, H. Q. Ngo, P. Frenger, and E. G. Larsson, "Ubiquitous cell-free massive MIMO communications," *EURASIP Journal on Wireless Communications and Networking*, vol. 2019, no. 1, p. 197, 2019.
- [78] E. Dahlman, S. Parkvall, and J. Skold, *5G NR: The next generation wireless access technology*. Academic Press, 2018.
- [79] E. Björnson and L. Sanguinetti, "Making cell-free massive MIMO competitive with MMSE processing and centralized implementation," *IEEE Transactions on Wireless Communications*, 2019.
- [80] E. Damosso and L. M. Correia, "COST action 231: Digital mobile radio towards future generation systems: Final report," *European commission*, 1999.
- [81] E. Nayebi, A. Ashikhmin, T. L. Marzetta, and B. D. Rao, "Performance of cell-free massive MIMO systems with MMSE and LSFD receivers," in *2016 50th Asilomar Conference on Signals, Systems and Computers*, 2016, pp. 203-207: IEEE.

- [82] H. Q. Ngo, L.-N. Tran, T. Q. Duong, M. Matthaiou, and E. G. Larsson, "On the total energy efficiency of cell-free massive MIMO," *IEEE Transactions on Green Communications and Networking*, vol. 2, no. 1, pp. 25-39, 2017.
- [83] S. Buzzi and A. Zappone, "Downlink power control in user-centric and cell-free massive MIMO wireless networks," in *2017 IEEE 28th Annual International Symposium on Personal, Indoor, and Mobile Radio Communications (PIMRC)*, 2017, pp. 1-6: IEEE.
- [84] M. Bashar, K. Cumanan, A. G. Burr, M. Debbah, and H. Q. Ngo, "On the uplink max-min SINR of cell-free massive MIMO systems," *IEEE Transactions on Wireless Communications*, vol. 18, no. 4, pp. 2021-2036, 2019.
- [85] A. Anpalagan, M. Bennis, and R. Vannithamby, *Design and deployment of small cell networks*. Cambridge University Press, 2015.
- [86] Z. Li, "Intelligent on-demand radio resource provisioning for green ultra-small cell networks," University of York, 2016.
- [87] M. Haenggi, J. G. Andrews, F. Baccelli, O. Dousse, and M. Franceschetti, "Stochastic geometry and random graphs for the analysis and design of wireless networks," *IEEE journal on selected areas in communications*, vol. 27, no. 7, pp. 1029-1046, 2009.
- [88] H. ElSawy, E. Hossain, and M. Haenggi, "Stochastic geometry for modeling, analysis, and design of multi-tier and cognitive cellular wireless networks: A survey," *IEEE Communications Surveys & Tutorials*, vol. 15, no. 3, pp. 996-1019, 2013.
- [89] P. Cardieri, "Modeling interference in wireless ad hoc networks," *IEEE Communications Surveys & Tutorials*, vol. 12, no. 4, pp. 551-572, 2010.
- [90] J. G. Andrews, A. K. Gupta, and H. S. Dhillon, "A primer on cellular network analysis using stochastic geometry," *arXiv preprint arXiv:1604.03183*, 2016.
- [91] M. Haenggi, *Stochastic geometry for wireless networks*. Cambridge University Press, 2012.
- [92] S. N. Chiu, D. Stoyan, W. S. Kendall, and J. Mecke, *Stochastic geometry and its applications*. John Wiley & Sons, 2013.
- [93] S. Jing, D. N. Tse, J. B. Soriaga, J. Hou, J. E. Smee, and R. Padovani, "Multicell downlink capacity with coordinated processing," *EURASIP Journal on Wireless Communications and Networking*, vol. 2008, p. 18, 2008.
- [94] M. Xu, D. Guo, and M. L. Honig, "Two-cell downlink noncoherent cooperation without transmitter phase alignment," in *2010 IEEE Global Telecommunications Conference GLOBECOM 2010*, 2010, pp. 1-5: IEEE.
- [95] H. Wu, X. Tao, J. Xu, and N. J. I. C. L. Li, "Coverage analysis for CoMP in two-tier HetNets with nonuniformly deployed femtocells," vol. 19, no. 9, pp. 1600-1603, 2015.
- [96] A. H. Sakr and E. J. I. T. o. W. C. Hossain, "Location-aware cross-tier coordinated multipoint transmission in two-tier cellular networks," vol. 13, no. 11, pp. 6311-6325, 2014.
- [97] R. Nasri and A. Jaziri, "Tractable approach for hexagonal cellular network model and its comparison to poisson point process," in *2015 IEEE Global Communications Conference (GLOBECOM)*, 2015, pp. 1-6: IEEE.
- [98] R. Nasri and A. J. I. T. o. W. C. Jaziri, "Analytical tractability of hexagonal network model with random user location," vol. 15, no. 5, pp. 3768-3780, 2016.
- [99] S. A. Banani, R. S. Adve, and A. W. Eckford, "A perturbed hexagonal lattice to model basestation locations in real-world cellular networks," in *2015 IEEE Globecom Workshops (GC Wkshps)*, 2015, pp. 1-6: IEEE.

- [100] R. Tanbourgi, S. Singh, J. G. Andrews, and F. K. Jondral, "Analysis of non-coherent joint-transmission cooperation in heterogeneous cellular networks," in *2014 IEEE International Conference on Communications (ICC)*, 2014, pp. 5160-5165: IEEE.
- [101] S. Bassoy, M. A. Imran, S. Yang, and R. Tafazolli, "A Load-Aware Clustering Model for Coordinated Transmission in Future Wireless Networks," *IEEE Access*, vol. 7, pp. 92693-92708, 2019.
- [102] W. Lu and M. Di Renzo, "Stochastic geometry modeling of cellular networks: Analysis, simulation and experimental validation," in *Proceedings of the 18th ACM International Conference on Modeling, Analysis and Simulation of Wireless and Mobile Systems*, 2015, pp. 179-188.
- [103] S. Dawaliby, A. Bradai, Y. Pousset, and C. J. I. T. o. E. T. i. C. I. Chatellier, "Joint Energy and QoS-Aware Memetic-Based Scheduling for M2M Communications in LTE-M," vol. 3, no. 3, pp. 217-229, 2018.
- [104] X. Xiang, C. Lin, X. Chen, and X. J. I. T. o. V. T. Shen, "Toward optimal admission control and resource allocation for LTE-A femtocell uplink," vol. 64, no. 7, pp. 3247-3261, 2014.
- [105] M. Minelli, M. Ma, M. Coupechoux, and P. J. I. T. o. V. T. Godlewski, "Scheduling impact on the performance of relay-enhanced LTE-A networks," vol. 65, no. 4, pp. 2496-2508, 2015.
- [106] R. Irmer *et al.*, "Coordinated multipoint: Concepts, performance, and field trial results," *IEEE Communications Magazine*, vol. 49, no. 2, pp. 102-111, 2011.
- [107] D. Lee *et al.*, "Coordinated multipoint transmission and reception in LTE-advanced: deployment scenarios and operational challenges," *IEEE Communications Magazine*, vol. 50, no. 2, pp. 148-155, 2012.
- [108] L. Liu, Y. Zhou, V. Garcia, L. Tian, and J. Shi, "Load aware joint CoMP clustering and inter-cell resource scheduling in heterogeneous ultra dense cellular networks," *IEEE Transactions on Vehicular Technology*, vol. 67, no. 3, pp. 2741-2755, 2017.
- [109] D. Liu *et al.*, "User association in 5G networks: A survey and an outlook," *IEEE Communications Surveys & Tutorials*, vol. 18, no. 2, pp. 1018-1044, 2016.
- [110] C. Peel, Q. Spencer, A. L. Swindlehurst, and B. Hochwald, "Downlink transmit beamforming in multi-user MIMO systems," in *Processing Workshop Proceedings, 2004 Sensor Array and Multichannel Signal*, 2004, pp. 43-51: IEEE.
- [111] Q. H. Spencer, A. L. Swindlehurst, and M. Haardt, "Zero-forcing methods for downlink spatial multiplexing in multiuser MIMO channels," *IEEE transactions on signal processing*, vol. 52, no. 2, pp. 461-471, 2004.
- [112] E. Björnson, J. Hoydis, and L. Sanguinetti, "Massive MIMO networks: Spectral, energy, and hardware efficiency," *Foundations and Trends in Signal Processing*, vol. 11, no. 3-4, pp. 154-655, 2017.
- [113] A. Krishnamoorthy and D. Menon, "Matrix inversion using Cholesky decomposition," in *2013 signal processing: Algorithms, architectures, arrangements, and applications (SPA)*, 2013, pp. 70-72: IEEE.